UNIVERSITY OF
BIRMINGHAM

The Role of ApoE and

Homocysteine in the Pathogenesis

of Alzheimer's Disease

by

Amen Zafar

A thesis submitted to the
University of Birmingham
for the degree of
Master of Philosophy (MPhil)

School of Clinical and Experimental Medicince
Neuropharmacology and Neurobiology
Medical School
University of Birmingham
March 2012

Supervisor - Dr Zsuzsanna Nagy
Co-Supervisor - Professor Roy Bicknell

ABSTRACT

Alzheimer's disease (AD) is the most common cause of dementia, followed by cerebrovascular disease (CVD). The two diseases occur together in ~20% of the demented population. AD and CVD share two risk factors: elevated plasma homocysteine (Hcy) and apolipoprotein E (ApoE) genotype.

The aim of this study was to investigate the possible mechanism by which Hcy and ApoE may interact to alter cell cycle kinetics and neuronal physiology, potentially leading to the development of AD-related pathology.

Using brain samples and clinical data collected from 252 patients (including preclinical, mild and severe AD patients and control patients) we investigated the effect of elevated levels of Hcy and ApoE genotype on cognitive deficit and AD-related pathology. Furthermore, using retinonic acid induced differentiated SH-SY5Y human neuroblastoma cells we investigated the effects of Hcy and ApoE isoforms on AD-related protein expression, cell proliferation, cell survival and the methylation pattern of cell cycle regulatory genes.

The results from this study suggest that (i) Hcy affects the development of AD at multiple levels, cell cycle regulation, DNA methylation, induction of oxidative stress and direct effect on AD-type protein accumulation and (ii) these effects are modulated by the ApoE genotype.

ACKNOWLEDGEMENTS

TABLE OF CONTENTS

LIST OF ILLUSTRATIONS

LIST OF TABLES

ABBREVIATIONS

Aβ	β-amyloid
AD	Alzheimer's disease
ANOVA	Analysis of Variance
APP	Amyloid Precursor Protein
ApoE	Apolipoprotein E
ApoER2	ApoE receptor 2
CAMCOG	Cambridge Cognitive Examination
CBS	Cystathionine β-Synthase
CDKI	Cyclin Dependent Kinase Inhibitor
CSF	Cerebrospinal Fluid
CVD	Cerebrovascular Disease
DNA	Deoxyribonucleic acid
DNMTs	DNA methyltransferases
DF	Degree of Freedom
E	Entorhinal
ECD	Electrochemical detection
Hcy	Homocysteine
HPLC	High performance liquid chromatography
8-HG	8-hydroxyguanosine
4-HN	4-hydroxynonenal
L	Limbic

LDH	Lactate dehydrogenase
LDL	Low Density Lipoprotein
MAPK	Mitogen Activated Protein Kinase
MCI	Mild Cognitive Impairments
N	Neocortical
NFT	Neurofibrillary Tangles
NMDA	N-Methyl-D-Aspartate
OPTIMA	Oxford Project to Investigate Memory and Ageing
PDT	Population Doubling Time
PHF	Paired Helical Filaments
PI	Propidium Iodide
qPCR	Quantitative Real Time Polymerase Chain Reaction
RA	Retinoic Acid
SAH	S-adenosylhomocysteine
SAM	S-adenosyl methionine
SP	Senile Plaques
VLDLR	VLDL receptor

1. INTRODUCTION

1.1. Alzheimer's Disease

Alzheimer's disease (AD) is the most common neurodegenerative disease; the gradual cognitive decline is the main clinical feature of the disease. In the early stages of AD, patients present with mild cognitive impairments (MCI) such as amnesia which can initially be mistaken for normal age-related memory loss. As the disease progresses, the memory problems become more severe and interfere with daily living. Individuals develop aphasia (language impairment) and apraxia (impairment in the co-ordination of fine movements). At late stages psychosis and personality changes are also very common[195].

In a study carried out in 2006, the Delphi consensus[1], it was estimated that at the time there were 24.3 million people with dementia, of which half were considered to have AD. It is predicted that the number of new cases will double in the next 20 years[1]. The duration of the disease from onset of symptoms ranges from 5 to 10 years[195]. Given the duration of the disease and the long term care required, there is a heavy social and economical burden placed on family, carers and healthcare services. The development of diagnostic tests and therapeutic interventions is crucial for this most devastating disease.

1.1.1. Alzheimer's Disease Pathology

AD has two distinct pathological features that present in the brain; these are neurofibrillary tangles (NFT) and senile plaques (SP)[118, 195]. The NFT are composed of intracellular paired

helical filaments (PHF) formed from hyperphosphorylated microtubule-associated protein, tau[115]. Tau pathology eventually leads to loss of synapses and neuronal death as intracellular trafficking is disrupted[116, 134]. The plaques are composed of extracellular deposits of β-amyloid (Aβ) formed from the cleavage of amyloid precursor protein (APP). It is debatable whether the presence of plaques correlates with increase cell death[114]. These pathological processes contribute to loss of synapses and neuronal networks, leading to brain atrophy and dementia.

1.1.2. Cell Cycle Theory

In recent years, the cell cycle theory has gained popularity in AD research[2]. It is hypothesised that AD is caused by a re-activation of the cell cycle in aging differentiated neurones. In neurones of healthy elderly individuals, the neuronal entry into the cell cycle is followed by the activation of cell cycle regulatory mechanisms (e.g. cyclin dependent kinase inhibitors), which halt the progression of cell cycle and inhibit neurones from bypassing the G1/S transition point. In AD it is thought that neurones bypass this G1/S transition point due to a failure of the cell cycle regulatory mechanisms. Passed the G1/S transition point neurones are unable to re-differentiate. Cells replicate their DNA, but as neurones are unable to undergo cytokinesis, the cells remain suspended in the G2 cell phase. This leads to activation of aberrant intracellular mitogenic signalling resulting in upregulation of kinase activity and downregulation of phosphatases. This phenomena may explain the formation of both the tangle and plaque pathology seen in AD[2].

The re-activation of the cell cycle is seen in normal aging neurones and is thought to play a role in synaptic plasticity[3]. AD pathology is seen in regions of the brain that are associated with high synaptic plasticity, such as the hippocampus. This suggests that neurones that can

undergo synaptic plasticity are more vulnerable to aberrant mitogenic stimuli or failure in cell cycle regulation. The trigger that induces these neurones to leave their differentiated state and develop AD pathology is still unknown[3].
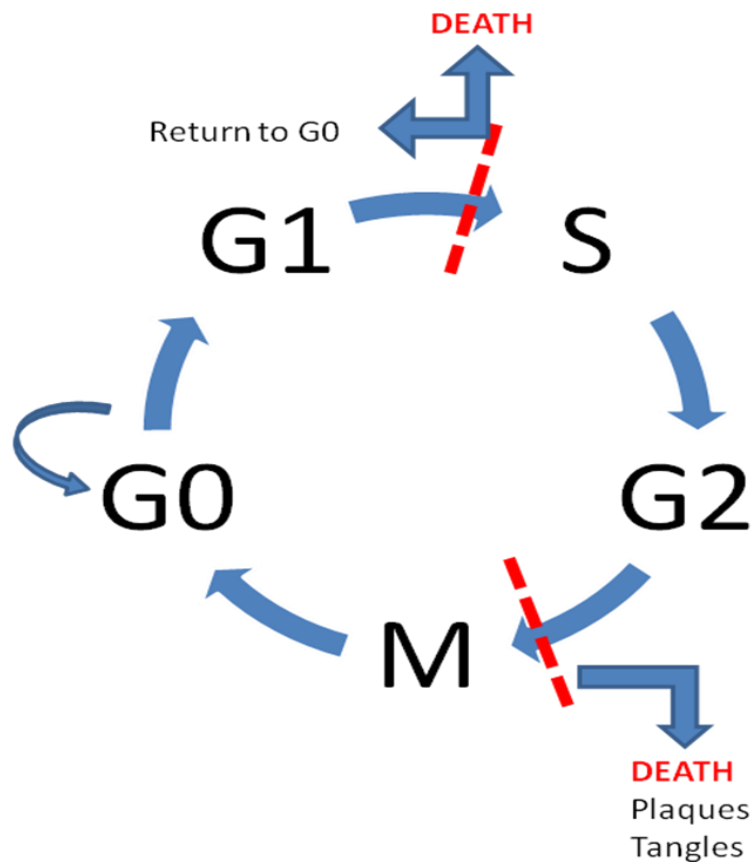
Figure 1

Cell cycle theory of Alzheimer's disease (adjusted from [2]).

1.1.3. Risk Factors

The study of known risk factors of AD has played an important role in exploring the pathogenesis of this disease. Old age is one of the risk factor best associated with AD[4]. There are other known risk factors that have been identified as predisposing individuals to developing AD; these include head trauma, hypertension, diabetes, depression, menopause and poor education [reviewed in [5] and [6]]. Furthermore, raised plasma homocysteine levels[7] and vascular disease[8] are seen as risk factors in AD and both these risk factors will be discussed further on in this chapter. While specific disease causing mutations have been identified on a small number of genes (APP, PS1 and PS2[157]); these mutations are responsible for the development of AD in less than 5% of patients. In the rest of AD patients, the disease cannot be accounted for by a single mutation. Nevertheless, the contribution of genetic factors to the disease is undeniable. The best known genetic risk factor for sporadic AD is the epsilon 4 variant of the apolipoprotein E gene (ApoE)[120].

As explained above AD is the main cause of dementia; the next leading cause is cerebrovascular disease (CVD), which includes stroke, carotid stenosis, and aneurysms. CVD alone accounts for ~16% of dementia cases, and CVD with AD makes up 20% of all dementia cases[191]. A number of studies have shown that the clinical symptoms of AD are more severe when patients have CVD, suggesting that the occurrence of the two diseases is pathogenically linked. A number of CVD risk factors have been associated with AD, e.g. hypertension and diabetes[192]. Two other common risk factors of CVD and AD are elevated plasma Hcy levels and ApoE4 genotype; both are the focus of this study.

1.2. Apolipoprotein E

Apolipoprotein E (ApoE) is a constituent of chylomicrons and very low density lipoprotein (VLDL); its primary function is lipid transport and metabolism. In the central nervous system, ApoE is involved in various aspects of neuronal repair and neuroprotection. In the brain ApoE is mainly secreted by astrocytes and has a role in cholesterol homeostasis, lipid distribution to regenerating axons, synaptic remodelling and remyelination of schwann cells[9;10].

The ApoE gene is located on chromosome 19q13.2 and consists of 3 introns and 4 exons; encoding a 317 amino acid precursor protein. Following post-translational splicing a 299 amino acid (34.2kda) ApoE glycoprotein is generated. The ApoE N-terminal domain contains the LDL receptor binding region (residues 1-191), while the C-terminal domain contains the lipid binding region (residues 222-299)[11]. The ApoE gene is polymorphic with three alleles (ε2, ε3, and ε4), producing three isoforms; ApoE2, ApoE3, and ApoE4. The ApoE isoforms differ in amino acid residues at positions 112 and 158. ApoE2 has a cysteine residue at both sites, ApoE3 has cysteine at 112 and arginine at 158 and ApoE4 has arginine at both sites[11]. Six genotypes are generated from these polymorphisms; 3 homozygous (ε2ε2, ε3ε3, ε4ε4) and 3 heterozygous (ε2ε3, ε2ε4, ε3ε4). The polymorphisms have an influence on the levels of protein produced; ApoE2 levels in plasma are higher than ApoE3 and ApoE4. The differing amino acid residues at the two positions (i.e. 112 and 158) alter the conformation of the N-terminal domain and influence the functionality of ApoE[12]. ApoE2 has been associated with hyperlipoproteinemia, which can lead to atherosclerosis and CVD. The cysteine residue at positions 112 and 158 in ApoE2 results in a poor binding of the N-terminal to receptor binding sites; this decreased binding activity of ApoE2 results in elevated cholesterol levels[13]. In AD the ApoE ε2 allele has be found to have a protective effect. The ApoE3 genotype is

common in all human populations[14], and this genotype is considered as the 'neutral' ApoE genotype in AD[15]. A large number of studies have linked ApoE4 to AD [Reviewed in [15]]. There is an increased frequency of the ApoE ε4 allele in late on-set familial and sporadic AD patients[16]. With increasing number of ApoE ε4 alleles the risk of developing AD increases from 20 to 90%, the age of onset of the disease decreases from 84 to 68 years[17] and the rate of cognitive decline increases[18]. These studies suggest a dosage effect of ApoE4. Post-mortem studies have found that ApoE ε4 carriers have significantly more neuritic plaques and tangles in neocortical regions of the brain compared to non-carriers[19;20]. However, the ApoE4 genotype is only a risk factor for AD, meaning that the presence of this variant does not necessarily cause AD[21;22]. Furthermore, in some ethnic groups the ApoE ε4 allele has no association with AD[14]. These studies suggest that the ApoE4 genotype alone is neither necessary nor sufficient for AD development, and this risk factor may work in combination with other factors to have a role in the pathogenesis of AD.

The mechanism by which the ApoE ε4 allele has a role in generating AD-type pathology is still unclear [reviewed in[23]]. However, a number of mechanisms have been postulated. These briefly include a direct interaction of ApoE with beta amyloid: the binding efficiency of the isoforms to beta amyloid was found as follows; ApoE2 > ApoE3 >> ApoE4. It has been suggested that ApoE has a role in the clearance of beta amyloid; and the binding efficiency of the different isoforms is reflected in the association of the isoforms with Aβ aggregation[24] and senile plaque formation in AD[25]. ApoE has also been shown to have an isoform-dependent effect on tau phosphorylation and tangle formation[26]. The role of ApoE in lipid distribution is also thought to play a part in AD development[27]. Furthermore, isoform-specific effects on neuronal repair and synaptogenesis have also been observed[28].

1.3. Homocysteine

Homocysteine (Hcy) is a sulfur-containing non-essential amino acid with a free-thiol group. It is a metabolite of methionine formed as a byproduct of the folate cycle[29]. The diagram below illustrates the pathway of Hcy metabolism.
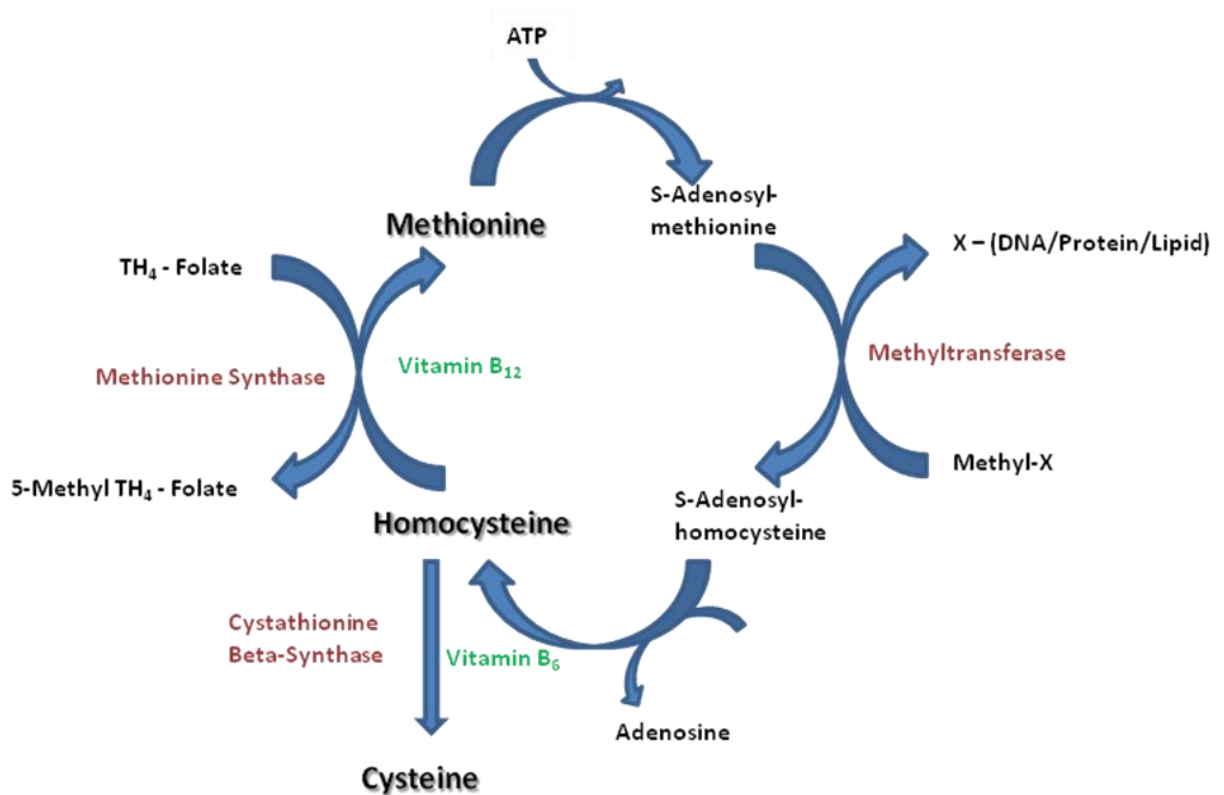
Figure 2

Homocysteine metabolism in the folate cycle. Hcy is an intermediate product generated from the demethylation of methionine. Hcy can be remethylated to methionine in the presence of methionine synthase and folate/vitamin B_{12}. Hcy can also be catabolised to cysteine via the transsulfuration pathway, and this is dependent on cystationine beta synthase (CBS) and vitamin B_6.

Methionine is converted to s-adenosyl methionine (SAM); this is the most important methyl donor in the body. After losing its methyl group SAM is converted to s-adenosylhomocysteine (SAH). SAH is then hydrolysed to generate Hcy and adenosine; this is a reversible reaction and equilibrium favors the synthesis of SAH. Hcy can be remethylated to methionine in the presence of vitamin B_{12}, folate, and 5-methyltetrahydrofolate. When methionine is in excess Hcy is irreversibly converted into cysteine by cystathionine β-synthase (CBS) in the presence of vitamin B_6. The distribution of Hcy depends on metabolic status; therefore any deficiencies in vitamins/enzymes in the pathway would lead to an imbalance in Hcy homeostasis and alter plasma Hcy levels[29].

Normal levels of plasma Hcy levels range between 5 to 15µmol/L. Hyperhomocysteinemia describes increased levels of plasma Hcy. Levels are defined as moderate (15 to 30µmol/L), intermediate (30 to 100µmol/L) and severe (>100µmol/L). Plasma Hcy levels increase with age, which may be a result of a decline in renal function[30]. The levels of Hcy in the cerebral spinal fluid (CSF) is 5-30% of that of plasma[31], suggesting that transport of Hcy in the brain is highly regulated, protecting the brain from increased levels of Hcy[32;33].

Elevated plasma Hcy levels have been reported in AD patients relative to controls[34;35], and the levels of Hcy appear to correlate with disease progression[34;36]. AD patients with high plasma Hcy levels show rapid medial temporal lobe atrophy[37], higher number of silent brain infarctions, and a greater rate of cognitive decline[38-40]. This relationship between Hcy and cognitive functioning is also seen in homocystinuria. Homocystinuria is a genetic disorder which causes severe hyperhomocysteinemia due to cystathionine beta-synthase deficiency. The main clinical symptom of homocystinuria is mental retardation, suggesting that Hcy

influences cognitive performance. Furthermore, in a study by Nilsson et al[41] oral folate supplementation given to patients with mild to moderate dementia and elevated Hcy levels was found to lead to a significant improvement in cognitive performance; whereas patients with mild to moderate dementia and normal plasma Hcy levels showed no improvement. While these studies do not prove that a relatively small increase in Hcy levels causes cognitive deficit, it is clear that early vitamin supplementation aimed at reducing plasma Hcy levels may halt or at least delay cognitive decline in AD patients. This is further supported by the systematic review of the handful of trials into the effect of folate in the elderly[193].

Although elevated plasma Hcy is an acknowledged risk factor for AD, the mechanism by which it contributes to the pathogenesis of the disease is not fully understood. It has been suggested that Hcy may trigger β-amyloid aggregation[42] and tau hyperphosphorylation[43]. Hcy has also been found to cause oxidative stress[44;45], and is neurotoxic through its action via a glutamate receptor agonist[46]. Alternatively, changes in Hcy levels could induce epigenetic changes via altering DNA and histone methylation[47-49]. There is little doubt that excess Hcy in the elderly is harmful, however the role of this amino acid in AD development is still a matter of debate and requires further study.

1.4. DNA Methylation

Epigenetics describes the regulation of genomic function which is independent of the DNA sequence. This can include DNA methylation, histone acetylation and results in changes in chromatin and chromosome structure. Epigenetic modifications allow regulation of gene

transcription and gene expression, and therefore have a significant influence on cellular function.

DNA methylation involves the addition of a methyl group from s-adenosyl methionine (SAM) to a cytosine residue on the DNA sequence. High levels of DNA methylation is found in CpG islands that occur close to promoter regions of a gene. This prevents binding of transcription factors and allows the regulation of gene expression. DNA methylation is influenced by the methylation potential, which refers to the ratio of metabolites in the folate cycle. As the cycle is influenced by dietary intake of vitamin B_6, B_{12}, folate and methionine, dietary variation could potentially affect DNA methylation and result in the alteration of gene expression. Since Hcy is an important part of the methylation cycle, dysregulation of DNA methylation may be one of the mechanisms by which elevated Hcy levels alter gene expression and lead ultimately, via the cell cycle alterations, to the degeneration of neurones in AD.

1.5. Possible Interactions Between ApoE and Homocysteine

Elevated plasma Hcy levels and ApoE4 genotype are common risk factors in both AD and CVD. A recent study suggests that the effects of plasma Hcy levels on cognitive performance are dependent on ApoE genotype[50]. Given that ~70% of plasma Hcy is plasma protein-bound, of which ~30% is lipoprotein-bound, a chemical interaction between Hcy and ApoE is a plausible explanation[51]. Hcy forms disulfide bonds with cysteine residues on lipoproteins[51-53]. Therefore, structural characteristics of the lipoproteins would influence Hcy binding. As each ApoE isoform has a different number of cysteine residues, they could interact differently with Hcy. ApoE2 has two free cysteine residues; therefore its binding capacity for Hcy would be

greater than that of either ApoE3 or ApoE4. The presence of ApoE2 may reduce the amount of free circulating Hcy, thus protecting the brain from the harmful effects of this amino acid. This scenario may explain the protective role of ApoE2 in AD. On the other hand, the binding of Hcy to ApoE could potentially result in a change in the function of the lipoprotein. In view of this, we hypothesise that Hcy may have a differential isoform effect on the activity of ApoE.

Interaction between ApoE and Hcy could also occur indirectly via common signaling pathways (summarised in Figure 3). Hcy is a glutamate receptor agonist, acting on NMDA receptors, that directly increases calcium influx into neurones, activating a number of downstream kinase pathways, e.g. MARK pathway[54]. Binding of ApoE to ApoE receptor 2 (ApoER2) and VLDL receptor (VLDLR) induces tyrosine phosphorylation of Dab1 at the cytoplasmic domain. This leads to the activation of NMDA receptors and increases calcium influx into neurones (see Figure 3). ApoE also activates several signalling pathways (including the MARK pathway) via the LDL receptor family.
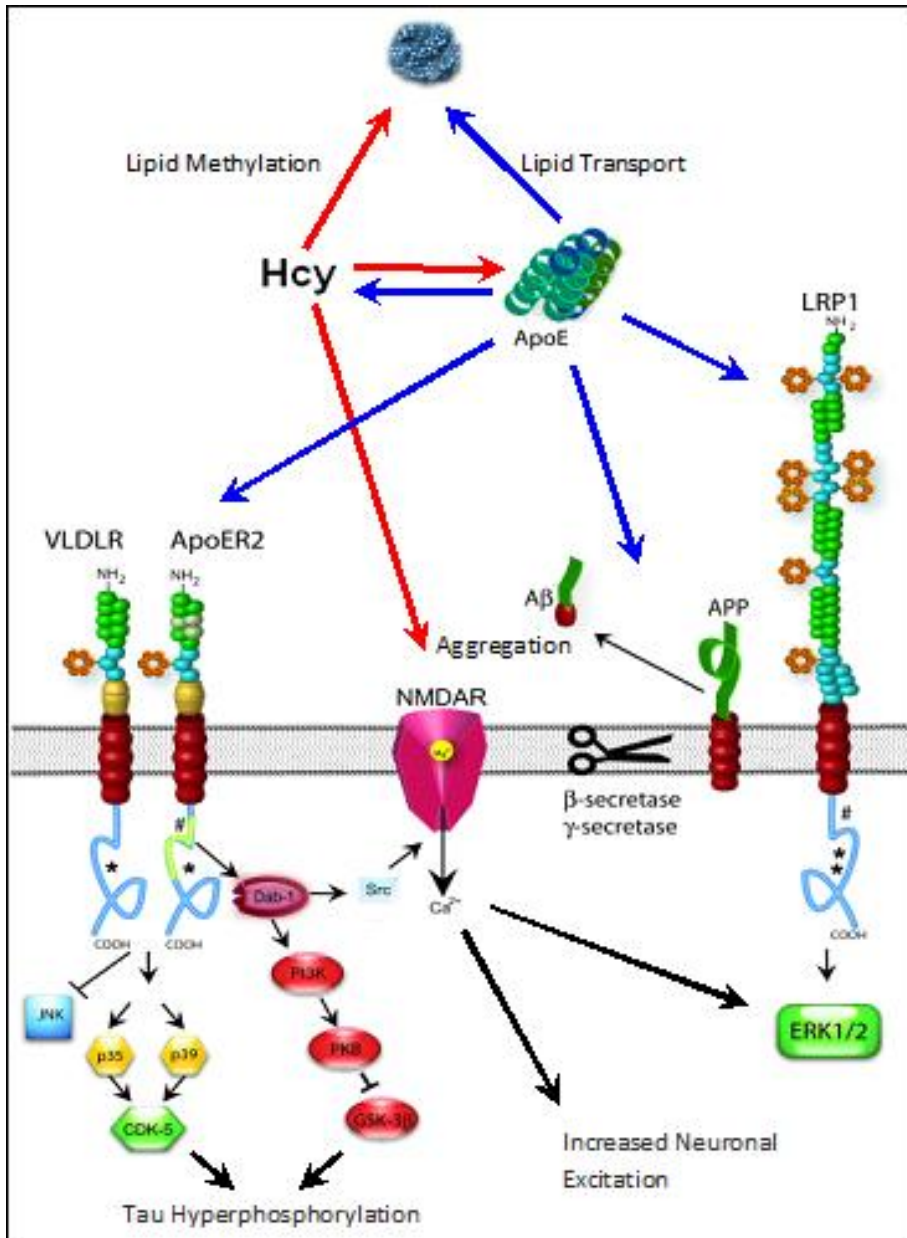
Figure 3

Diagrammatic illustration of possible interactions of ApoE and Hcy [Adjusted from[55]].

1.6. ApoE, Homocysteine and the Cell Cycle

ApoE has been shown to inhibit proliferation of smooth muscle cells, mediated through cell cycle arrest at the G_0/G1 transition point[56]. However this effect is isoforms-dependent, with ApoE4 shown to be less effective at inhibiting smooth muscle cell proliferation than the other isoforms (ApoE2 > ApoE3 > ApoE4)[57;58]. Hcy on the other hand, has been shown to stimulate cell proliferation. In a study also involving smooth muscle cells, high levels of Hcy induced increased cyclin A expression and cell proliferation[59]. However in a recent study, Hcy was found to inhibit endothelial cell proliferation through altering DNA methylation of the cyclin A promoter. This was associated with increased SAH levels, reduced activity of DNA methyltransferases (DNMTs) and increased histone acetylation at the promoter region[49]. These studies highlight the possibility that Hcy induced alterations in the methylation pattern of cell cycle related genes may have opposing effects in different cell types. This raises the possibility that in AD, the aberrant expression of cell cycle related genes is due to Hcy induced changes in their promoter methylation.

Studies have shown that both ApoE and Hcy influence the cell cycle individually. Therefore it is possible that the interaction of the two risk factors, whether directly or indirectly, could generate a differential cell cycle response depending on the ApoE isoform.

2. SUMMARY OF THE RESEARCH PROPOSAL

Alzheimer's disease (AD) is the most common cause of dementia in the developed world, followed by cerebrovascular disease (CVD). The two diseases occur together in ~20% of the demented patient population[191]. AD and CVD share two risk factors: elevated plasma Hcy level and apolipoprotein E genotype. A recent study suggests that plasma Hcy level and ApoE genotype may not represent independent risk factors for cognitive decline. The aim of this project is to investigate the possible mechanism by which Hcy and ApoE may interact to alter neuronal physiology, potentially leading to the development of AD-related pathology. We plan to investigate three hypotheses.

Hypothesis 1. Since elevated levels of plasma Hcy are a recognised risk factor for Alzheimer's disease, we hypothesis that elevated levels of Hcy are associated with more severe pathology and cognitive deficit in Alzheimer's disease patients.

Hypothesis 2. We hypothesise that the effect of Hcy are dependent on the ApoE genotype.

Hypothesis 3. We will investigate the effect that Hcy has on cell proliferation, cell survival and the methylation pattern of cell cycle regulatory genes. We hypothesise that Hcy contributes to the development of AD by affecting the neuronal cell cycle, and that the effect of Hcy on the cell cycle is modulated in an ApoE isoform-dependent manner. Since prior literature shows inconsistent and cell-type specific effects for both Hcy and ApoE we are unable to predict the measures of interactions (as hypothesised in Hypothesis 2 and Hypothesis 3).

3. METHODS

3.1. Patients

We used human brain tissue from the Thomas Willis brain bank (brain tissue collected by OPTIMA). The 206 patients included in this study (64 control patients (entorinal stage), 57 mild AD patients (limbic stage) and 85 severe AD patients (neocortical stage)) were all participants of the Oxford Project to Investigate Memory and Ageing (OPTIMA) study. Patient numbers were not based on power calculations, but on sample availability. Without preliminary data on the experimental variation of different measures we could not perform power calculations. Patient numbers in this study are lower than most neuropathology based studies. The donated brain tissue is stored by the Thomas Willis brain bank, while OPTIMA holds the wealth of collected longitudinally clinical information. We have results of yearly cognitive tests (CAMCOG and MMSE) and plasma Hcy levels. The tissues collected by the brain bank have been characterised in detail by a consultant neuropathologist using standard diagnostic protocols (CERAD protocol and Braak staging for AD). The extent of the contribution of any vascular pathology to the clinical dementia was determined by the clinical neuropathologist)[192].

3.2. Extraction of RNA, DNA and Protein

3.2.1. TRI-Reagent Method

TRI Reagent$^®$ is a ready-to-use reagent which allows simultaneous isolation of RNA, DNA and proteins from samples. 100mg of brain tissue was homogenised in 1ml TRI-reagent (Sigma Aldrich). The sample was incubated at room temperature for 5 minutes, and 100µl 1-bromo-3-chloropropane was added. The solution was shaken vigorously for 15 seconds, incubated at room temperature for 2 minutes and centrifuged at 12,000g for 15 minutes at 4°C. The mixture separated into 3 layers: a lower red phenol-chloroform phase (protein), interphase (DNA) and the colourless upper aqueous phase (RNA).

3.2.1.1. RNA extraction

The aqueous phase was transferred to a clean eppendorf tube for subsequent RNA extraction. The RNA was precipitated from the aqueous phase by adding 500µl isopropanol and mixed by inversion. The sample was stored at room temperature for 5 min, and then centrifuged at 12,000g for 8 minutes at 4°C. The RNA pellet was washed in 1ml 75% ethanol and subsequently centrifuged at 7,500g for 5 minutes at 4°C. Supernatant was discarded and the pellet was air dried for 30 minutes at room temperature. The pellet was then dissolved in 100µl water. The sample was treated with DNase, 1 unit per µg (Promega). RNA was re-extracted with TRI-reagent (as described above) and sample stored at 4°C.

3.2.1.2.DNA extraction

After the removal of the aqueous phase (for RNA extraction) the remaining two layers of the samples were centrifuged at 12,000g for 15 minutes at 4°C and any remaining aqueous phase was removed. The solution was mixed with 300μl of ethanol and centrifuged at 12,000g for 5 minutes at 4°C to produce a DNA pellet. The supernatant was transferred to a clean tube for subsequent protein extraction. The DNA pellet was washed on the shaker for 1 hour in 0.1M sodium citrate in 10% ethanol. The sample was centrifuged at 12,000g for 5 minutes; supernatant discarded and washes repeated twice. The DNA pellet was then washed for 30 minutes in 1.5ml 75% ethanol and centrifuged at 2,000g for 5 minutes. The pellet was air dried overnight and then dissolved in 400μl nuclease free water. DNA concentration and purity were measured using spectrophotometry (NanoDrop-1000 Spectrophotometer). All samples were diluted to a final concentration of 25ng/μl and stored at 4°C.

3.2.1.3.Protein extraction

The protein was precipitated from the supernatant as collected above by addition of 3 volumes acetone. After 15 minutes incubation at room temperature, the sample was centrifuged at 12,000g for 10 minutes at 4°C. The supernatant was discarded and the pellet was washed three times in 1.2ml of 0.3M guanidine hydrochloride in 95% ethanol and 2.5% glycerol; sample was spun at 8,000g for 5 minutes and supernatant removed. A final wash was performed in 1.2ml ethanol containing 2.5% glycerol; sample was again spun at 8,000g for 5 minutes. The protein pellet was air dried for 1 hour and dissolved in RIPA buffer (0.1M NaCl, 10mM TrisHCl, 1mM EDTA, 400μg/ml PMSF, 2μg/ml aprotinin and 1% SDS). Protein

concentration and purity were measured using spectrophotometry. All samples were diluted to a final 1mg/ml concentration and stored at -70°C.

3.2.2. DNA Extraction using QIAGEN Genomic-tips

The QIAGEN Genomic-tips together with the Genomic DNA Buffer Set (Blood & Cell Culture DNA Maxi Kit, Qiagen) provide a reliable method for the isolation of pure high–molecular-weight genomic DNA directly from tissue samples. The purification procedure is based on the selective binding of genomic DNA to the anion-exchange resin in the genomic tip.

400mg of brain tissue (lateral temporal lobe) was homogenised and transferred to 19ml of Buffer G2 containing RNase A (204U) and RNAse T1 (100U). The sample was vortexed and incubated at 37°C for 30 minutes. Proteinase K (300U) was added to the sample, vortexed and incubated at 50°C for 2 hours.

The Qiagen genomic tip was equilibrated with 10ml of Buffer QBT. The sample was vortexed for 20 seconds and applied to the equilibrated genomic tip. The genomic tip was washed twice with 15ml Buffer QC, and DNA was eluted with 15ml of Buffer QF (50°C). DNA was precipitated with 10.5ml of isopropanol and gently mixed. Strings of DNA were collected with an inoculating loop and transferred to 1ml of 70% ice-cold ethanol. The DNA was spun at 3000g for 20 minutes at 4°C, supernatant discarded, and pellet air dried overnight. The pellet was dissolved in 500µl nuclease free water and incubated at 55°C for 2 hours. DNA

concentration and purity were measured using spectrophotometry. The A_{260}:A_{230} ratio was greater than 1.7 and the A_{260}:A_{280} ratio was greater than 1.8. The DNA samples were stored at 4^oC.

3.3. Brain Homocysteine

The OPTIMA study subjects have regular plasma Hcy measurements collected longitudinally. However the levels of Hcy in the brain are known to be quite different to that of plasma. High performance liquid chromatography (HPLC) with electrochemical detection (ECD) was used to measure levels of free Hcy in the brain samples[61].

3.3.1. Brain Tissue

Occipital lobe samples were used to measure the levels of free Hcy in the brain. 10mg of brain tissue was homogenised in 1ml of RIPA buffer (0.1M NaCl, 10mM TrisHCl, 1mM EDTA, 1% protease inhibitor cocktail). The samples were spun at 13,000g for 5 minutes, and the supernatant collected for analysis.

3.3.2. HPLC with ECD

High pressure liquid chromatography coupled to electrochemical detection (HPLC-ECD) on a boron-doped diamond (BDD) working electrode was used for measurement of Hcy and methionine levels in brain tissue samples. The HPLC-ECD method was optimised from the

Bailey et al protocol taken from Methods in Molecular Biology[60]. The method has a high sensitivity and specificity as determined previously. We have not repeated the quality control experiments for the performance of the assay[60, 61, 196].

The HPLC system consisted of a Coulchem II Multielectrode Detector (ESA Analytical, UK), 5021A Conditioning Cell (ESA Analytical, UK), 5014B Microdialysis Cell (Phenomenex, UK) and a 5040 Analytical Cell containing the BDD electrode (ESA Biosciences, UK). Samples were injected into the HPLC system through a 7726 Rheodyne 6-port injection valve (IDEX Health & Science Group, USA) using a 50μl Rheodyne 2" Syringe (SGC, USA). The mobile phase was pumped through the system using a 580 twin-reciprocating pump (ESA Analytical, UK), passing through a vacuum degasser (Shodex, USA). Data was collected and analysed using the Prime Data Acquisition and Reporter software (HPLC Technology, UK).

The optimal operating potential for detection of Hcy and methionine on the BDD electrode was at 1400mV, initially a 1900mV potential was applied for 30 seconds. The mobile phase was composed of 25mM sodium dihydrogen phosphate (NaH_2PO_4), 1.4mM 1-octane sulfonic acid and 7% acetonitrile. All chemicals used were of HPLC electrochemical grade. How the mobile phase was made was crucial for HPLC-ECD as small changes would influence trace analysis. 3.9g NaH_2PO_4 and 432mg 1-octane sulfonic acid was dissolved in 800ml of polished deionised polished water (18.2MΩ-cm). The pH was adjusted to pH 2.65. The solution was made up to 1L with polished deionised water and mixed. 70ml was removed and discarded before 70ml of acetonitrile was added. The final solution was vacuum filtered through a Nylon-66 Filter (pore size 0.2μm). The flow rate of the mobile phase was set at 0.8ml/min on the pump.

To make the HPLC-ECD composite standard 100µl of 1mM homocysteine (Sigma Aldrich, UK) and 50µl of 1mM methionine (Sigma Aldrich, UK) were mixed and the solution made up to 10ml with polished deionised water. For HPLC-ECD sample preparation, supernatant (see 3.3.1) was thawed, and 25µl added to 225µl of polished deionised water. This was vortexed for 30 seconds and stored on ice for 10 minutes. 250µl of 0.1M perchloric acid was added to the sample, vortexed for another 30 seconds before being transferred to a 3kDa cut-off centrifugal filter unit (Millipore, USA). The samples were centrifuged for 30 minutes at 14,000g at 4°C and the filtrate stored on ice until injection.

3.4. ELISA

3.4.1. ELISA: Quantitative protein expression studies from brain tissue

ELISA (enzyme linked immunosorbant assay) was performed to measure the expression of proteins in the brain. Proteins studied and the primary and secondary antibodies are listed in Table 1.

Protein samples were thawed and diluted to 10µg/ml in 0.1M carbonate buffer (pH 9.6). Each sample was represented in triplicates; 100µl of diluted protein was added per well and incubated overnight at 4°C. Following the removal of the coating solution (using an Elx405 96-well plate washer, BioTek) 200µl blocking solution (PBS containing 1%BSA) was added to each well and plates were incubated at room temperature for 2 hours. Blocking solution was removed by aspiration and 100µl of the primary antibody was added to each well and incubated overnight at 4°C. Following the washes with PBST (PBS/0.1% tween20), the plates were incubated for 2 hours at room temperature with 100µl of biotinylated secondary antibody. This was followed by rigorous washing and incubation in 100µl of Streptavidin-HRP (1:200, R&D Systems). Immunoreactivity was visualized with o-phenylenediamine dihydrochloride (Sigma Aldrich), a peroxidase substrate. The reaction was stopped by adding 25µl of 4M H_2SO_4. Absorbance was read at 490nm with a plate reader (Opsys MR^{TM} microplate reader, Dynex).

For each ELISA assay we used a calibration curve that allowed the quantification of protein in our samples. For the cell cycle related proteins the standard curve was prepared from a rapidly

dividing cell line (Flp-In™ T-Rex™ 293 cells; Invitrogen). The cells were cultured for several days (to attain rapid growth without reaching confluence). Protein was extracted from the cells using Cytobuster (Novagen) containing 1% Protease Inhibitor Cocktail (Sigma Aldrich). The protein standard was spun at 15,000g for 10 minutes. Supernatant was transferred to clean a tube and used to carry out 2-fold serial dilutions in Cytobuster containing 1% Protease Inhibitor Cocktail.

For β-amyloid, AT8, DCII, 4-hydroxynonenal and 8-hydroxyguanosine labelling the standard sample for the calibration curve was derived from the brain tissue of a patient with Alzheimer's disease. For NeuN labelling the standard was derived from a brain tissue sample from a healthy elderly individual.

Data was expressed as arbitrary units obtained from the optical density measurements and the calibration curve which was generated from serial dilutions of the standard protein sample. Constructing a calibration curve on each ELISA plate allowed each measurement to be given an arbitrary value relative to the calibration curve (see Figure 4).

Table 1

List of proteins studied and the concentration of primary/secondary antibodies used for

ELISAs.

Protein Measured	Primary Antibody Concentration	Secondary Antibody Concentration
Mouse monoclonal amyloid-β	1:5000, Dako	Biotinylated polyclonal rabbit anti-mouse immunoglobulin (1:2000, Dako)
Mouse monoclonal PHF-Tau, AT8	1:1000, Innogenetics	Biotinylated polyclonal rabbit anti-mouse immunoglobulin (1:2000, Dako)
Mouse monoclonal Alzheimer's disease tau, DCII	1:500, Sigma Aldrich	Biotinylated polyclonal rabbit anti-mouse immunoglobulin (1:2000, Dako)
Goat polyclonal 8-hydroxyguanosine	1:2000, AbD Serotec	Biotinylated polyclonal rabbit anti-goat immunoglobulins (1:2000, Dako)
Goat polyclonal 4-hydroxynonenal	1:4000, Abcam	Biotinylated polyclonal rabbit anti-goat immunoglobulins (1:2000, Dako)
Mouse monoclonal neuronal nuclei, NeuN	1:1000, Chemicon	Biotinylated polyclonal rabbit anti-mouse immunoglobulin (1:2000, Dako)

Original Calibration Curve

$y = 2.9877x - 0.2855$
$R^2 = 0.9917$
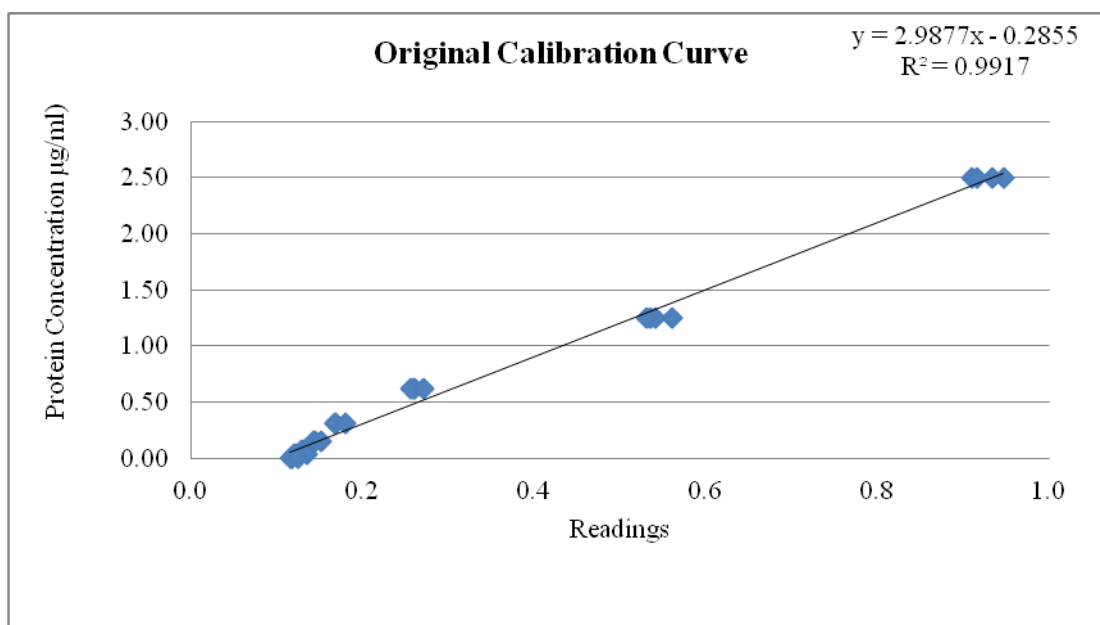
Figure 4

ELISA Calibration Curve. (x-axis - optical density measurements, y-axis - standard protein sample concentration, µg/ml)

3.5. DNA Methylation

3.5.1. % Global of DNA Methylation

Global DNA Methylation from DNA extracted from the lateral temporal lobe was measured by HPLC by our collaborators in Leicester University. See Sandhu J et al, 2009 for the method used[61].

3.5.2. Methylation Status of CDKIs

Custom-made Methyl-Profiler DNA Methylation PCR Arrays were purchased from SABiosciences. The Arrays allow simultaneous profiling of DNA methylation of five CDKI gene promoter regions (p16^{INK4a}, p15^{INK4b}, p27^{kip1}, p21^{cip1} and p57^{kip2}).

Using the Methyl-Profiler™ Arrays and PCR primers together with the DNA Methylation Enzyme Kit we can analyse the methylation status of CpG islands in the promoter region of CDKI genes. Four digests (M_o, M_s, M_d, M_{sd} - see Figure 5) were set up to detect different methylated DNA fractions using real-time PCR. The product of a mock digest (M_o) contained all of the input genomic DNA. The product of the methylation-sensitive (M_s) restriction enzyme (Enzyme A) digest contained hypermethylated DNA sequences, while the product of the methylation-dependent (M_d) restriction enzyme (Enzyme B) digest contained unmethylated DNA sequences. And finally the product of a double digest (M_{sd}) measured the background and the success of both enzymatic digestions.
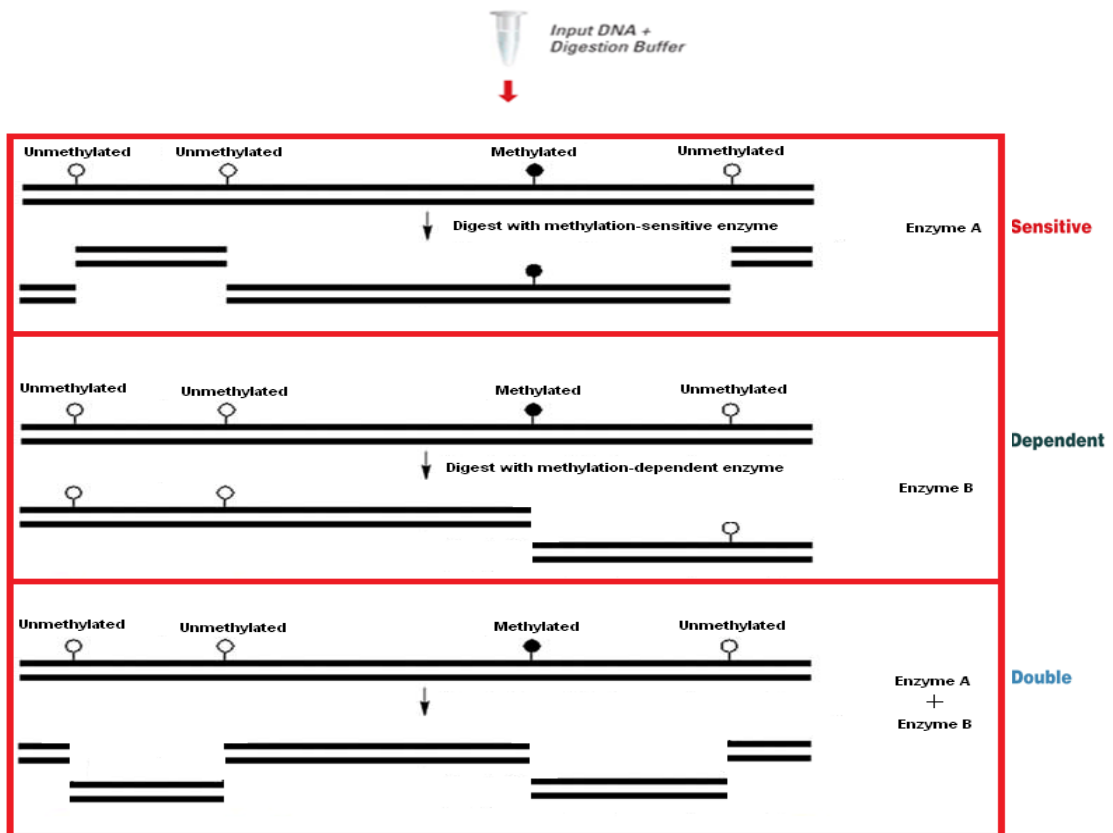
Figure 5

Using DNA Methylation Enzymes (i.e. Enzyme A and Enzyme B) can set up four reactions to detect different methylated DNA fractions using real-time PCR.

Using the two digestion enzymes (i.e. Enzyme A and Enzyme B), four digests are performed to detect different DNA methylation fractions. We prepared the four restriction digest as following (see Table 2).

Table 2

Setting up four restriction digests using Enzyme A and Enzyme B.

	Mo	Ms	Md	Msd
Nuclease-free H$_2$O	8.62	7.42	7.42	6.22
5X Digestion Buffer	3.6	3.6	3.6	3.6
enzyme A	0	1.2	0	1.2
enzyme B	0	0	1.2	1.2
BSA	0.18	0.18	0.18	0.18
Genomic DNA 25ng/µl (1µg)	**5.6**	**5.6**	**5.6**	**5.6**
Total	**18**	**18**	**18**	**18**

The digests were incubated overnight at 37°C in a thermal cycler. Enzymes were inactivated at 65°C for 20 minutes following digestion.

The RT² SYBR® Green/ROX® qPCR master mix contained all of the optimized reagents and buffers needed for SYBR® Green based real-time PCR. The master mix includes buffer, HotStart DNA Taq polymerase, nucleotides and ROX® (used as a reference dye to normalise the qPCR instruments, Stratagene Mx3000p). For each of the four DNA digests an individual

PCR cocktail was prepared and carefully added to the PCR array (see Table 3) and then placed in the Stratagene Mx3000p (see Table 4 for program setting).

Table 3

A. Setting up SYBR® Green based real-time PCR cocktails.

	M_o	M_s	M_d	M_{sd}
H$_2$O	75µl	75µl	75µl	75µl
PCR Master Mix	82.5µl	82.5µl	82.5µl	82.5µl
M_o Digest	7.5µl	-	-	-
M_s Digest	-	7.5µl	-	-
M_d Digest	-	-	7.5µl	-
M_{sd} Digest	-	-	-	7.5µl
Total	165µl	165µl	165µl	165µl

B. Samples were mixed and 25µl was carefully added to the PCR array:

Sample 1

Sample 2

Sample 3

Sample 4
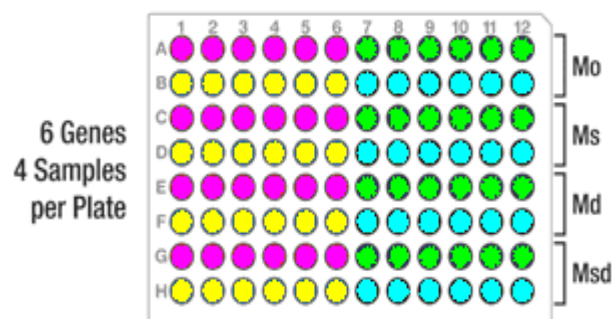
Table 4

The qPCR reaction was run in a two-step program on the Stratagene Mx3000p.

Cycles	Temperature	Duration
1	95°C	10 mins
40	97°C	15 secs
	72°C	1 min

3.5.2.1. Obtaining Cycle Threshold Values (C_t)

In real-time PCR a positive reaction is detected by accumulation of a fluorescent signal, the SYBR green dye binds to double stranded DNA and fluoresces. As more double stranded DNA amplicons are produced during the PCR reaction the intensity of the fluorescent emissions will increase. The cycle threshold (C_t) is defined as the number of cycles required for the fluorescent signal to cross the threshold (i.e. exceeds background level). C_t levels are inversely proportional to the amount of target nucleic acid in the sample (i.e. the lower the C_t level the greater the amount of target nucleic acid in the sample).

After the cycling program was completed for the Methyl-Profiler PCR arrays, the C_t values were obtained. The baseline and threshold values were manually set. To define the baseline, the linear view of the amplification plots was used and only readings from cycle number 2 through to the cycle just before the earliest visible amplification were selected. To define the threshold values, the log view of the amplification plots was used, and threshold values above

the background signal but within the lower third of the linear portion of the amplification curves were selected (see Figure 6).

Finally, all Ct values were transferred to an Excel analysis template file supplied by SABiosciences. The template automatically performs the calculations from the raw Ct values to determine the gene promoter methylation status. The template normalises the digest Ct values to the mock digest Ct values and finally the percentage of the DNA that is hypermethylated is calculated.

Figure 6

qPCR amplication plots. A. Linear View. B. Logarithmic View.

A
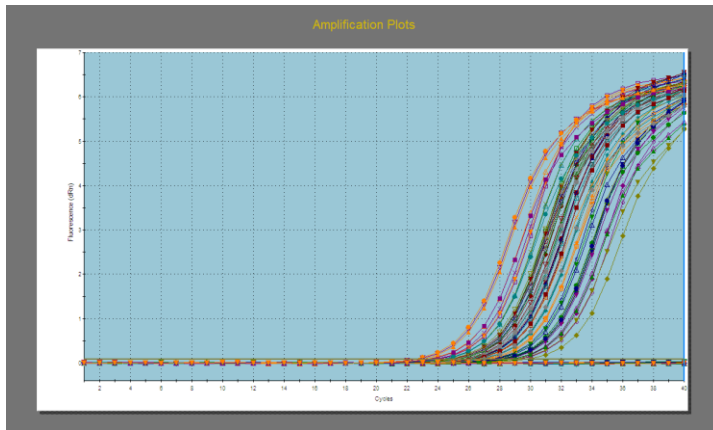
B
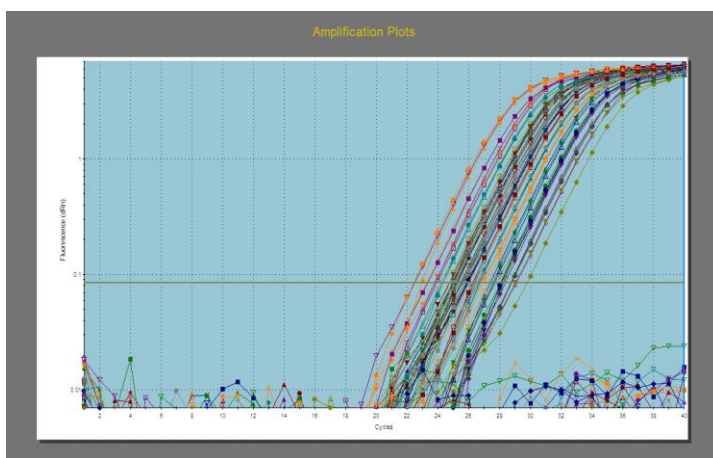
3.6. Cell Culture → 96-well format

3.6.1. SH-SY5Y Neuroblastoma Stock

SH-SY5Y human neuroblastoma cells were purchased from ECACC and grown in DMEM/F-12 1:1 supplemented with 10% FCS, 100U penicillin-streptomycin and 2mM L-glutamine, at 37°C in 5% CO_2, humidified atmosphere. Passage number did not exceed 20 and cells did not reach senescence. Cells were frozen (-80°C) in foetal calf serum containing 10% DMSO at a density of 5 million cells/ml.

3.6.2. Setting Up Cultures From Frozen Cells

Cells were washed in DMEM/F-12 1:1 (w/o glutamine) and suspended in culture medium (DMEM/F-12 1:1 supplemented with 10% FCS (PAA), 100U/ml penicillin-streptomycin (Invitrogen) and 2mM L-glutamine (Sigma Aldrich)) to achieve a cell density of 500,000 cells/ml. Cells were plated into 25cm^2 flasks, and allowed to settle for 48 hours at 37°C in 5% CO_2, humidified atmosphere. After the cells had settled, the culture medium was replaced with the same culture medium supplemented with 10μM retinoic acid (Tocris). The cells were allowed to differentiate for 5 days, with new culture medium containing 10μM retinoic acid replaced each day. At day six, the culture medium was removed and replaced with 2ml of 1mM EDTA in PBS. This was left on the cells for 10 minutes. Flasks were gently tapped to dislodge the cells, and the supernatant was transferred to DMEM/F-12 1:1 (w/o glutamine). Cells were washed and then suspended in culture medium supplemented in retinoic acid to achieve a cell density of 100,000 cells/ml. Cells were plated in 96-well flat bottom tissue

culture treated plates (Becton Dickinson) and 100µl cell suspension was dispensed into each well (10,000 cells/well). Cells were allowed to settle for 24 hours at 37°C in a humidified incubator containing 95% air and 5% CO_2.

3.6.3. Treatment Schedules

On day 7 one batch of differentiated cells were collected and used as a control for propidium iodide, immunocytochemistry and LDH assay, see Table 5:

Table 5

Cell culture 8-day treatment schedule.

	Treatment	**Collection**
Day 0	Set up in Flask	-
Day 1	Grow	-
Day 2	10µM Retinoic Acid treatment	-
Day 3	10µM Retinoic Acid treatment	-
Day 4	10µM Retinoic Acid treatment	-
Day 5	10µM Retinoic Acid treatment	-
Day 6	Set up in 96-well plates - 10µM Retinoic Acid treatment	-
Day 7	Drug + ApoE Isoforms treatment	Control - 0hr collection
Day 8	-	24hr collection Treated Plates

The rest of the cells were treated with either D-L-homocysteine (10, 20, 40, 80, 160 µM) or L-Cysteine (5, 10, 20, 40, 80 µM) (Sigma Aldrich) in the presence of 5µg/ml human recombinant ApoE isoforms (2, 3, or 4) (BioVision). Drugs were diluted in culture medium supplemented with retinoic acid. 100µl of homocysteine solution was added per well, (see Table 6 for plate layout). Cells were left overnight at 37°C in a humidified incubator containing 95% air and 5% CO_2.

Table 6

96 Plate Layout

	1	2	3	4	5	6	7	8	9	10	11	12
A												
B												
C												
D	CONTROL (NO HCY, NO APOE)	Dose 1	Dose 2	Dose 3	Dose 4	Dose 5	CONTROL (NO HCY, NO APOE)	Dose 1	Dose 2	Dose 3	Dose 4	Dose 5
E												
F												
G												
H												

Note - Identical cultures were also set up in 25cm^2 flasks to obtain large enough cell numbers to allow RNA and DNA extraction for subsequent gene expression and methylation analysis.

3.6.4. Collection Of Cells

Identical sets of culture plates were collected for different assays. From plates collected for immunocytochemistry the supernatant was gently aspirated and cells were fixed (in-situ) with 100μl of Glyo-Fixx (Shandon-Thermo Scientific) for 2 hours followed by incubation with 100μl of 85% ice-cold ethanol. (Note - The plates collected for cytometry were fixed with 85% ice-cold ethanol only).

From the plates collected for LDH (cell proliferation and survival assay) 50μl of supernatant was removed from each well and transferred to a clean 96-well plate (for the measurement of dead cells) and stored at -20°C until LDH Assay was performed.

In the 25cm^2 flasks at day 8, the culture medium was removed and replaced with 2ml of 1mM EDTA in PBS. This was left on the cells for 10 minutes. Flasks were gently tapped to dislodge the cells, and the supernatant was transferred to DMEM/F-12 1:1 (w/o glutamine). Cells were washed, supernatant removed, and pellet frozen at -80°C. RNA, DNA and Protein Extraction were performed as described on page 16.

3.6.5. Immunocytochemistry

3.6.5.1.Phospho-Tau (AT8) and Beta-Amyloid

Ethanol was aspirated from the wells. 100µl of Blocking Solution (PBS, 0.1% triton X-100 and 5% BSA) was added to each well. Plates were incubated at room temperature for 30 minutes. Blocking solution was aspirated and 50µl of primary antibody was added; either mouse monoclonal amyloid-β (1:100, Dako) or mouse monoclonal PHF-Tau, AT8 (1:200, Innogenetics).

For the negative controls, PBS with 0.1% triton X-100 was applied instead of the primary antibody. From this step onwards, the control plates were treated exactly as the treated cultures. Plates were incubated overnight at 4°C.

Cells were washed twice with 200µl of PBS with 0.1% triton X-100. Primary antibodies were detected by incubating overnight at 4°C with 100µl of anti-mouse IgG - FITC (1:200, Abcam). Cells were washed twice with 200µl of PBS with 0.1% triton X-100, and 100µl of propidium iodide staining solution (100µg/ml RNase A, 10µg/ml Propidium iodide 0.1% Triton-X-100) was added to each well (see Table 7 for plate set up). Plates were incubated at 37 °C for 20 minutes and protected from the light.

Table 7

96 well plate set up for immunocytochemistry:

	1	2	3	4	5	6	7	8	9	10	11	12
A												
B												
C												
D		Zero day control, labelled with Beta Amyloid <u>or</u> AT8, and stain with PI						Negative control for immuno-cytochemistry				
E												
F												
G												
H												

3.6.5.2. Measurement and Acumen Explorer® Analysis

The Acumen Explorer® Microplate Cytometer (TTP LabTech Ltd) was used to scan the 96-well cell cultures in situ. Propidium iodide was used to measure DNA content and to establish the cell cycle phase of individual cells. Furthermore, using antibodies to label tau and beta amyloid we could carry out secondary analysis to measure changes in protein expression and the expression of protein in different cell cycle phases. We used green-fluorescent for protein- and red-fluorescent for cell cycle analysis. Cytometry data was transferred to our standard mathematical model, which allowed calculation of the length of the different phases of the cell cycle and protein content.

3.6.6. **Cyto Tox 96® Non-Radioactive Cytotoxicity Assay**

The number of dead cell in the cultures was determined using a commercially available kit (CytoTox 96 non-radioactive Cytotoxicity Assay, Promega) that quantitatively measures lactate dehydrogenase (LDH) release upon cell lysis. The method relies on the conversion of a tetrazolium salt by LDH into a red formazan product. SY-SH5Y cells diluted in culture medium where used to generate a calibration curve.

Cell culture supernatant samples (see 3.6.4) were thawed and kept at 4^oC before use. 50μl of ice-cold reconstituted substrate buffer was added to each well. Plates were incubated at room temperature and protected from light. Reaction was stopped with 50μl of stop solution and absorbance read at 490nm. Cell numbers are directly proportional to the absorbance values which represent LDH activity. The number of cells that have died in the cultures were derived from the standard curve containing set cell numbers of the same type. The Hcy-induced change in cell death was calculated as the ratio of dead cells in Hcy treated cultures and controls and expressed as a percentage.

3.7. Statistics

Statistical analysis was carried out using the MedCalc® software package. Kruskall Wallis analysis was used if data was not normally distribution. Two factor analysis of variance (ANOVA) and multi-factor analysis of variance (MANOVA) was used to analyse the interactions between Hcy levels and ApoE genotype. Multiple regression analysis was used to analyse Hcy levels as a continuous variable. Furthermore, to analyse variables independent of disease severity z-scores were generated for each variable. This gave a measure of the standard deviation from the group mean. In some instances we have dichotomised continuous variables into binary categories (such as 'smaller than' or 'greater than' the observed group mean). The binary transformation allows for the use of logistic regression to test for the possible predictors of an outcome[194]. If the p-values were < 0.05 then this was regarded as statistically significant. Note - due to the relatively low patient number no age and sex correction were possible.

4. RESULTS

4.1. The Effect of Homocysteine and ApoE on the Development of AD (HYPOTHESIS 1 and HYPOTHESIS 2)

We analyzed the effect of the ApoE genotype and plasma as well as brain Hcy levels on markers of disease severity and evolution in a cohort of Alzheimer's disease patients and controls. The number of samples analysed was not based on power calculations, but was determined by tissue availability.

4.1.1. The Effect of Homocysteine on Disease Severity

We defined disease severity based on Braak Staging[62]. Using one-way analysis of variance (ANOVA) we found that the levels of plasma Hcy (as measured at most three years before death) was not different in the different patient groups (Figure 7). Additionally the frequency of elevated plasma Hcy levels (above the accepted normal 15 μM) was not different in these groups (see Figure 8 and Table 8 for Chi-square test). However, we found that patients suffered from additional vascular pathology, elevated plasma Hcy levels were associated with more severe Alzheimer-type pathology (Figure 9).
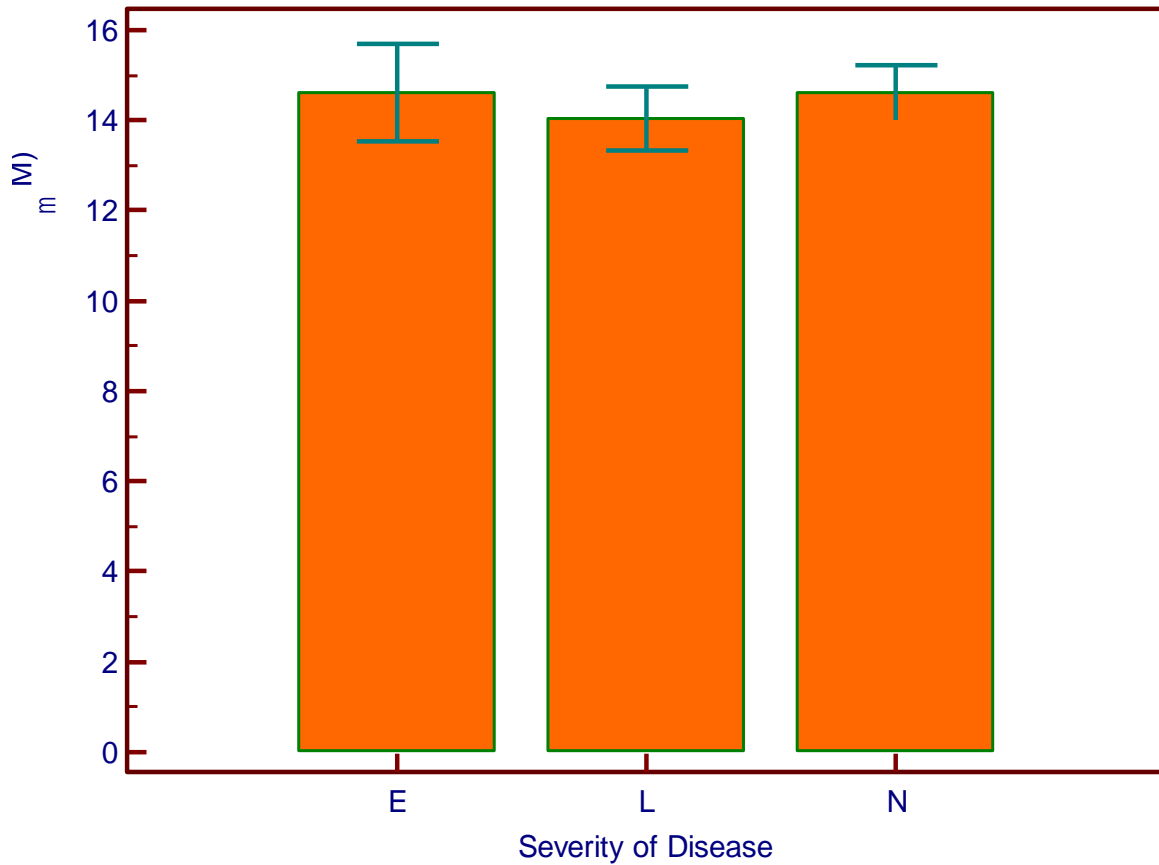
Figure 7

A one-way analysis of variance (ANOVA) was conducted with the levels of plasma Hcy as the dependent variable and the severity of disease as the independent variable. Plasma Hcy levels (absolute values, μM) on y-axis and disease severity (E = entorhinal, L = limbic, and N = neocortical) on x-axis. Error bars represent standard error of the mean. Top of bars represent mean. (p = 0.850, df = 2).
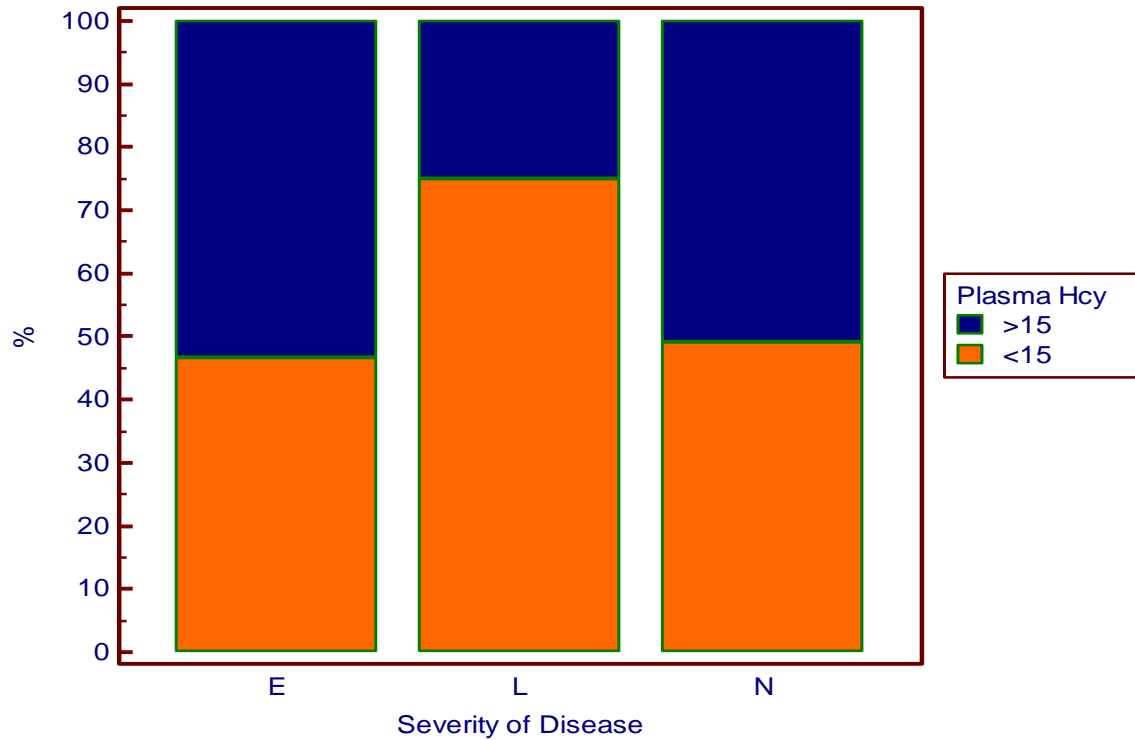
Figure 8

Effect of disease severity on the distribution of patients with different plasma Hcy levels. A Chi-square test was conducted with the severity of disease as the dependent variable and the plasma Hcy levels as the independent variable. Plasma Hcy levels (<15 and >15µM - absolute values) and disease severity (E = entorhinal, L = limbic, and N = neocortical). (p = 0.1128, df = 2).

Table 8

Frequency of elevated plasma Hcy in individuals in different stages of AD. Disease severity - pre-clinical (entorhinal), mild (limbic) and severe (neocortical).

	Severity of Disease			Relative Frequency
	Pre-clinical AD	**Mild AD**	**Severe AD**	
<15µM	7 - (8.3%)	15 - (17.9%)	24 - (28.6%)	54.8%
>15µM	8 - (9.5%)	5 - (5.9%)	25 - (29.8%)	45.2%
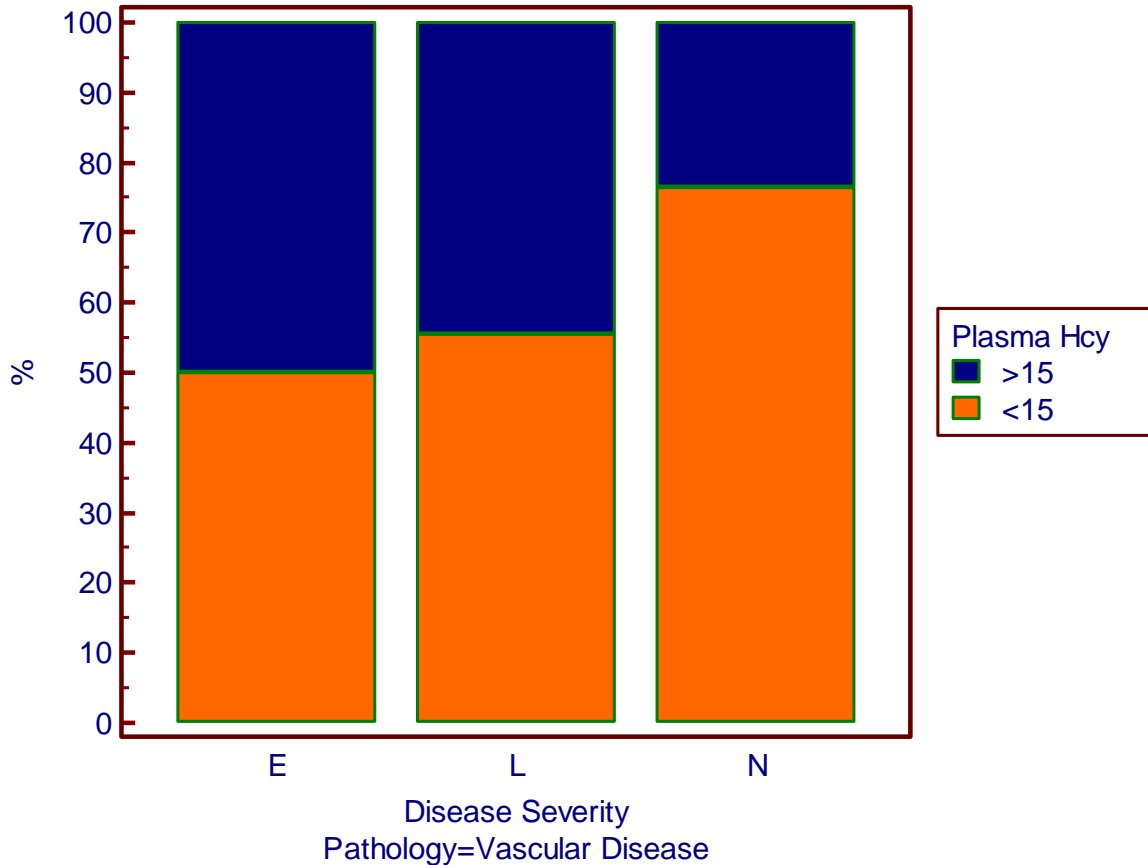
Figure 9

Effect of disease severity on the distribution of plasma Hcy levels in patients with additional vascular disease. A Chi-square test was conducted with the severity of disease as the dependent variable and the plasma Hcy levels as the independent variable. Plasma Hcy levels (<15 and >15μM - absolute values) and disease severity (E = entorhinal, L = limbic, and N = neocortical). (p = 0.1779, df = 2).

We have also found that disease free survival (age of onset in demented patients and age at death in the non-demented elderly) was significantly higher in patients with elevated plasma Hcy levels (p=0.04), see Figure 10.

Using the age of onset and the age of death we calculated the duration of the disease in demented patients. Z-scores were calculated for each patient group (to avoid the effect of disease severity on disease duration). We found that the patients with elevated levels of plasma Hcy had a significantly shorter disease duration (p=0.024) than patients with normal plasma Hcy level, see Figure 11.
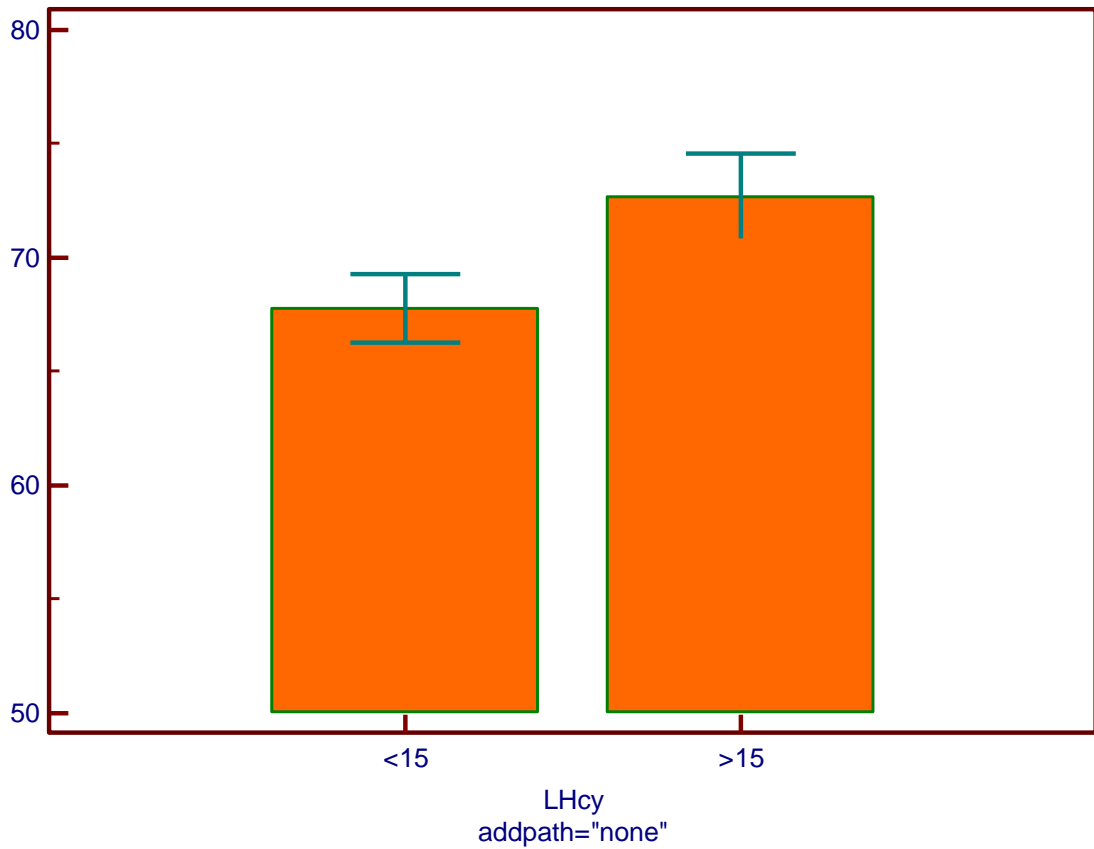
Figure 10

The effect of plasma Hcy on disease free survival. An ANOVA was conducted with the disease free survival as the dependent variable and the levels of plasma Hcy as the independent variable. Age of disease free survival (on y-axis) and plasma Hcy levels dichotomised to smaller than or greater than 15µM (on x-axis). ($p = 0.04$, df = 1). Error bars represent standard error of the mean. Top of bars represent mean.
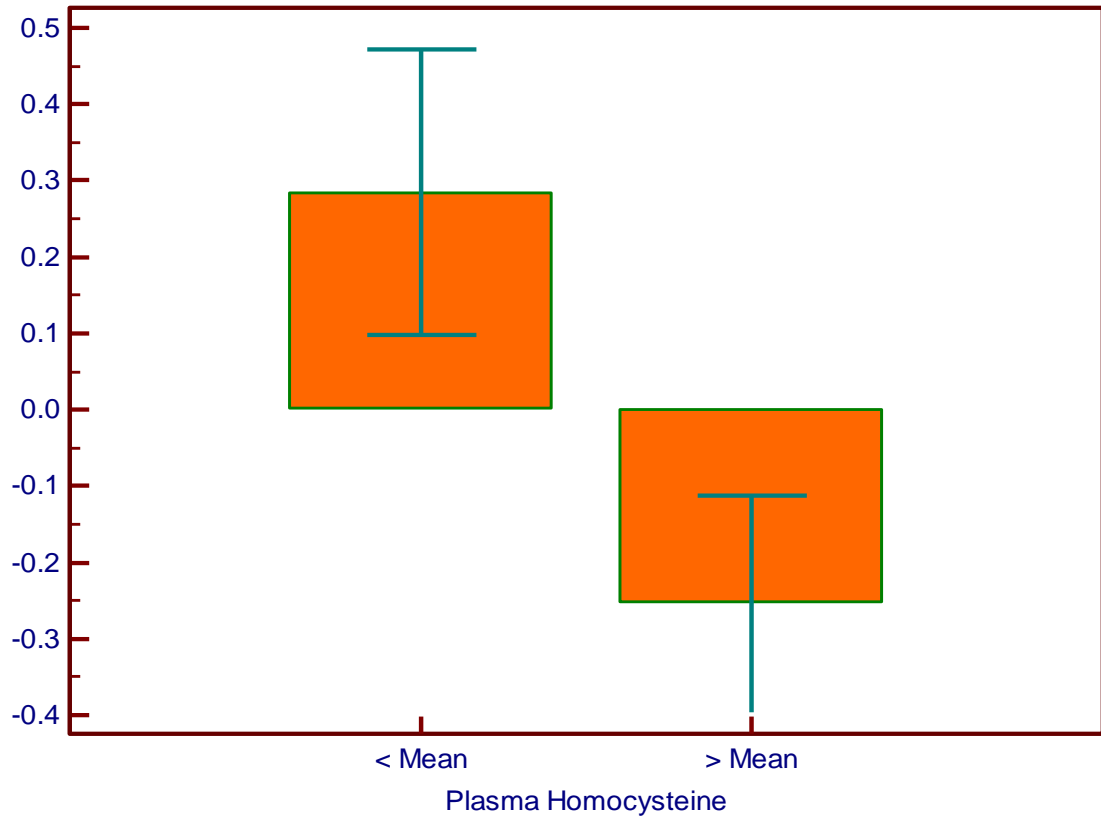
Figure 11

The effect of plasma Hcy on disease duration. An ANOVA was conducted with the disease duration as the dependent variable and the levels of plasma Hcy as the independent variable. z-score values for disease duration (on y-axis) and plasma Hcy levels dichotomised to smaller than or greater than the mean of the group (on x-axis). ($p = 0.024$, df = 1). Error bars represent standard error of the mean. Top of bars represent mean.

Similar analysis was performed to study the effects of brain Hcy measurements. We found a weak trend showing that the levels of brain Hcy decreased with increasing severity of AD (Figure 12 and Table 9). No association was found between brain Hcy levels and age of onset or disease duration (data not shown).

Table 9

Frequency of elevated brain Hcy in different stages of AD. Disease severity - pre-clinical (entorhinal), mild (limbic) and severe (neocortical).

	Severity of Disease			Relative Frequency
	Pre-clinical AD	**Mild AD**	**Severe AD**	
Brain Hcy < mean	7 - 13.5%	5 - 9.62%	22 - 42.3%	65.4%
Brain Hcy > mean	6 - 11.5%	4 - 7.69%	8 - 15.3%	34.6%
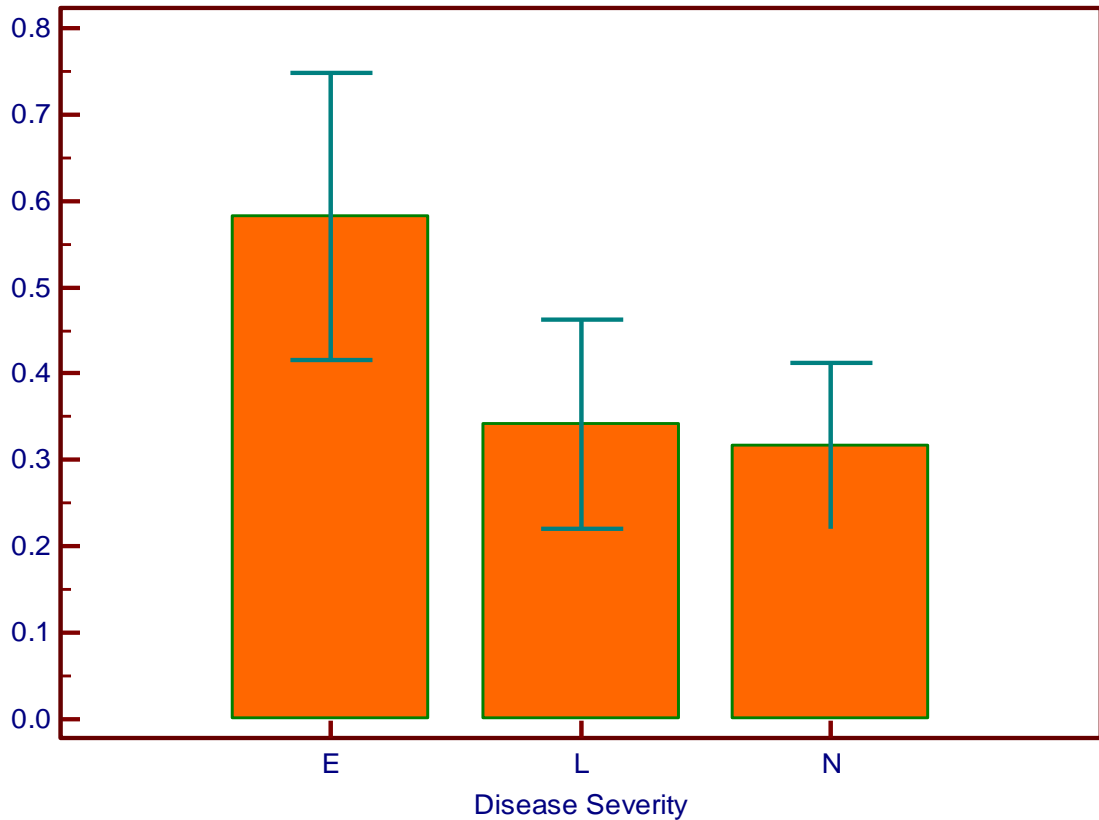
Figure 12

Analysis of brain Hcy levels and disease severity. A Kruskal-Wallis test was conducted with the levels of Brain Hcy as the dependent variable and the disease severity as the independent variable. Brain Hcy levels (absolute values normalized to protein concentration, µM/g of protein) on y-axis and disease severity (E = entorhinal, L = limbic, and N = neocortical) on x-axis. (p = 0.1316, df = 2). Error bars represent standard error of the mean. Top of bars represent mean.

To analyse the relationship between ApoE genotype and disease severity we dichotomised the ApoE genotypes into two groups: ApoE ε4 non-carriers (allele = 0) and carriers (either one or two ε4 alleles = 1). We found significantly higher percentage of ApoEε4 carriers among neocortical stage patients (see Figure 13 and Table 10).

Using z-score values for age of onset and disease duration, we found that the age of disease onset was earlier and the duration of disease much longer in ApoE4 carriers compared to non-carriers, although these associations were not statistically significant (see Figure 14 and Figure 15).

Table 10

Frequency of ApoE4 genotype in different stages of AD. Disease severity - pre-clinical (entorhinal), mild (limbic) and severe (neocortical). (chi-squared = $p < 0.0001$).

	Severity of Disease			Relative Frequency
	Pre-clinical AD	**Mild AD**	**Severe AD**	
ApoE ε4 non-carriers	14 - (15.7%)	14 - (15.7%)	15 - (16.9%)	48.3%
ApoE ε4 carriers	2 - (2.2%)	7 - (7.9%)	37 - (41.6%)	51.7%
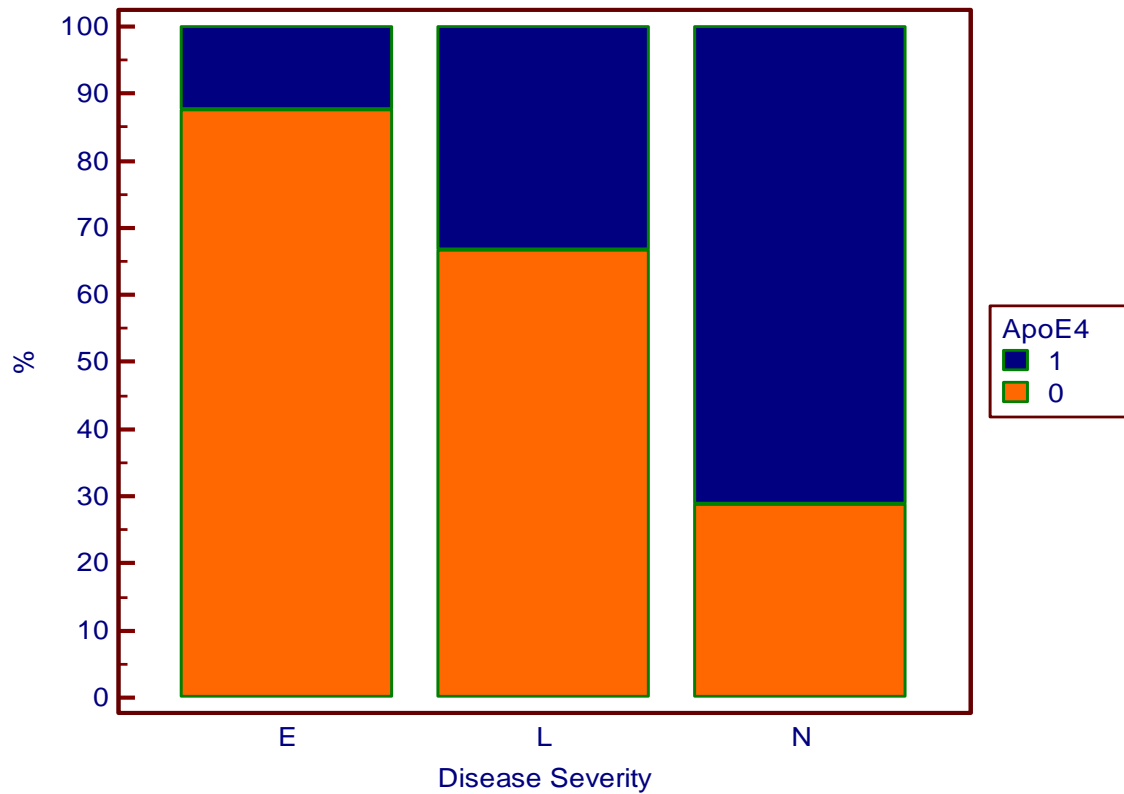
Figure 13

Analysis of ApoE4 genotype and disease severity. A Chi-square test was conducted with the severity of disease as the dependent variable and the ApoE4 genotype as the independent variable. ApoEε4 non-carriers (no ApoEε4 allele = 0) and ApoEε4 carriers (either one or two alleles = 1). Disease severity (E = entorhinal, L = limbic, and N = neocortical) on x-axis. (p < 0.0001, df = 2).
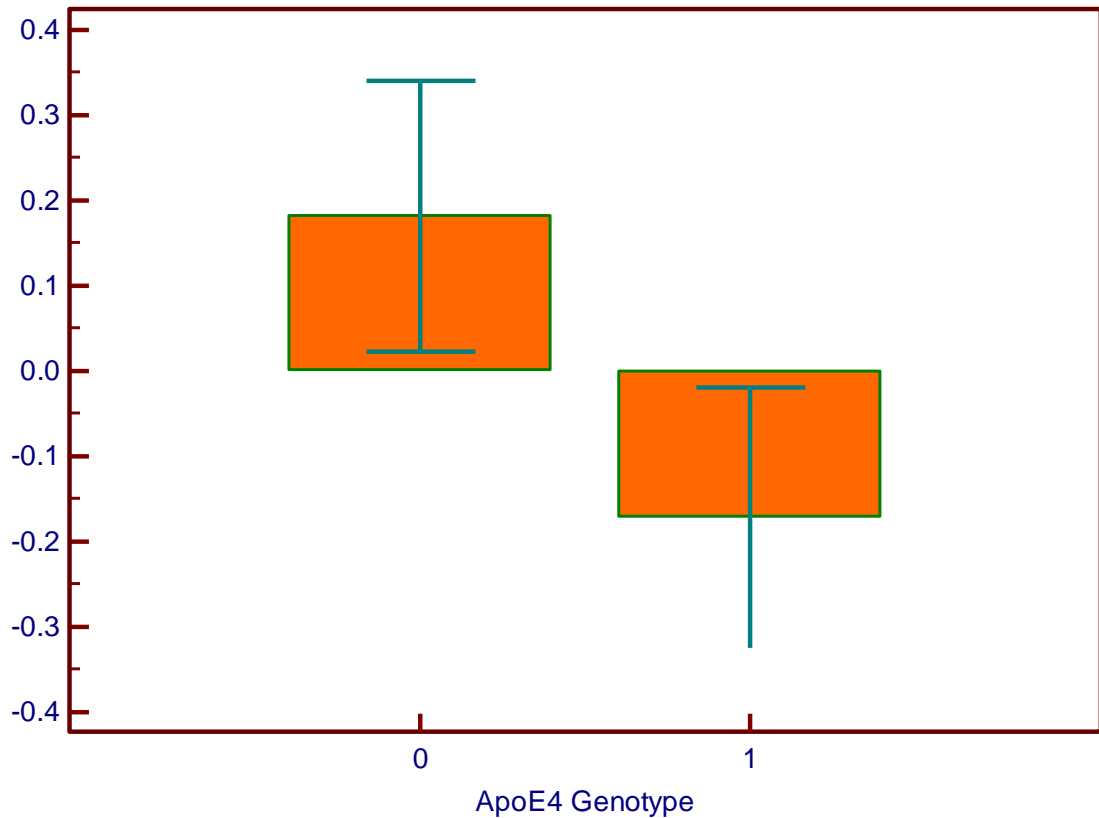
Figure 14

Analysis of ApoE4 genotype and age of onset. A Kruskal-Wallis test was conducted with the age of last normal as the dependent variable and the ApoE4 genotype as the independent variable. ApoEε4 non-carriers (no ApoEε4 allele = 0) and ApoEε4 carriers (either one or two alleles = 1) on x-axis. Age of onset (dichotomised to smaller than or greater than the mean of the group) on y-axis. (p = 0.1397, df = 1). Error bars represent standard error of the mean. Top of bars represent mean.
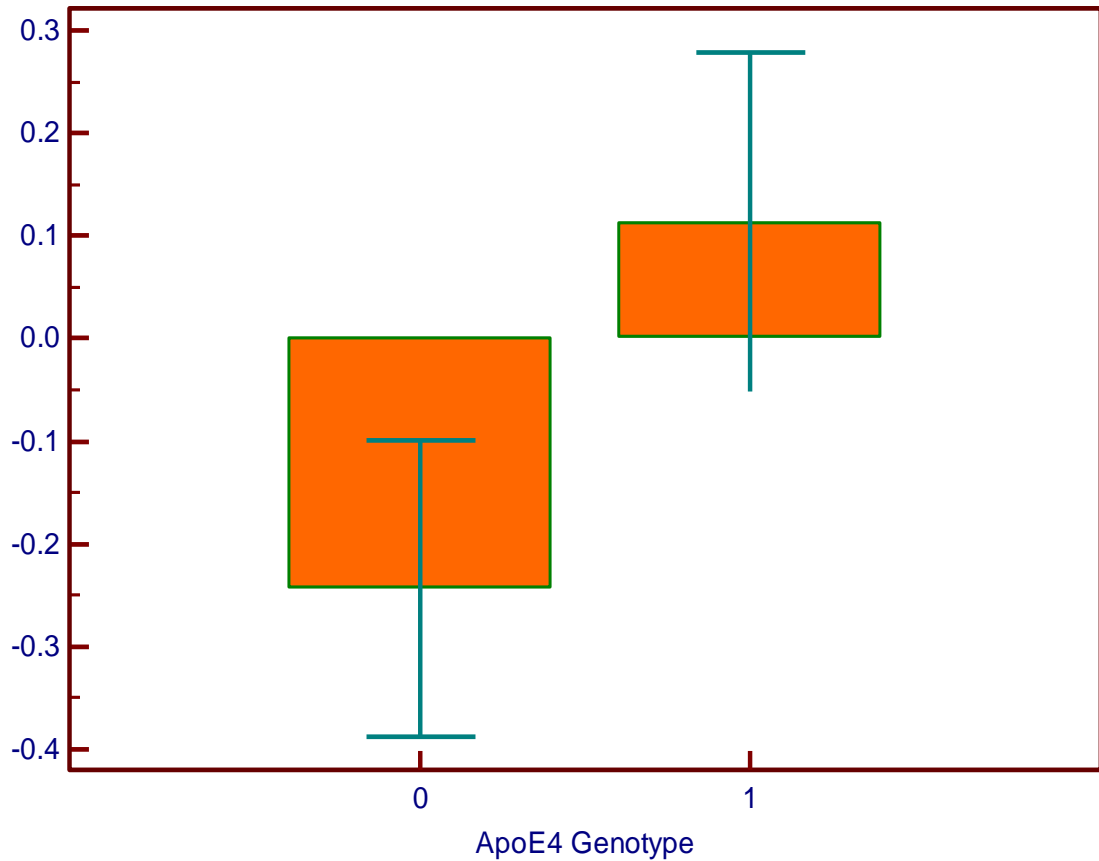
Figure 15

Analysis of ApoE4 genotype and disease duration. A Kruskal-Wallis test was conducted with the disease duration as the dependent variable and the ApoE4 genotype as the independent variable. ApoEε4 non-carriers (no ApoEε4 allele = 0) and ApoEε4 carriers (either one or two alleles = 1) on x-axis. Disease duration (dichotomised to smaller than or greater than the mean of the group) on y-axis. ($p = 0.1830$, df = 1). Error bars represent standard error of the mean. Top of bars represent mean.

We carried out two way analysis of variance to assess whether the effect of plasma Hcy on disease duration (see Figure 10) was dependent on the ApoE genotype. The analysis indicates that the effect of Hcy, in terms of accelerating the disease process is mainly present in patients with the ApoE4 allele but not in patients who do not carry the ApoE4 (see Figure 16).
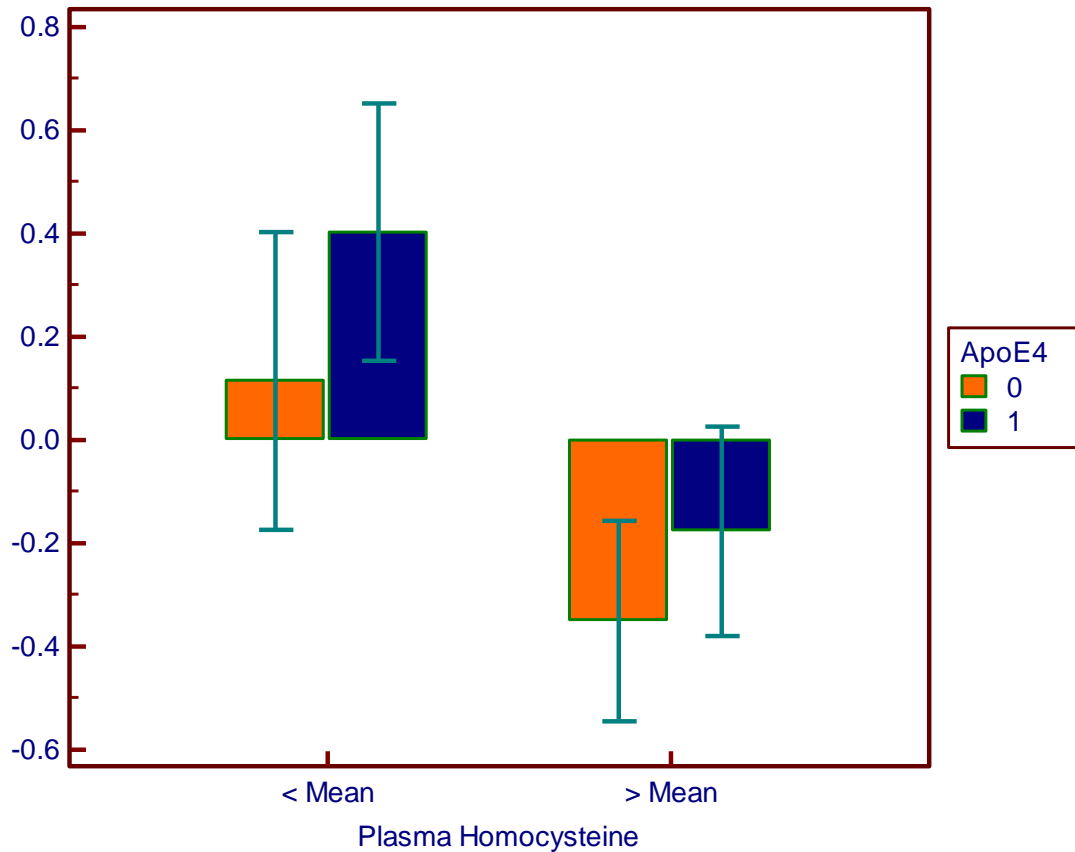
Figure 16

The combined effect of plasma Hcy and ApoEε4 genotype on disease duration. An ANOVA was conducted with the disease duration as the dependent variable and the levels of Hcy and the ApoE4 genotype as the independent variables. z-score values for disease duration on y-axis and plasma Hcy levels (dichotomised to smaller than or greater than the mean of the group) on x-axis. ApoEε4 non-carriers (no ApoEε4 allele = 0) and ApoEε4 carriers (either one or two alleles = 1). Error bars represent standard error of the mean. Top of bars represent mean.

4.1.2. The Effect of Homocysteine on Cognitive Function

We have relied on CAMCOG scores taken from the last cognitive assessment before death (not more than 6 months prior to death) to analyse cognitive function. Plasma Hcy levels had no effect on the final cognitive status of the patients (data not shown). Brain Hcy levels did not influence the CAMCOG score either (data not shown).

As the percentage of ApoE4 carriers is significantly higher in neocortical stage patients than entorhinal or limbic stage patients, (Figure 13) the analysis of ApoE ε4 effect on cognitive function was carried out using CAMCOG scores normalised to disease severity. The ApoE genotype did not influence the CAMCOG score or loss of CAMCOG score per disease month (data not shown). Finally, two-way analysis of variance was used to analyse the combined effect of Hcy and ApoE4 genotype on cognitive function. Including the ApoE genotype in the analysis did not alter the lack of effect Hcy has on cognitive function (see Figure 17).
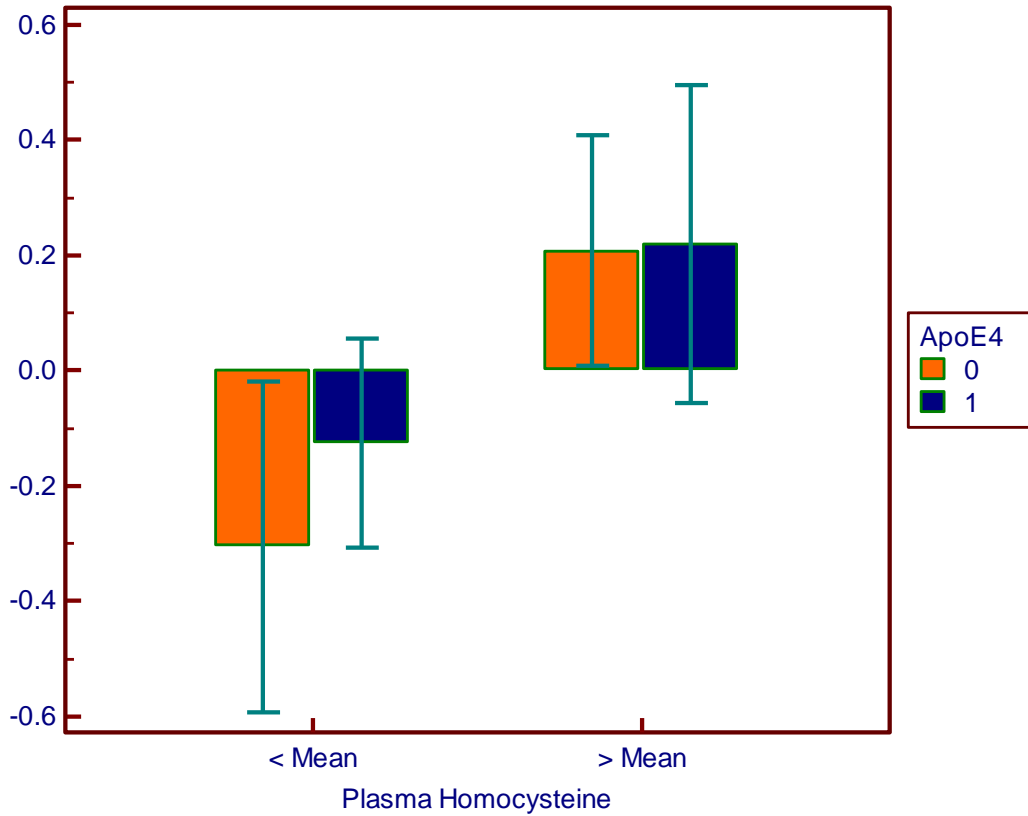
Figure 17

The combined effect of plasma Hcy and ApoEε4 genotype on CAMCOG score. An ANOVA was conducted with CAMCOG scores as the dependent variable and the levels of Hcy and the ApoE4 genotype as the independent variables. z-score values for CAMCOG score on y-axis and plasma Hcy levels (dichotomised to smaller than or greater than the mean of the group) on x-axis. ApoEε4 non-carriers (no ApoEε4 allele = 0) and ApoEε4 carriers (either one or two alleles = 1). Error bars represent standard error of the mean. Top of bars represent mean.

4.1.3. The Effect of Homocysteine on Pathology

We analysed the effect of Hcy on the accumulation of AD-type pathology and oxidative stress. AD-related pathology (AT8-positive phospho-tau, DC11 positive NFTs and beta amyloid), synaptic remodelling, synaptic density and oxidative stress markers were analysed separately for the three different lobes (i.e. lateral temporal, frontal and occipital lobe).

Tau phosphorylation and NFT formation

We investigated the relationship between disease severity and tau-related pathology using two antibodies: AT8 and DC11. AT8 recognises hyperphosphorylated tau (p-tau) prior to tangle formation, while DC11 detects hyperphosphorylated tau present in tangles. The amount of p-tau significantly increases with AD progression (see Figure 18).
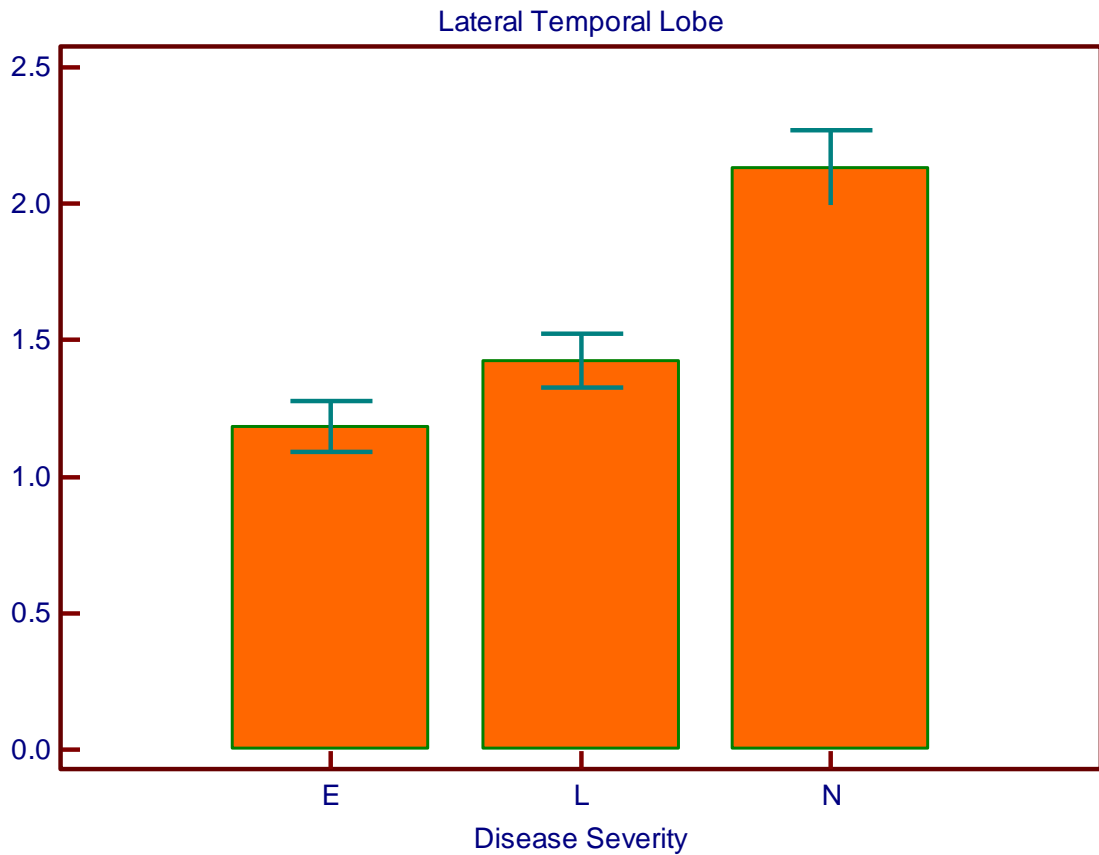
Figure 18

Analysis of p-tau in the lateral temporal lobe and disease severity. An ANOVA was conducted with AT8 expression as the dependent variable and the disease severity as the independent variable. AT8 expression (absolute values) on y-axis. Disease severity (E = entorhinal, L = limbic, and N = neocortical) on x-axis. ($p < 0.001$, $df = 2$). Error bars represent standard error of the mean. Top of bars represent mean.

Depending on the distribution of data, parametric ANOVA test or non-parametric Kruskal-Wallis test were used to analyse the effect of elevated plasma Hcy on the accumulation of AD-type pathology. We found that patients with elevated plasma Hcy levels had higher AT8 and DC11 expressed in all brain regions. The same is seen with brain Hcy levels. Statistically significant differences were only found with DC11 expression in the lateral temporal lobe in patients with elevated plasma Hcy ($p = 0.0256$) and elevated brain Hcy levels ($p = 0.0404$), see Figure 19.
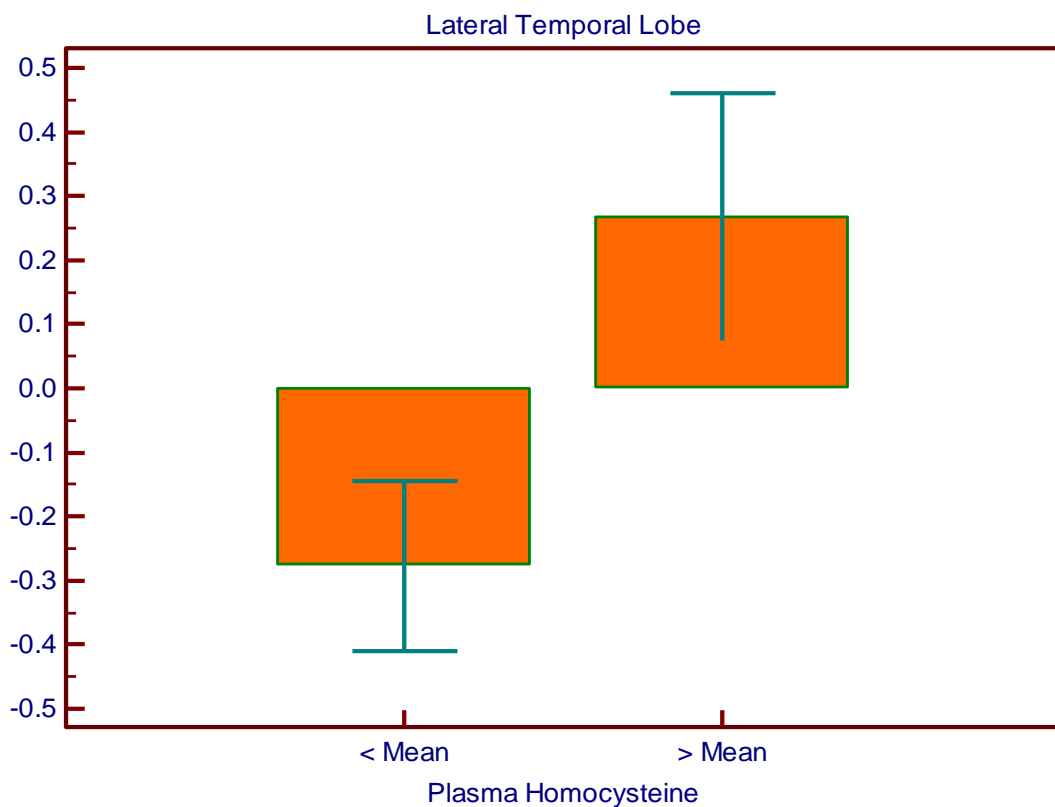
Figure 19

A - Plasma Homocysteine Levels
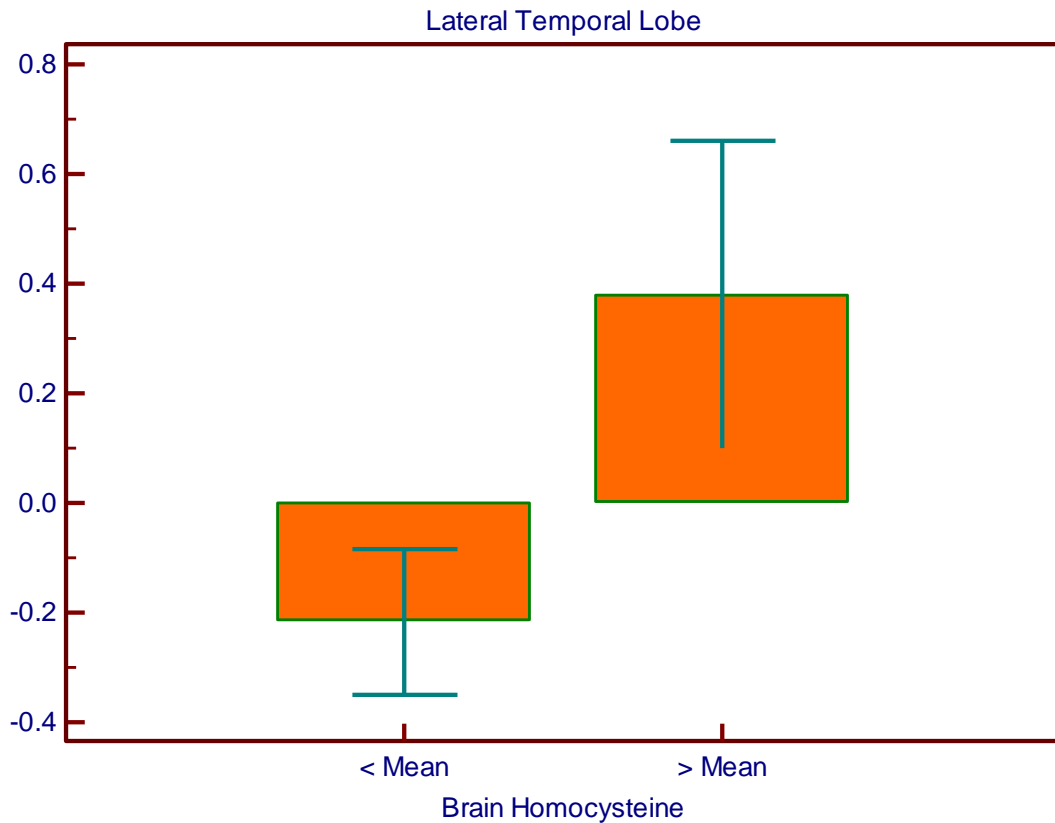
Figure 19

B - Brain Homocysteine Levels

Effect of Hcy levels on the accumulation of tangle pathology in the lateral temporal lobe. An ANOVA was conducted with DC11 expression as the dependent variable and the levels of plasma/brain Hcy as the independent variable. z-score values for DC11 expression on y-axis. Plasma/brain Hcy levels (dichotomised to smaller than or greater than the mean of the group) on x-axis. $p = 0.0256$, $df = 1$ and $p = 0.0404$, $df = 1$ respectively. Error bars represent standard error of the mean. Top of bars represent mean.

The ApoE genotype did not influence the expression of DC11 in the lateral temporal lobe (see

Figure 20).
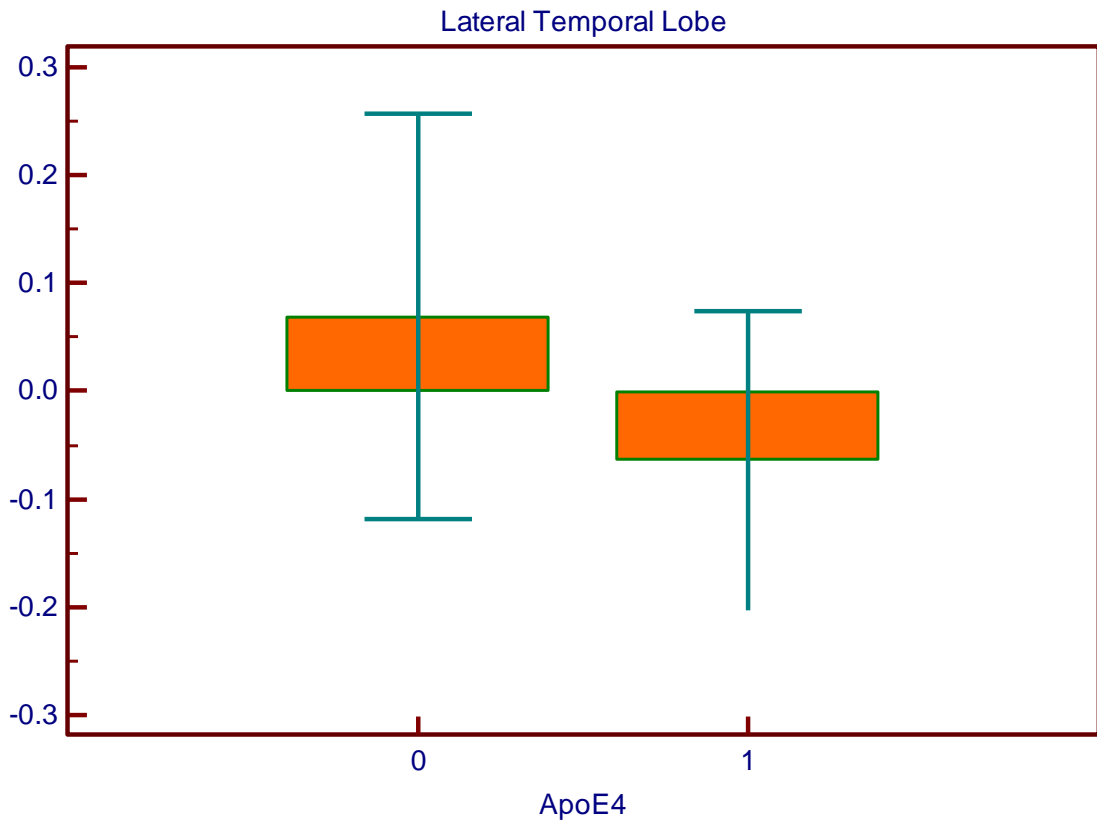
Figure 20

Analysis of ApoE4 genotype and tangle pathology in the lateral temporal lobe. A Kruskal-

Wallis test was conducted with DC11 expression as the dependent variable and the ApoE4

genotype as the independent variable.z-score values for DC11 expression on y-axis. ApoEε4

non-carriers (no ApoEε4 allele = 0) and ApoEε4 carriers (either one or two alleles = 1) on x-

axis. (p = 0.569, df = 1). Error bars represent standard error of the mean. Top of bars

represent mean.

Two-way analysis of variance was used to analyse the combined effect of Hcy level and ApoE4 genotype on DC11 expression in the lateral temporal lobe. We found that this relationship became non-significant in ApoE ε4 carriers in the lateral temporal lobe (see Figure 21). This interaction between ApoE4 and Hcy levels was even more pronounced, and statistically significant (p=0.033, df = 1) if we taken into account the brain Hcy (see Figure 22).
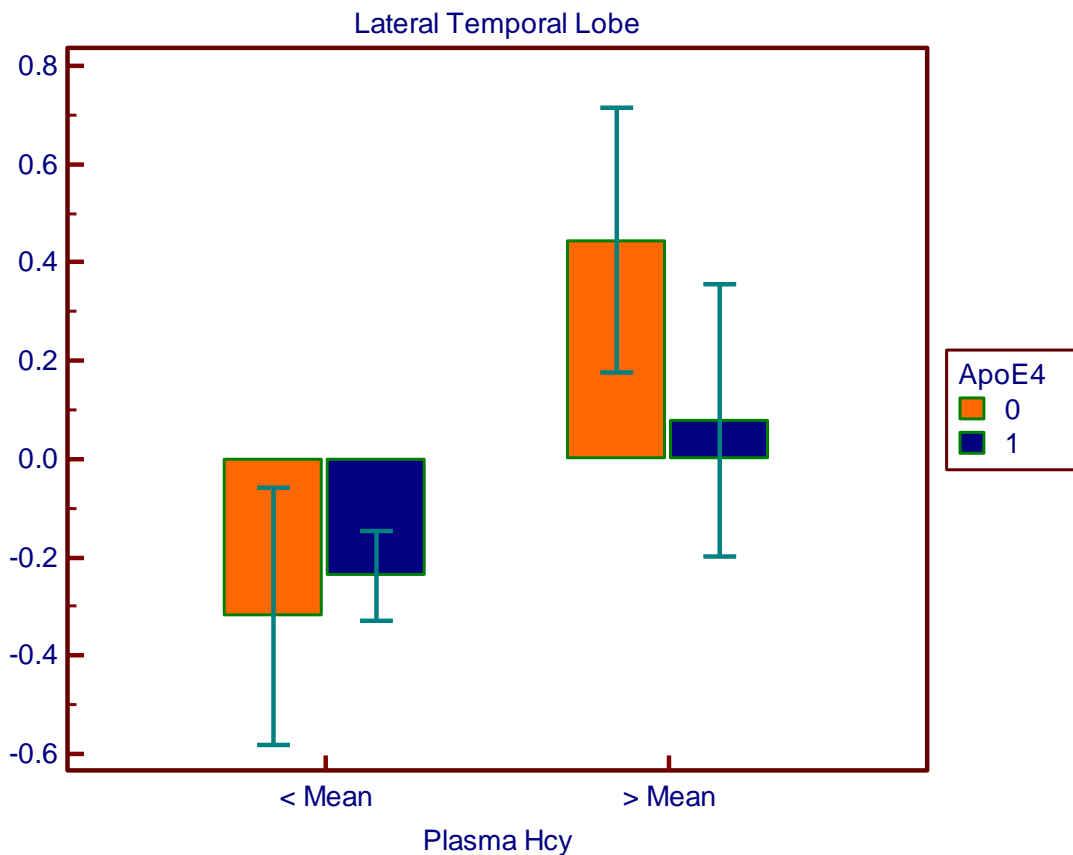
Figure 21

Two way analysis of variance. The combined effect of plasma Hcy and ApoEε4 genotype on tangle pathology in the lateral temporal lobe. An ANOVA was conducted with the DC11 expression as the dependent variable and the plasma Hcy levels and the ApoE4 genotype as the independent variable. z-score values for DC11 expression on y-axis and plasma Hcy levels (dichotomised to smaller than or greater than the mean of the group, µM) on x-axis.

ApoEε4 non-carriers (no ApoEε4 allele = 0) and ApoEε4 carriers (either one or two alleles = 1). Error bars represent standard error of the mean. Top of bars represent mean.
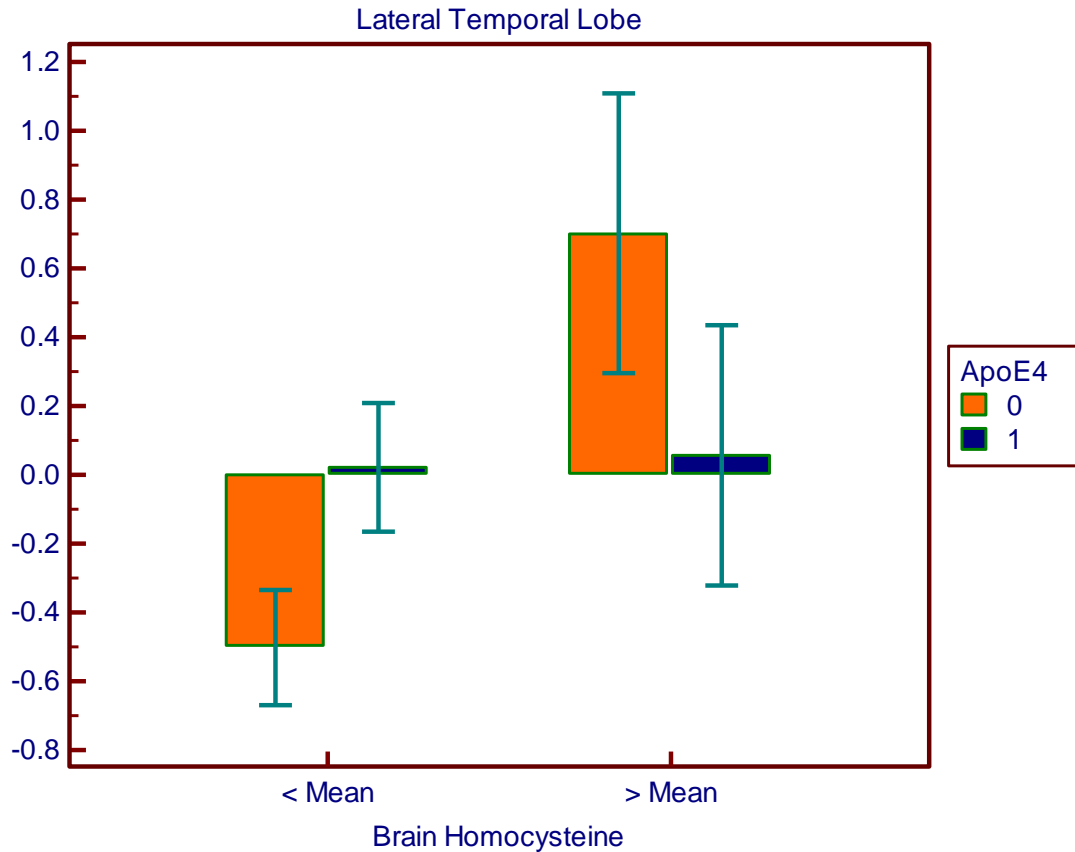
Figure 22

Two way analysis of variance. The combined effect of brain Hcy and ApoEε4 genotype on tangle pathology in the lateral temporal lobe. An ANOVA was conducted with the DC11 expression as the dependent variable and the brain Hcy levels and the ApoE4 genotype as the independent variable. z-score values for DC11 expression on y-axis and brain Hcy levels (dichotomised to smaller than or greater than the mean of the group, μM) on x-axis. ApoEε4 non-carriers (no ApoEε4 allele = 0) and ApoEε4 carriers (either one or two alleles = 1). Error bars represent standard error of the mean. Top of bars represent mean.

<u>Beta Amyloid</u>

One of the hallmarks of AD is extracellular insoluble amyloid plaques composed of beta amyloid. Kruskal-Wallis test was used to investigate if beta amyloid expression related to disease severity. The expression of beta amyloid in the frontal and occipital lobe significantly increased with AD progression (see Figure 23).
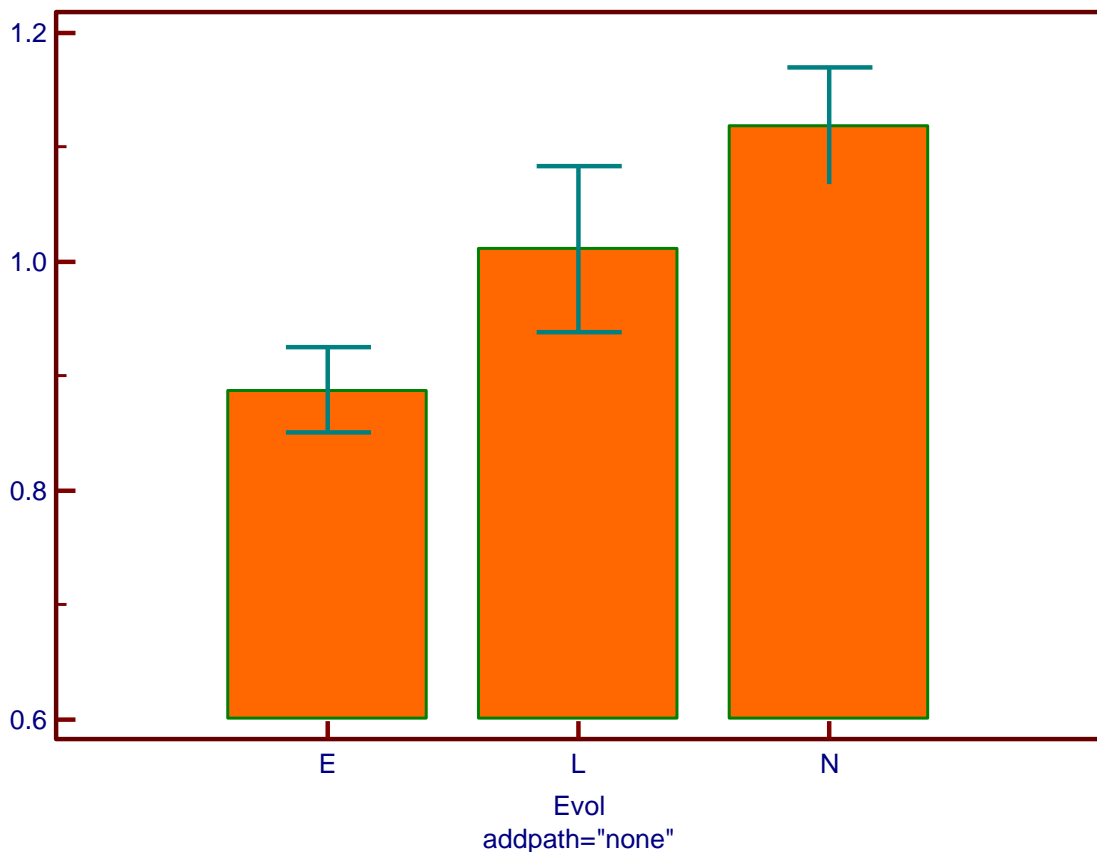
Figure 23

Relationship between disease severity and beta amyloid accumulation. A Kruskal-Wallis test was conducted with the beta amyloid expression as the dependent variable and the disease severity as the independent variable. z-score values for beta amyloid expression in the frontal lobe on the y-axis. Disease severity (E = entorhinal, L = limbic, and N = neocortical) on x-axis. ($p = 0.0101$, df = 2). Error bars represent standard error of the mean. Top of bars represent mean.

Using z-scores we analysed the effect of Hcy on beta-amyloid expression independently of disease severity. Kruskal-Wallis analysis showed that beta amyloid expression in the temporal lobe was significantly increased in patients with elevated brain Hcy levels (see Figure 24). A similar trend is seen with plasma Hcy levels (Figure 25), although results failed to reach statistical significance.

Lateral Temporal Lobe

Brain Homocysteine
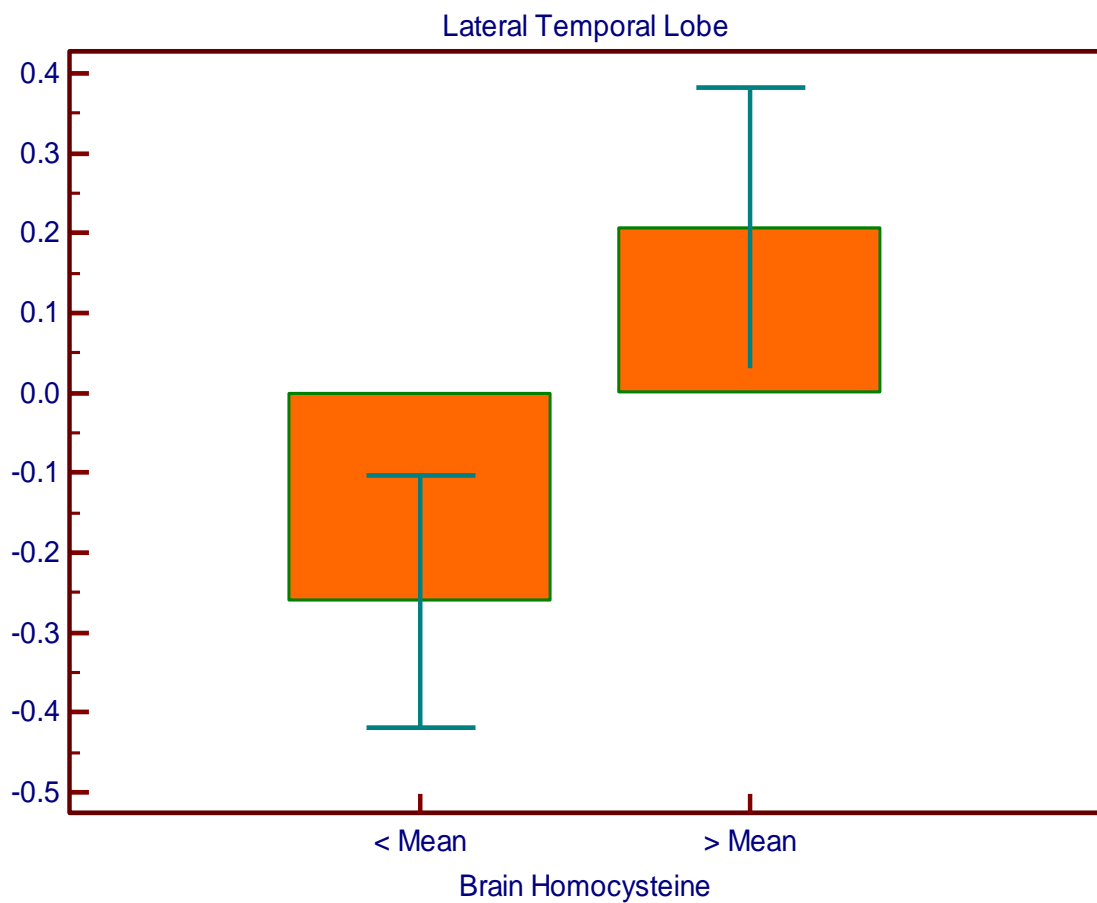
Figure 24

Effect of brain Hcy levels on the accumulation of beta amyloid in the lateral temporal lobe. A Kruskal-Wallis test was conducted with the beta amyloid expression as the dependent variable and the brain Hcy levels as the independent variable. z-score values for beta amyloid expression on y-axis. z-score values for brain Hcy levels (dichotomised to smaller than or

greater than the mean of the group, µM/protein) on x-axis. (p = 0.0499, df = 1). Error bars represent standard error of the mean. Top of bars represent mean.

.
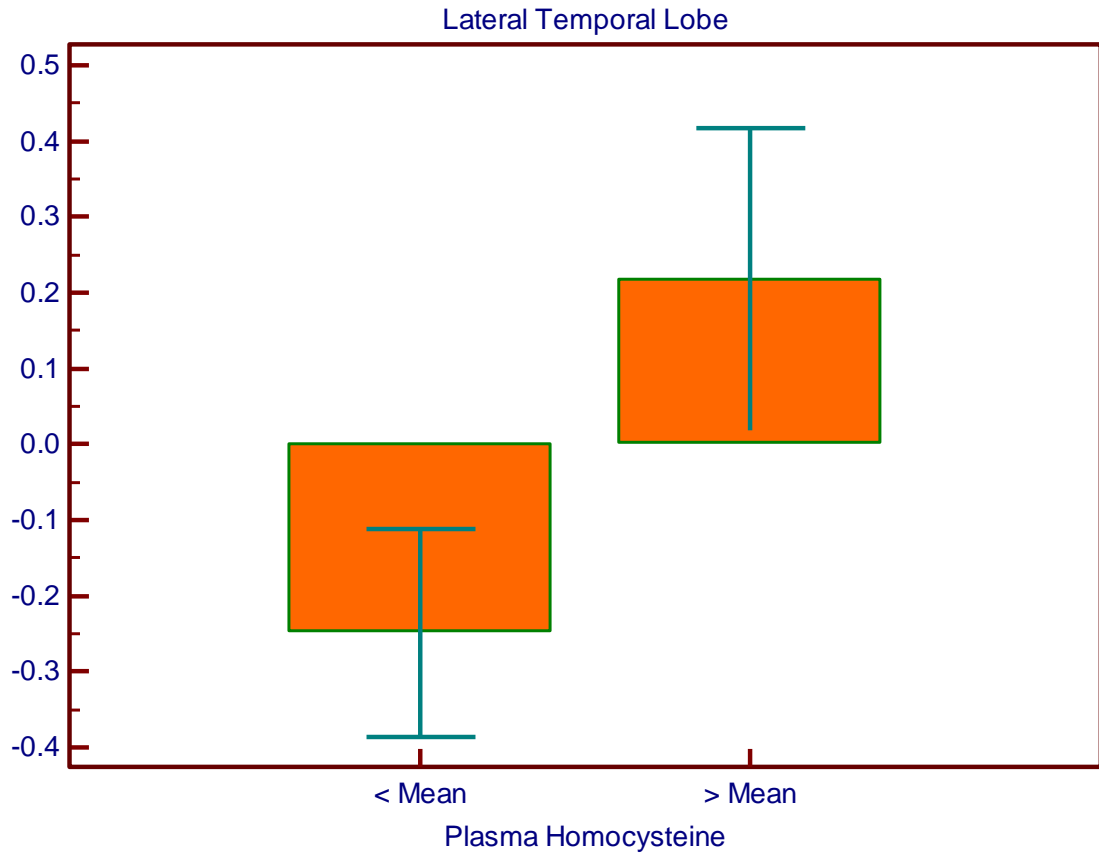
Figure 25

Effect of plasma Hcy levels on the accumulation of beta amyloid in the lateral temporal lobe. A Kruskal-Wallis test was conducted with the beta amyloid expression as the dependent variable and plasma Hcy levels as the independent variable. z-score values for beta amyloid expression on y-axis. z-score values for plasma Hcy levels (dichotomised to smaller than or greater than the mean of the group, µM/protein) on x-axis. (p = 0.1639, df = 1). Error bars represent standard error of the mean. Top of bars represent mean.

Beta amyloid expression in the lateral temporal lobe was significantly higher in ApoEε4 carriers (see Figure 26) than non-carriers. Two-way analysis of variance was used to analyse the combined effect of Hcy levels and ApoE4 genotype on beta amyloid expression in the lateral temporal lobe. ApoEε4 non-carriers with high plasma Hcy levels were found to have significantly higher levels of beta amyloid in the temporal lobe, while in ApoE4 carriers plasma Hcy levels had no significant effect. Similar interactions was seen when brain Hcy levels were used to analyse the data (see

Figure **27** and Figure 28).
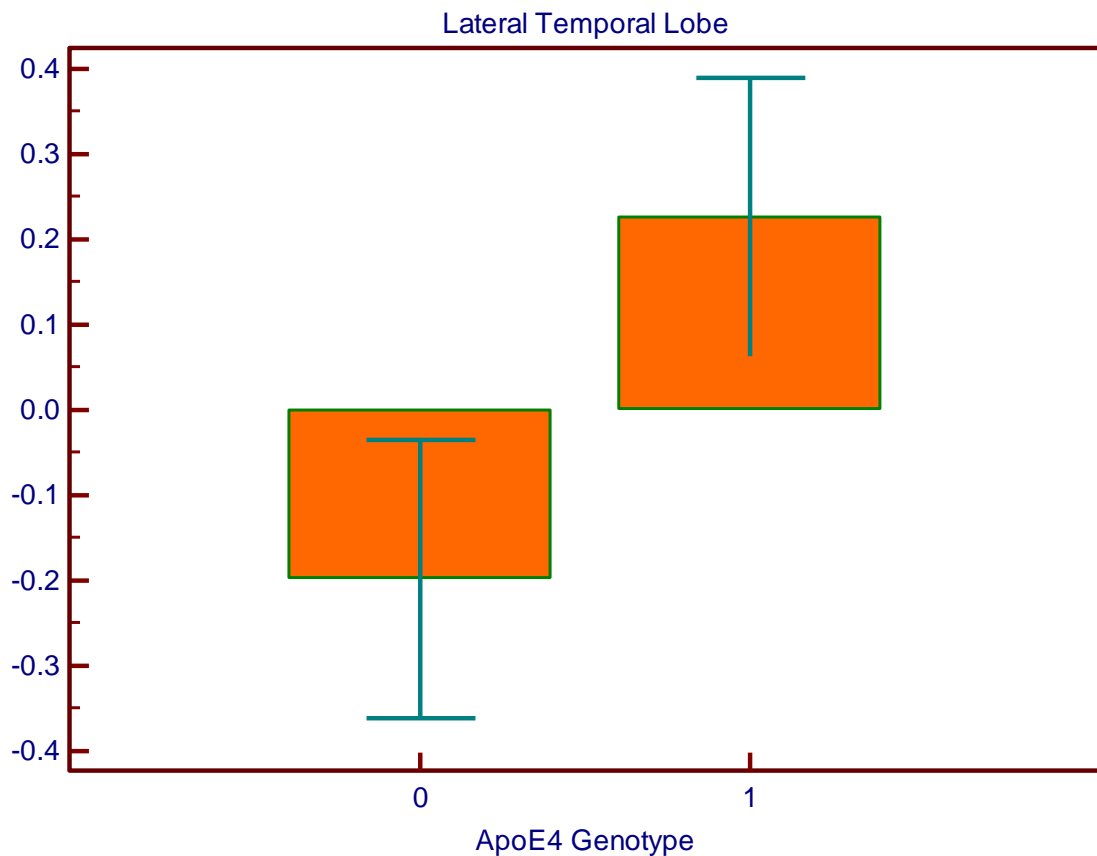
Figure 26

Analysis of ApoE4 genotype and beta amyloid expression in the lateral temporal lobe. A Kruskal-Wallis test was conducted with the beta amyloid expression as the dependent variable and the ApoE genotype as the independent variable. z-score values for beta amyloid

expression on y-axis. ApoEε4 non-carriers (no ApoEε4 allele = 0) and ApoEε4 carriers (either one or two alleles = 1) on x-axis.(p = 0.0415, df = 1). Error bars represent standard error of the mean. Top of bars represent mean.
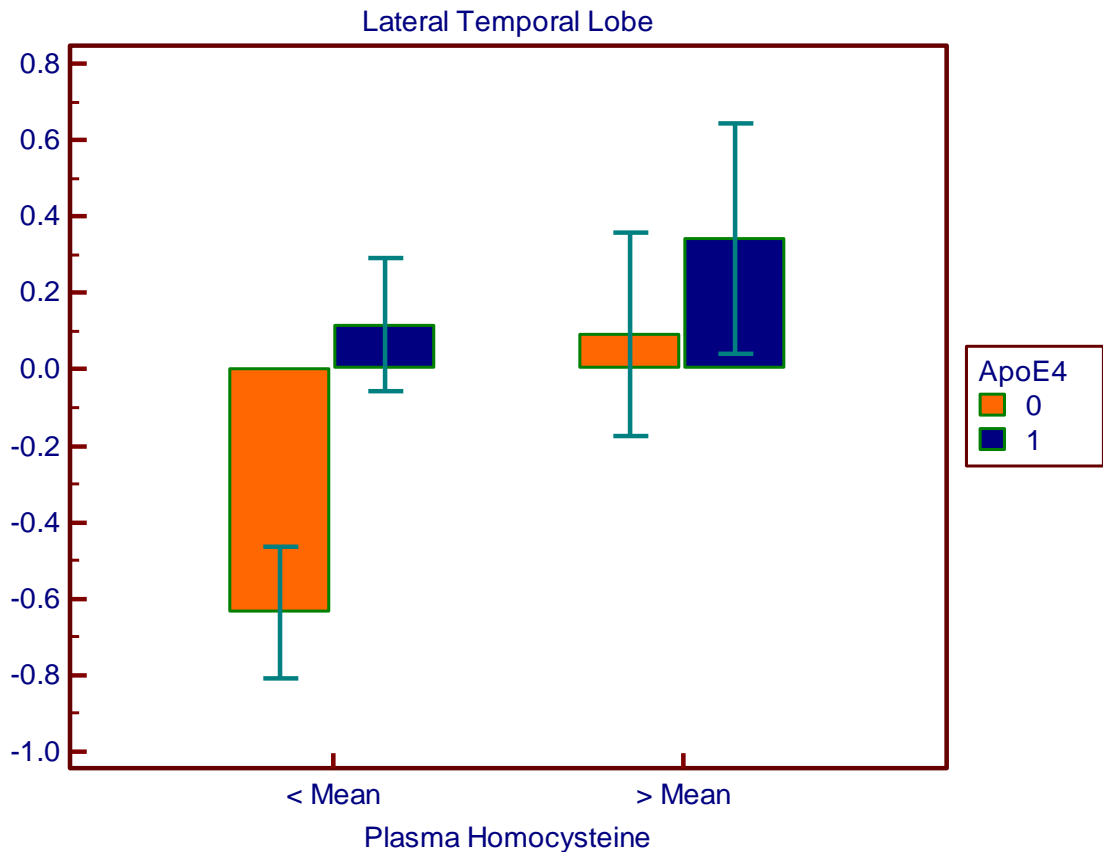
Figure 27

Two way analysis of variance. The combined effect of plasma Hcy and ApoEε4 genotype on beta amyloid expression in the lateral temporal lobe. An ANOVA was conducted with beta amyloid expression as the dependent variable and the levels of plasma Hcy and the ApoE4 genotype as the independent variables. z-score values for beta amyloid expression on y-axis and plasma Hcy levels (dichotomised to smaller than or greater than the mean of the group, μM) on x-axis. ApoEε4 non-carriers (no ApoEε4 allele = 0) and ApoEε4 carriers (either one or two alleles = 1). Error bars represent standard error of the mean. Top of bars represent mean.

Lateral Temporal Lobe
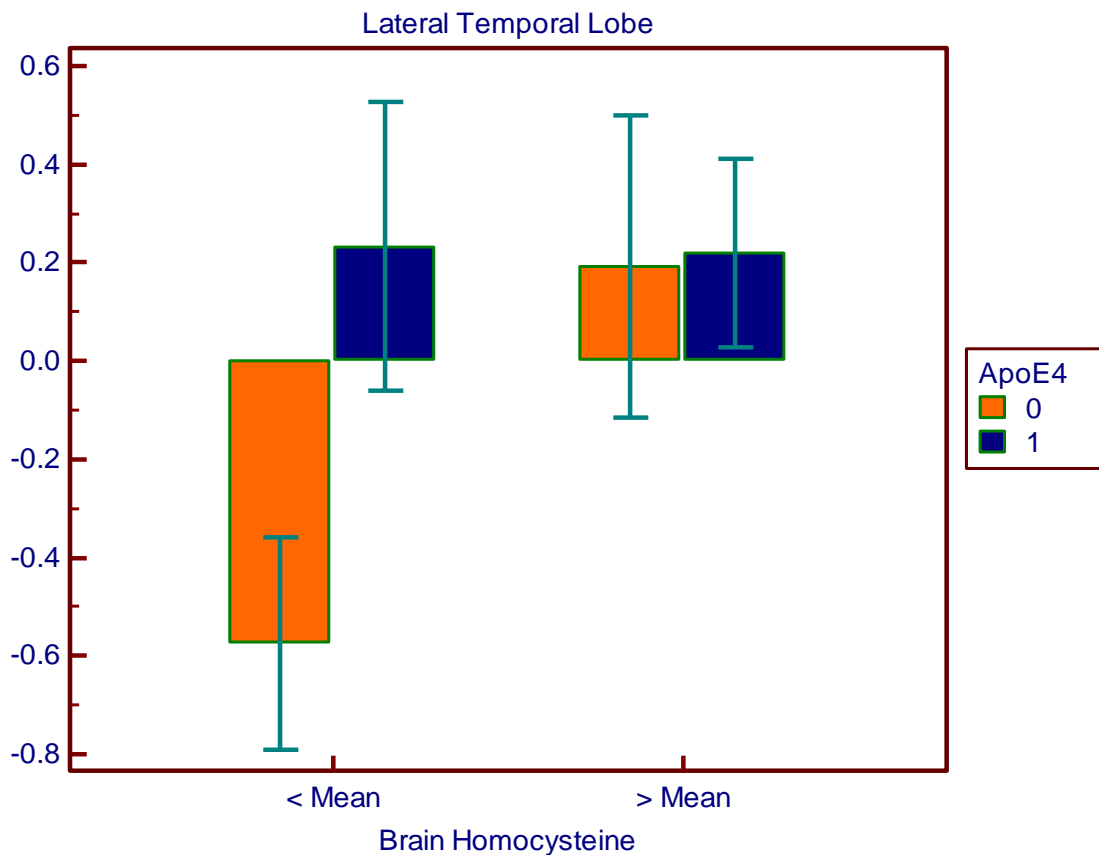
Figure 28

Two way analysis of variance. The combined effect of brain Hcy and ApoEε4 genotype on beta amyloid expression in the lateral temporal lobe. An ANOVA was conducted with beta amyloid expression as the dependent variable and the levels of brain Hcy and the ApoE4 genotype as the independent variables. ƶ-score values for beta amyloid expression on y-axis and brain Hcy levels (dichotomised to smaller than or greater than the mean of the group) on x-axis. ApoEε4 non-carriers (no ApoEε4 allele = 0) and ApoEε4 carriers (either one or two alleles = 1). Error bars represent standard error of the mean. Top of bars represent mean.

4.1.4. The Effect of Homocysteine on Oxidative Stress

4-hydroxynonenal (4-HN) and 8-hydroxyguanosine (8-HG) were used as markers of oxidative stress. ANOVA was used to investigate the relationship between disease severity and the expression of these oxidative stress markers. We found no significant relationship between oxidative stress and disease progression (data not shown).

Logistic regression analysis was used to investigate the relationship between oxidative stress markers and Hcy levels. 4-HN expression in the lateral temporal lobe positively correlated with brain Hcy levels (close to significance $p = 0.0608$, see Table 11). The ApoEε4 genotype did not influence this relationship. Furthermore, 4-HN expression in the frontal lobe positively correlated with brain Hcy levels (see Table 12). In the frontal lobe of ApoEε4 carriers the Hcy-induced 4-HN levels were significantly lower than in those without the ApoE4 allele (Table 12). This interaction is also reflected in the fact that high brain Hcy levels are associated with increased 4-HN expression primarily in ApoE4 carriers, but not in patients who do not have this isoform (see Figure 29). 8-HG expression in the frontal lobes also showed a positive correlation to brain Hcy levels; however the ApoEε4 genotype did not influence this relationship (see Table 13, $p = 0.0022$).

Table 11

Relationship of 4-HN expression in the lateral temporal lobe with Hcy levels and ApoEε4 genotype. A logistic regression analysis was conducted using z-score values dichotomised to smaller than or greater than the mean of the group. With 4-HN expression in the lateral temporal lobe as the dependent variable and the levels of Hcy and the ApoE4 genotype as the independent variables.ApoEε4 non-carriers (no ApoEε4 allele = 0) and ApoEε4 carriers (either one or two alleles = 1). p=0.0608.

Variable	4-HN Lateral Temporal Lobe		
	Coefficient	**Std. Error**	**P**
Brain Hcy levels	0.7066	0.4198	0.0924

Table 12

Relationship of 4-HN expression in the frontal lobe with Hcy levels and ApoEε4 genotype. A logistic regression analysis was conducted using z-score values dichotomised to smaller than or greater than the mean of the group. With 4-HN expression in the frontal lobe as the dependent variable and the levels of Hcy and the ApoE4 genotype as the independent variables. ApoEε4 non-carriers (no ApoEε4 allele = 0) and ApoEε4 carriers (either one or two alleles = 1). p=0.0057.

Variable	4-HN Frontal Lobe		
	Coefficient	**Std. Error**	**P**
Brain Hcy levels	0.7437	0.3897	0.0564
ApoE4	-1.6105	0.6493	0.0131
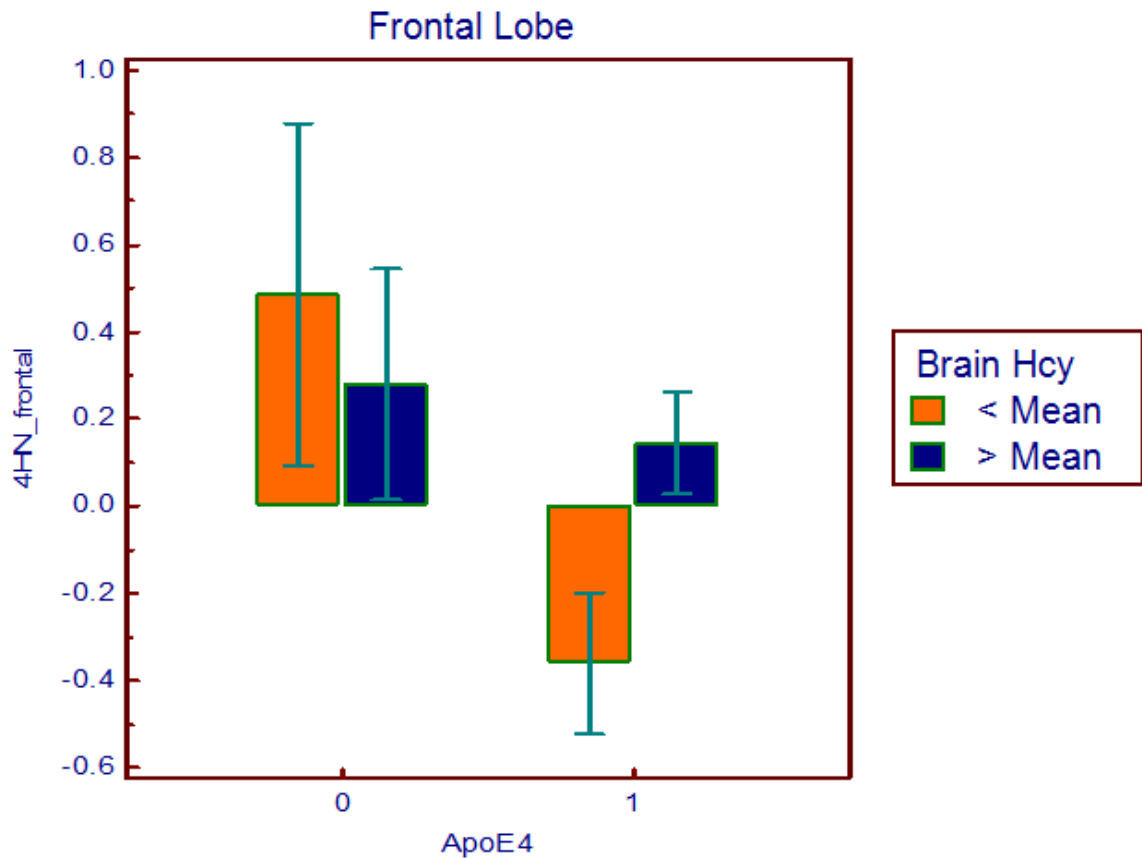
Figure 29

The relationship of brain Hcy, ApoEε4 genotype and 4-HN expression in the frontal lobe. A ANOVA was conducted using 4-HN expression in the frontal lobe as the dependent variable and the levels of Hcy and the ApoE4 genotype as the independent variables.z-score values for 4-HN expression in the frontal lobe on y-axis. ApoEε4 non-carriers (no ApoEε4 allele = 0) and ApoEε4 carriers (either one or two alleles = 1) on x-axis. z-score values for brain Hcy levels (dichotomised to smaller than or greater than the mean of the group, μM). Error bars represent standard error of the mean. Top of bars represent mean.

Table 13

Relationship of 8-HG expression in the frontal lobe with Hcy levels and ApoEε4 genotype. A logistic regression analysis was conducted using z-score values dichotomised to smaller than or greater than the mean of the group. With 8-HG expression in the frontal lobe as the dependent variable and the levels of Hcy and the ApoE4 genotype as the independent variables. ApoEε4 non-carriers (no ApoEε4 allele = 0) and ApoEε4 carriers (either one or two alleles = 1). p=0.0022.

Variable	8-HG Frontal Lobe		
	Coefficient	Std. Error	P
Brain Hcy Levels	1.3484	0.5649	0.0170

4.1.5. Relationship Between Brain Homocysteine and Plasma Homocysteine Levels

Levels of Hcy in the CSF have been reported to be 5-30% of that of plasma. We used brain tissue to measure levels of Hcy; this allowed us to analyse if there was any relationship between the levels of Hcy in the brain and the levels measured in plasma within the last 4 years prior to death. The Hcy levels were normalized for disease severity and transformed to z-scores values (see Methods). This allowed us to study the relationship between brain Hcy and plasma Hcy levels, independent of disease severity. We found no association between the two variables (see Figure 30).

Hcy is an intermediary in sulfur-amino acid metabolism and is a link between methionine and folate. Taking this into consideration we decided to look at the relationship between Hcy and methionine level. Firstly, we analysed the relationship between brain Hcy and brain methionine levels. We found no association between the two variables (see Figure 31) and the Hcy/methionine ratio in the brain was mainly determined by the brain Hcy levels (R^2 value = 86.8%, $p<0.0001$; see Figure 32).
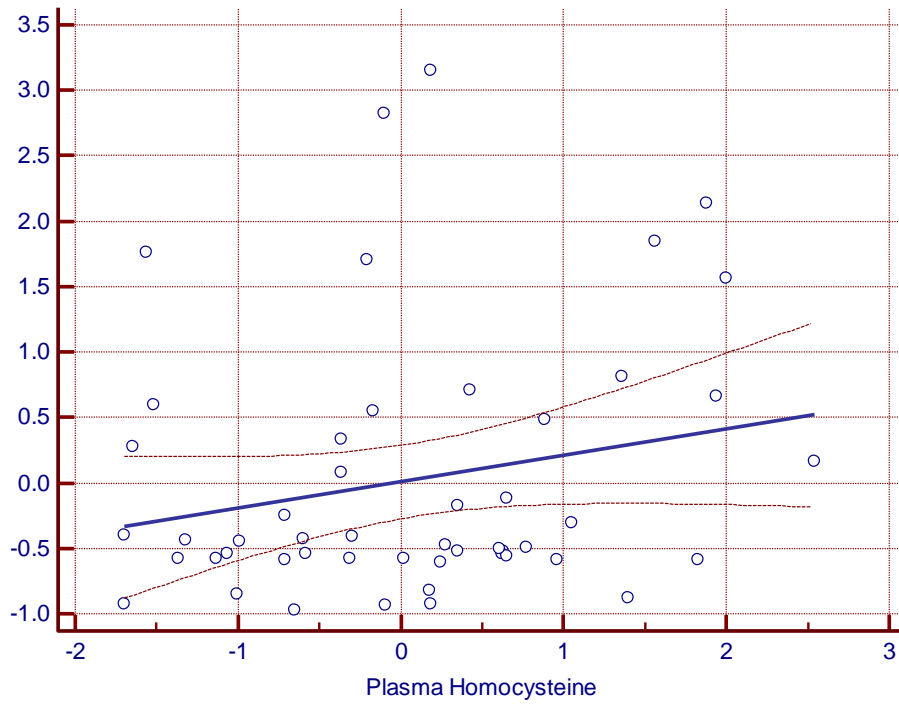
Figure 30

Correlation analysis of brain Hcy levels and plasma Hcy levels (z-scores), R^2 value = 21.9%,

p = 0.1266.
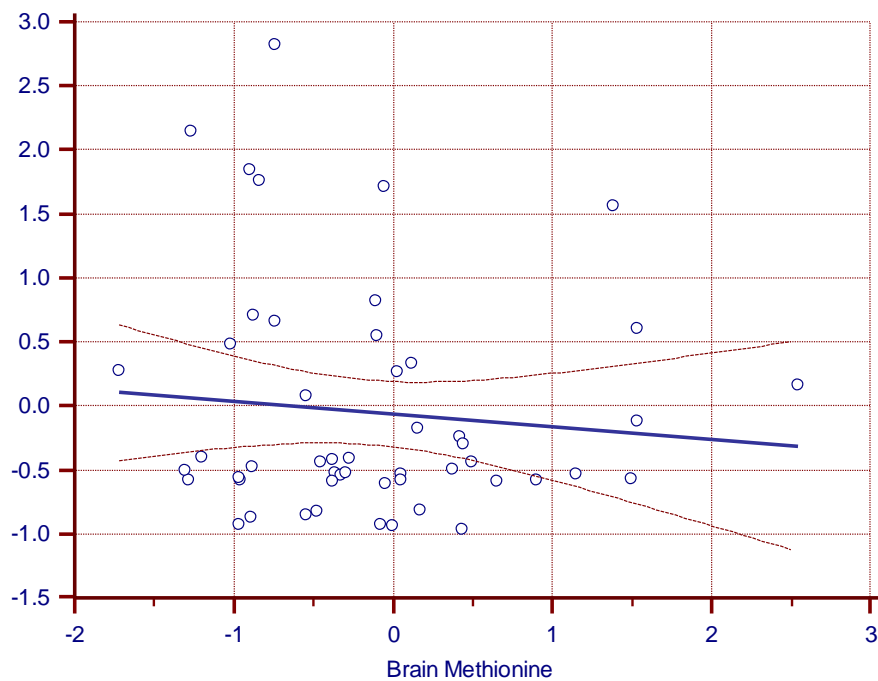
Figure 31

Correlation analysis of Hcy and methionine levels in the brain (z-scores), R^2 value = 0.8%, p = 0.518.
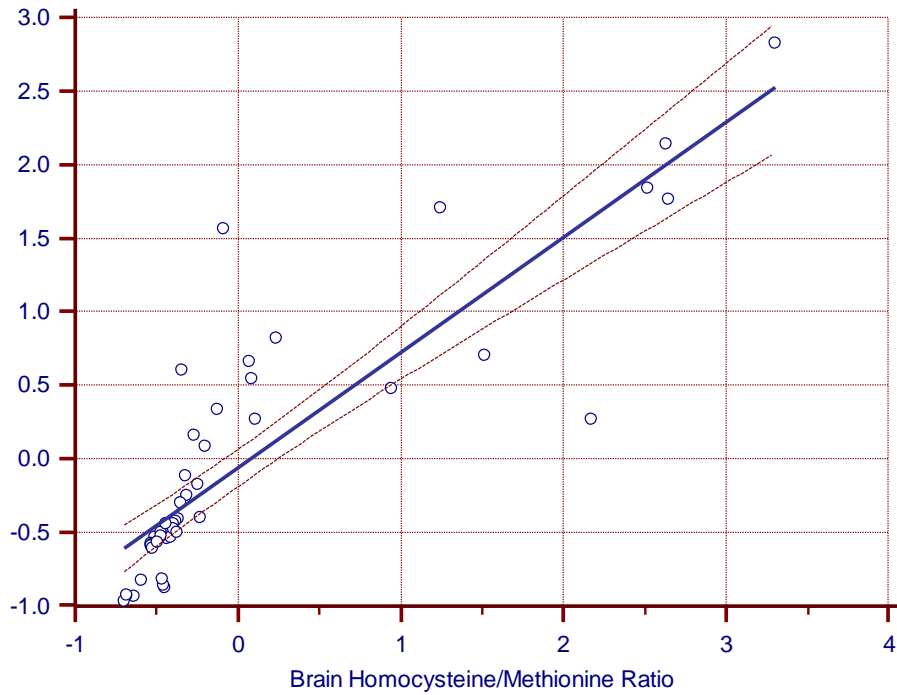
Figure 32

Correlation analysis of brain Hcy and brain Hcy/methionine ratio (z-scores), R2 value = 86.8%, p<0.0001.

4.1.6. Global DNA Methylation

Any change in the Hcy/methionine ratio could potentially result in changes to the methylation capacity. In consideration of this, we decided to analyse global DNA methylation. Firstly, we investigated the relationship between global DNA methylation and disease severity. We found a trend showing that the % of global methylated DNA was reduced in patients with neocortical stage AD compared to that of patients in an entorhinal or limbic stage of AD (see Figure 33).
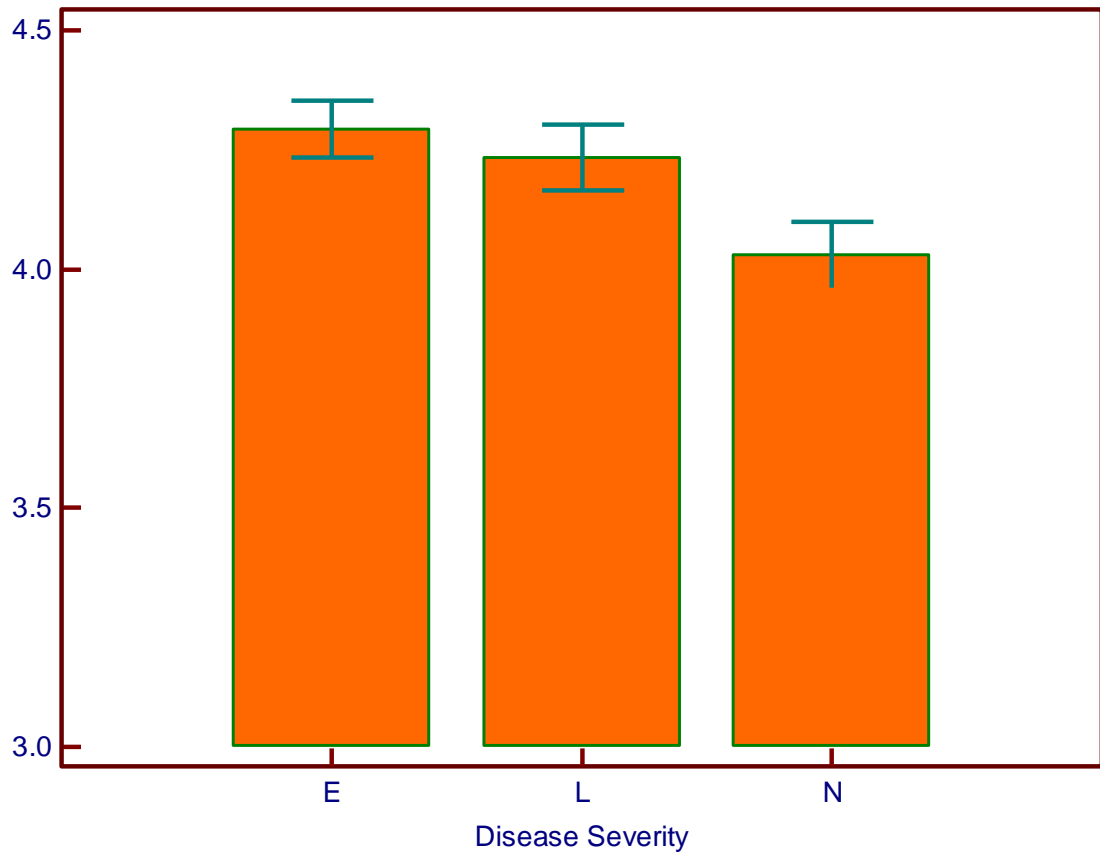
Figure 33

A Kruskal-wallis test was conducted using the % of global DNA methylation as the dependent variable and the disease severity as the independent variables. % of global DNA methylation (absolute values) on y-axis and disease severity (E = entorhinal, L = limbic, and N = neocortical) on x-axis. (p = 0.0901, df = 2). Error bars represent standard error of the mean. Top of bars represent mean.

Next using the z-score values we decided to look at the relationship between global DNA methylation and Hcy levels (both in brain and plasma). There was no association between global DNA methylation and Hcy levels. Furthermore, analysis using methionine levels and the Hcy/methionine ratio yielded no significant relationship with global DNA methylation (data not shown). Additionally we found that the presence or absence of the ApoEε4 allele did not alter this pattern (see Table 14).

ApoEε4 carriers were found to have a slightly reduced global DNA methylation compared to non- carriers (see Figure 34), although the result failed to reach statistical significance. However this can be interpreted as a larger number of neocortical stage patients being ApoEε4 carriers.
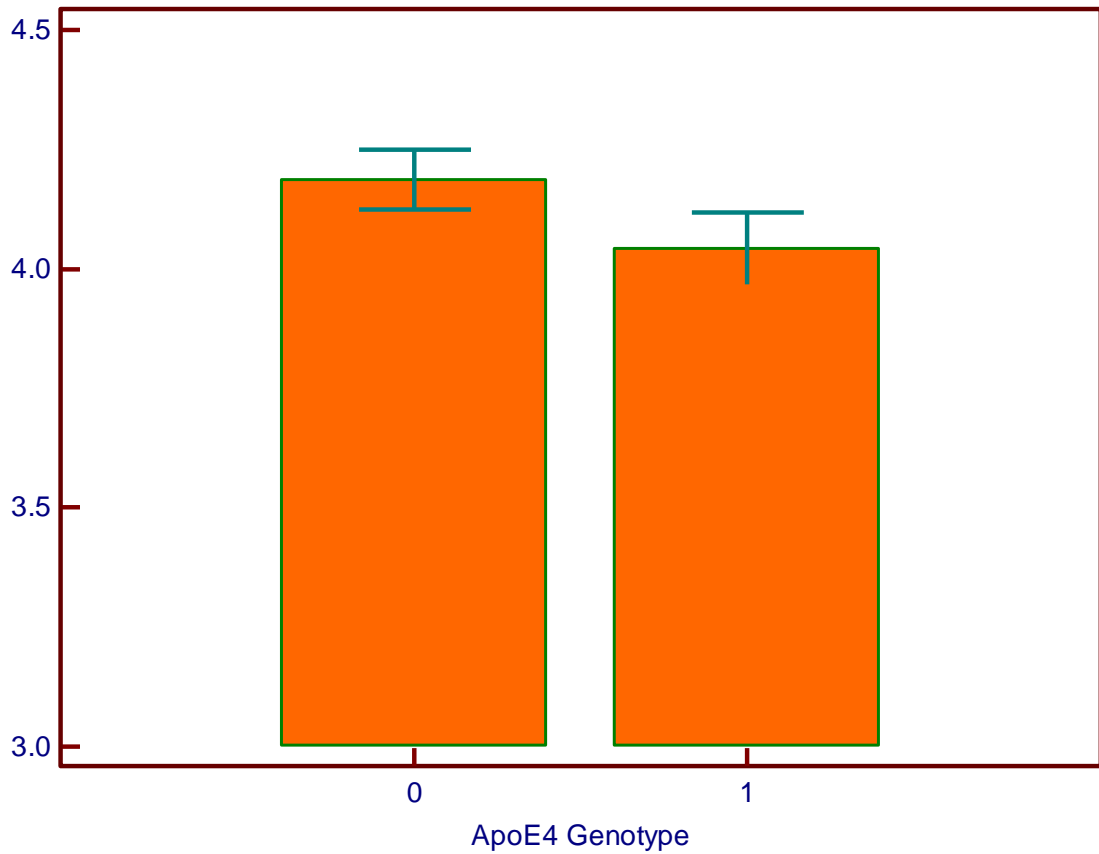
Figure 34

Analysis of ApoE4 genotype and % of global DNA methylation. A Kruskal-wallis test was conducted using the % of global DNA methylation as the dependent variable and the ApoE4 genotype as the independent variables. % of global DNA methylation (absolute values) on y-axis. ApoEε4 non-carriers (no ApoEε4 allele = 0) and ApoEε4 carriers (either one or two alleles = 1) on x-axis. (p = 0.150, df = 1). Error bars represent standard error of the mean. Top of bars represent mean.

Table 14

Multiple regression analysis with % global methylation as the dependent variable and Hcy measurements (z-score values) and ApoEε4 genotype as independent variables. p = 0.054.

Independent variables	% Global Methylation Status		
	Coefficient	**Std. Error**	**P**
ApoE4	-0.2289	0.1134	0.0540

Variables not included in the model
Plasma Hcy levels
Brain Hcy levels
Brain Hcy/methionine ratio
Brain methionine levels

4.1.7. The Effect of Homocysteine on the Methylation of Cyclin Dependent Kinase Inhibitor Genes

Following our analysis of global DNA methylation, we decided to investigate the relationship between Hcy and the methylation status of CDKI genes.

Firstly, we investigated the relationship between CDKI methylation (absolute values) and disease severity to see if the methylation of CDKI genes changed at different stages of AD. Using Kruskal-Wallis analysis we found no relationship between the severity of disease and the methylation of CDKI genes (data not shown).

Using z-score values, the effect of Hcy and ApoEε4 genotype on CDKI methylation was analysed by multiple regression analysis. We found, with a backward regression model, a number of independent variables (brain Hcy levels and Hcy/methionine ratio) that contributed to the p16^{INK4a} methylation status. ApoEε4 genotype had no effect on p16 ^{INK4a} methylation (see Table 15). The promoter methylation of the other CDKI genes was not affected by Hcy levels in the brain (data not shown).

Table 15

Multiple regression analysis with p16^{INK4a} methylation as the dependent variable and Hcy measurements (z-score values) and ApoEε4 genotype as independent variables. p = 0.053.

Independent variables	p16^{INK4a} promoter methylation		
	Coefficient	Std. Error	P
Brain Hcy Levels	1.0204	0.4071	0.0227
Brain Hcy/Methionine ratio	-1.0056	0.3911	0.0198

Variables not included in the model
Plasma Hcy Levels
Brain Methionine Levels
ApoE4

4.1.8. The Effect of Homocysteine on Protein Expression of Cyclin Dependent Kinase Inhibitors

After analysing CDKI methylation status, we next wanted to investigate if the levels of Hcy influenced the expression of CDKI at the protein level.

Firstly we decided to see if the levels of CDKI were altered at different stages of AD. We found trends showing that levels of CDKI (p16^{INK4a}, p21^{cip1}, p27^{kip1} and p57^{kip2}) were at their highest at later stages of AD. Using Kruskal-Wallis analysis, statistically significant differences were only found with p21^{cip1} expression in the lateral temporal and occipital lobe (see Figure 35 and Figure 36).

Using z-score values, we found that the methylation status of the CDKI genes did not correlate with the expression of the CDKI protein (data not shown).

Finally we analysed the relationship between Hcy levels and the expression of CDKIs. Plasma Hcy levels did not influence CDKI expression. Elevated levels of brain Hcy were significantly associated with decreased expression of p16^{INK4a} in the occipital lobe (Figure 37). Including ApoEε4 genotype in this analysis showed that the effect of the Hcy was stronger in patients who did not carry the ApoEε4 allele (Figure 38).

We also found that patients with elevated brain Hcy levels had significantly higher expression of p27 and p57 in the occipital lobe (Figure 39 and Figure 41 respectively). This Hcy-

associated increase in the expression of p27/p57 is only present in patients who are ApoE ε4 carriers (Figure 40 and Figure 42 respectively).
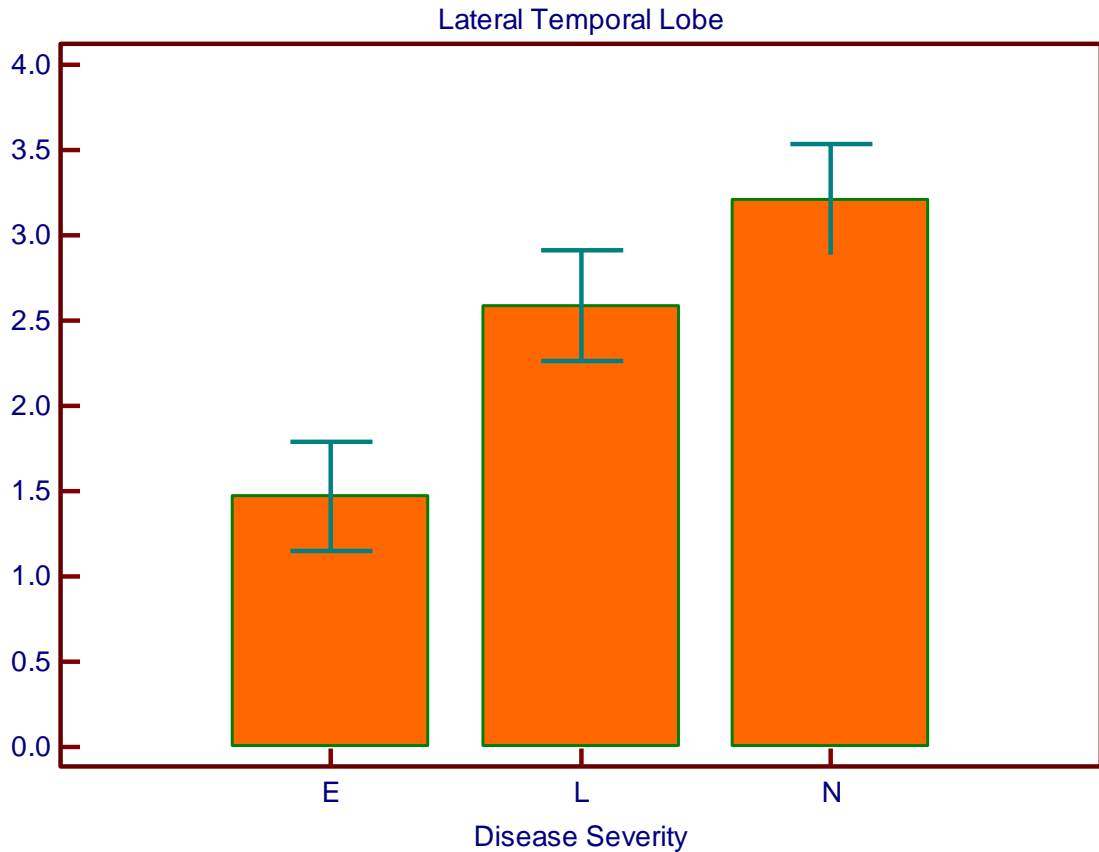
Figure 35

p21^{cip1} expression in the lateral temporal lobe of individuals in different stages of AD. A Kruskal-wallis test was conducted using p21 expression as the dependent variable and the disease severity as the independent variable. Disease severity on the x-axis (E = entorinal, L = Limbic, N = Neocortical); p21 expression in the lateral temporal lobe on the y-axis. (p = 0.0086, df = 2). Error bars represent standard error of the mean. Top of bars represent mean.
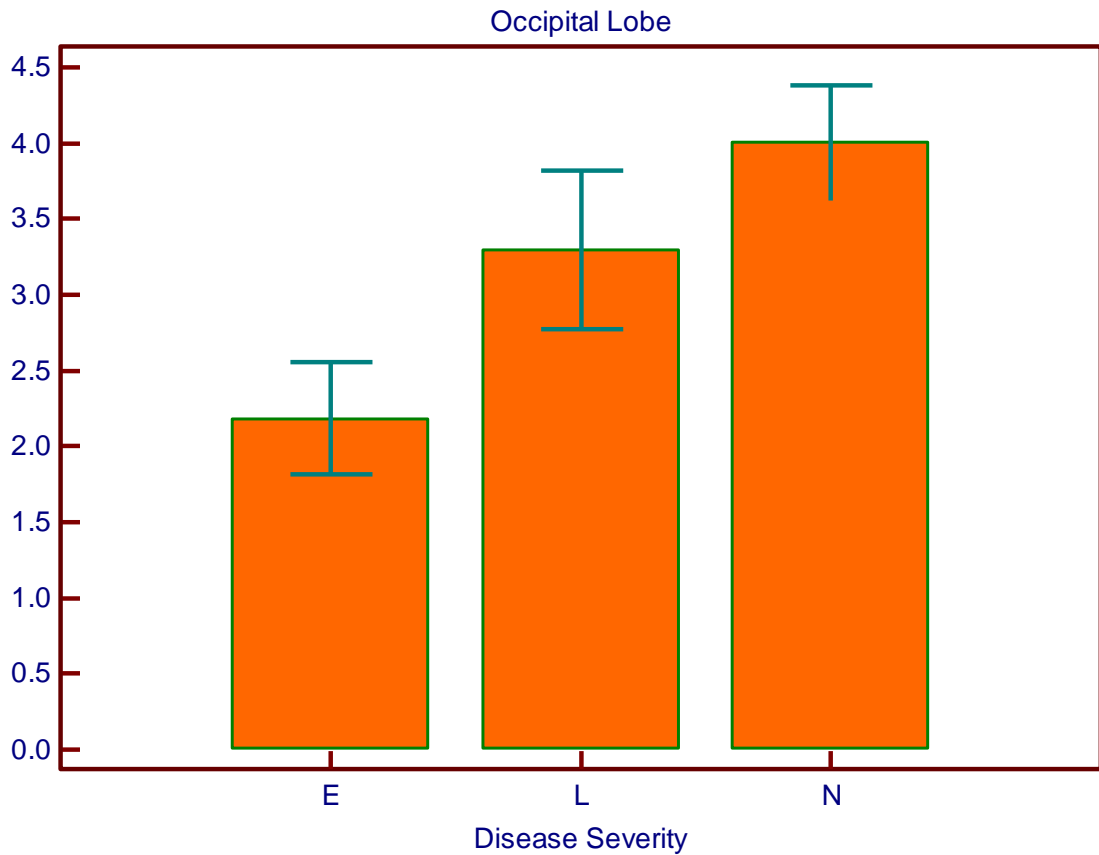
Figure 36

p21^{cip1} expression in the occipital lobe of individuals in different stages of AD. A Kruskal-wallis test was conducted using the p21 expression as the dependent variable and the disease severity as the independent variable. Disease severity on the x-axis (E = entorinal, L = Limbic, N = Neocortical); p21 expression in the occipital lobe on the y-axis. (p = 0.0362, df = 2). Error bars represent standard error of the mean. Top of bars represent mean.
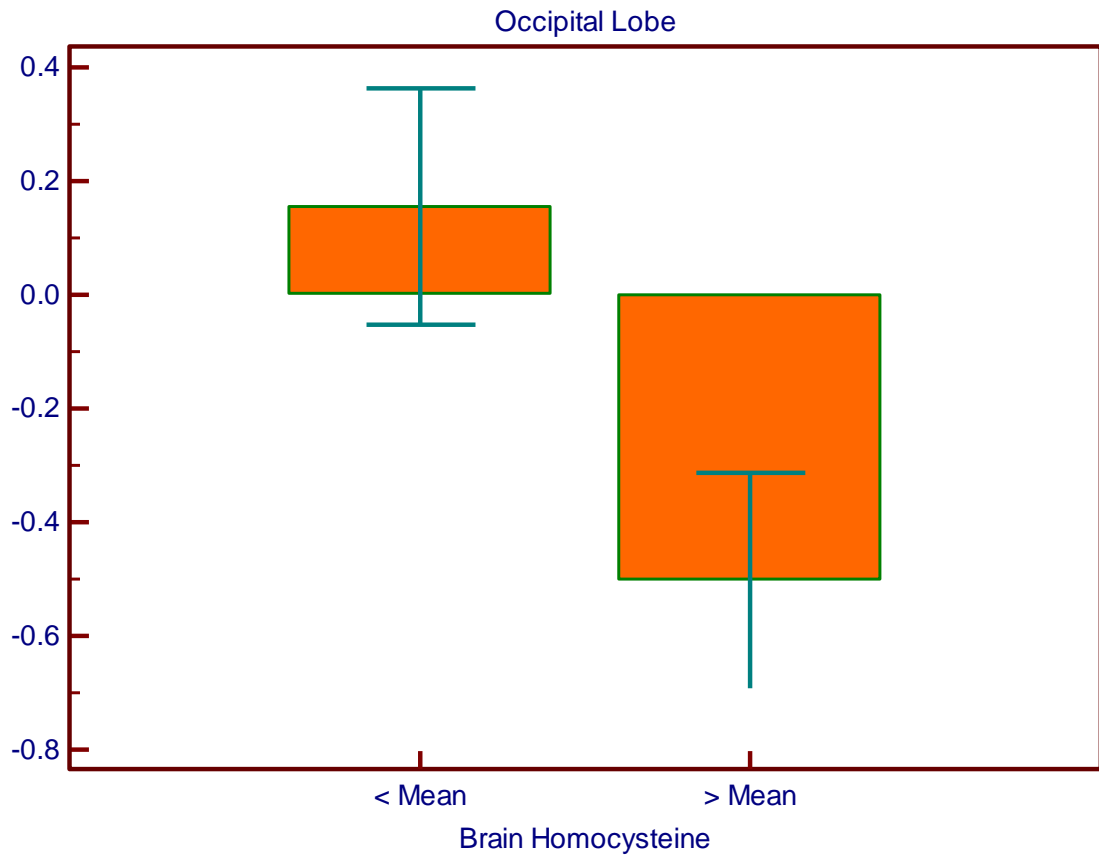
Figure 37

Effect of brain Hcy levels on p16^{INK4a} expression in the occipital lobe. A Kruskal-wallis test was conducted using p16 expression as the dependent variable and brain Hcy levels as the independent variables. z-score values for p16^{INK4a} expression in the occipital lobe on y-axis. z-score values for brain Hcy levels (dichotomised to smaller than or greater than the mean of the group) on x-axis. (p = 0.042, df = 1). Error bars represent standard error of the mean. Top of bars represent mean.
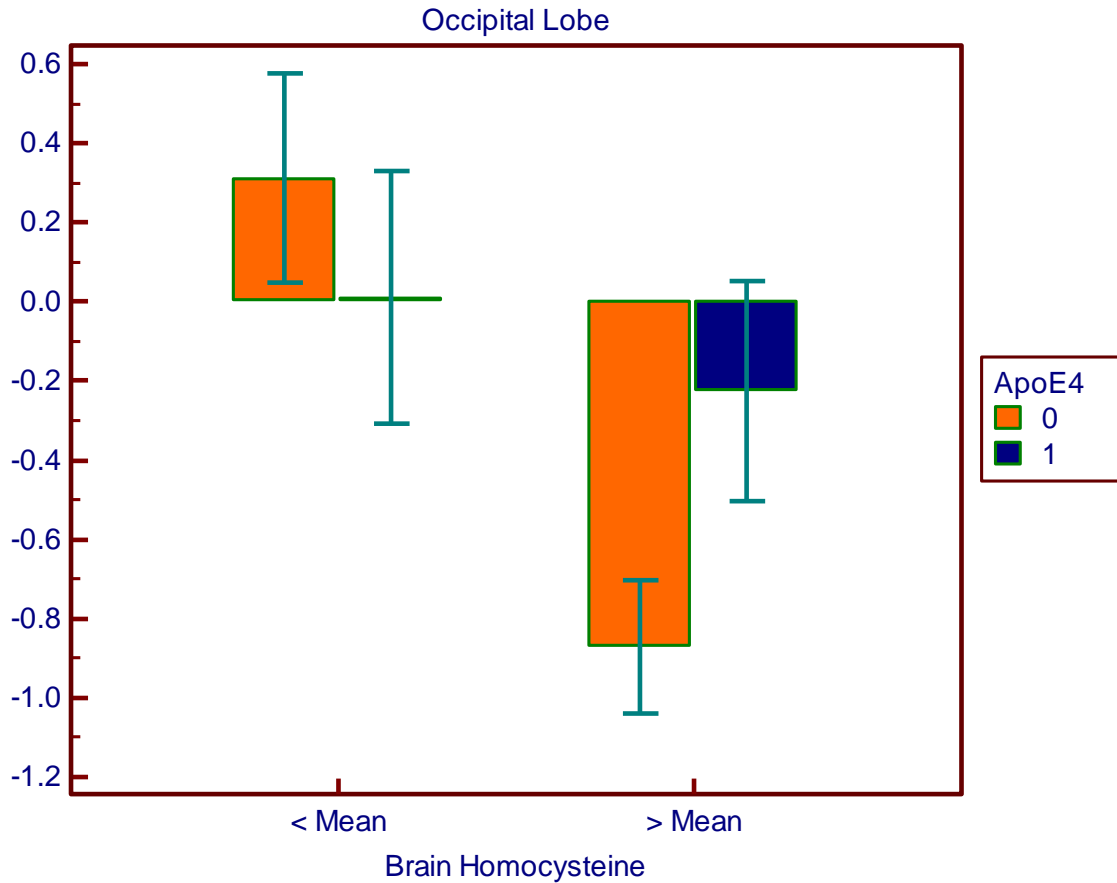
Occipital Lobe

Figure 38

The relationship of brain Hcy, ApoEε4 genotype and p16^{INK4a}expression in the occipital lobe. An ANOVA was conducted using p16 expression as the dependent variable and the brain Hcy levels and the ApoE4 genotype as the independent variables. z-score values for p16^{INK4a} expression in the occipital lobe on y-axis. z-score values for brain Hcy levels (dichotomised to smaller than or greater than the mean of the group, μM) on x-axis. ApoEε4 non-carriers (no ApoEε4 allele = 0) and ApoEε4 carriers (either one or two alleles = 1). (p = 0.139, df = 1). Error bars represent standard error of the mean. Top of bars represent mean.
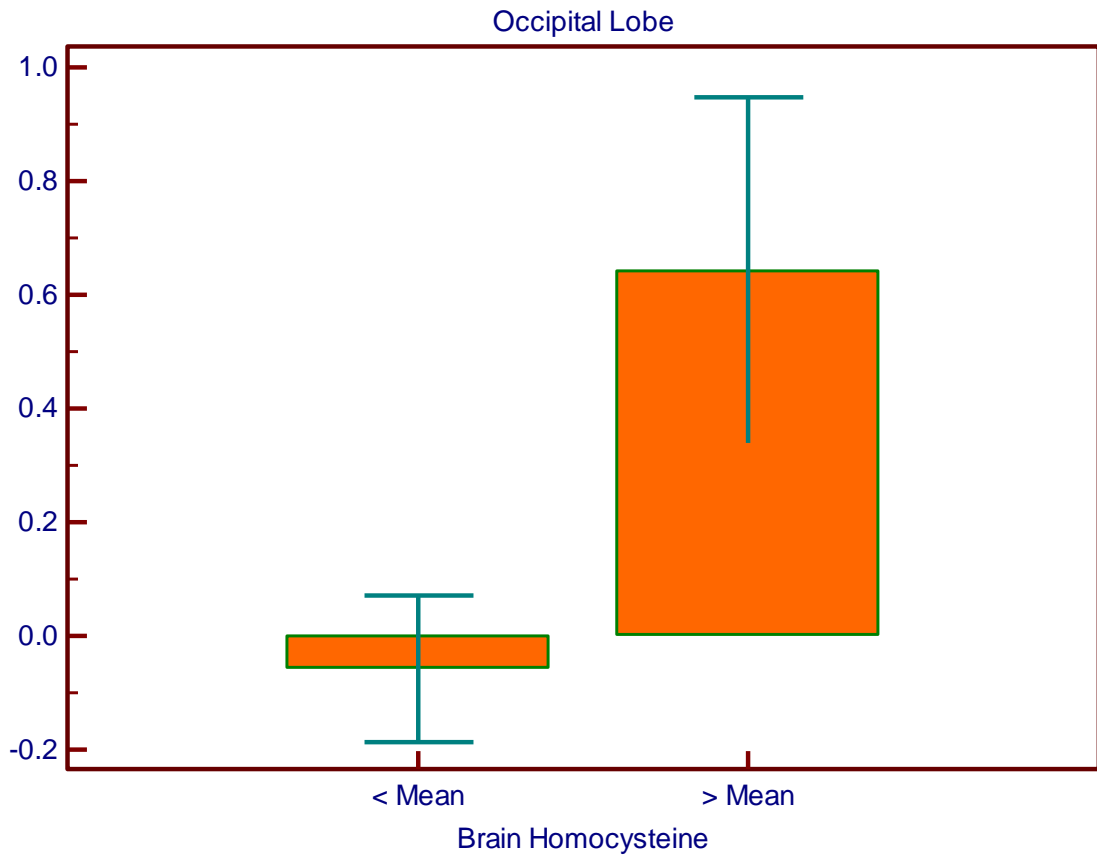
Figure 39

Effect of brain Hcy levels on p27[kip1] expression in the occipital lobe. A Kruskal-wallis test was conducted using p27 expression as the dependent variable and the brain Hcy levels as the independent variable. z-score values for p27[Kip1] expression in the occipital lobe on y-axis. z-score values for brain Hcy levels (dichotomised to smaller than or greater than the mean of the group) on x-axis. Kruskal wallis test. ($p = 0.018$, $df = 1$). Error bars represent standard error of the mean. Top of bars represent mean.
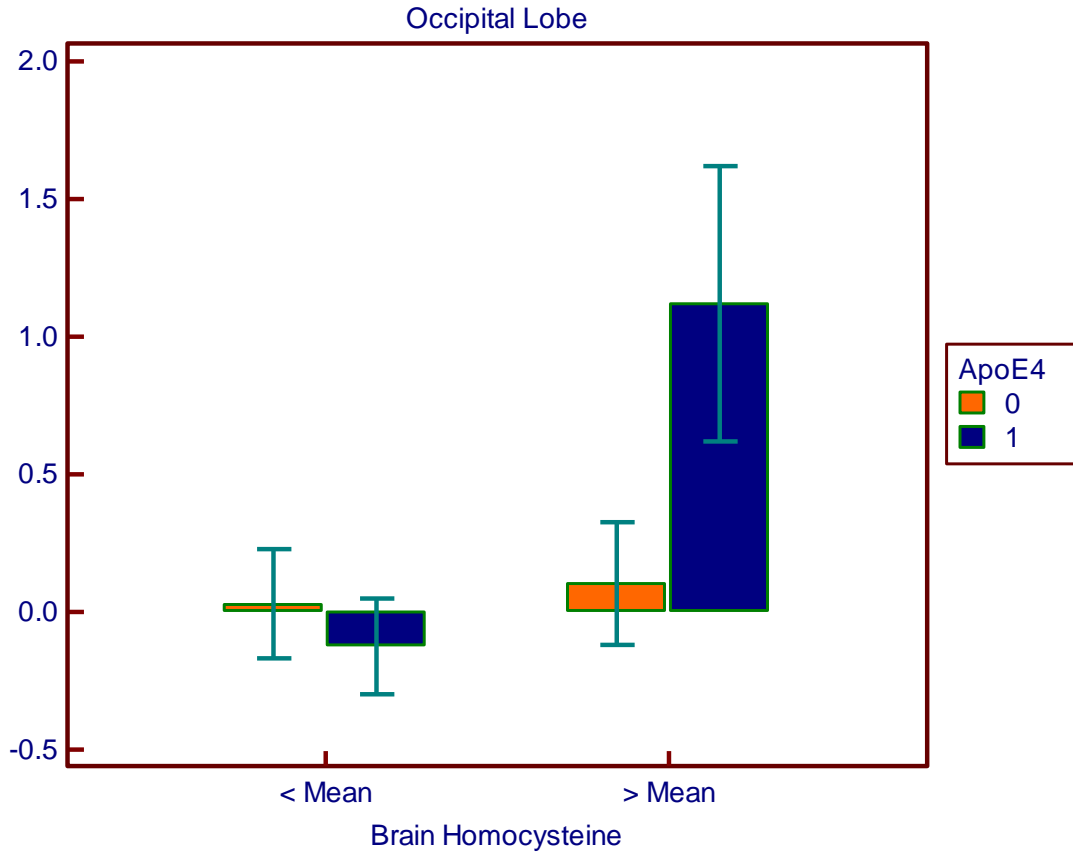
Figure 40

The relationship of brain Hcy, ApoEε4 genotype and p27[Kip1] expression in the occipital lobe. An ANOVA was conducted using p27 expression as the dependent variable and the brain Hcy levels and the ApoE4 genotype as the independent variables. z-score values for p27[Kip1] expression in the occipital lobe on y-axis. z-score values for brain Hcy levels (dichotomised to smaller than or greater than the mean of the group) on x-axis. ApoEε4 non-carriers (no ApoEε4 allele = 0) and ApoEε4 carriers (either one or two alleles = 1). ($p = 0.040$, df = 1). Error bars represent standard error of the mean. Top of bars represent mean.
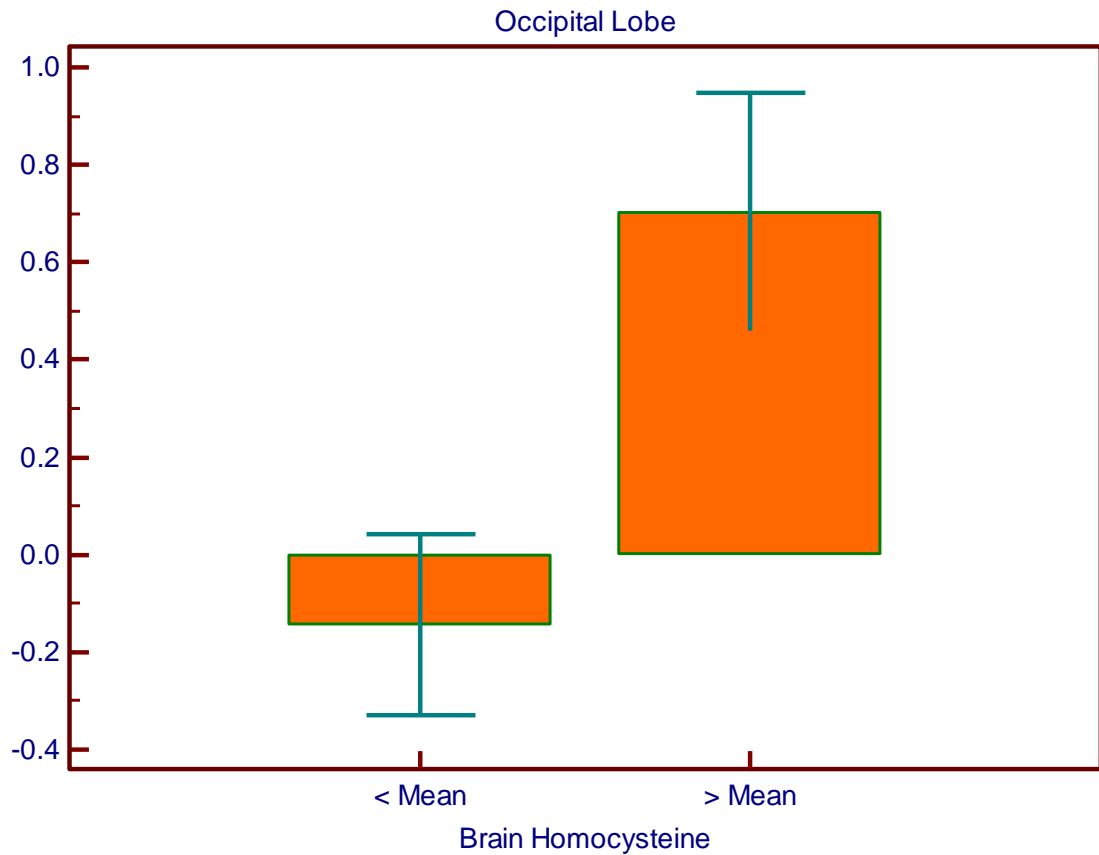
Figure 41

Effect of brain Hcy levels on p57^{Kip2} expression in the occipital lobe. A Kruskal wallis test was conducted using p57 expression as the dependent variable and the brain Hcy levels as the independent variable. z-score values for p57^{Kip2} expression in the occipital lobe on y-axis. z-score values for brain Hcy levels (dichotomised to smaller than or greater than the mean of the group) on x-axis. ($p = 0.005$, $df = 1$). Error bars represent standard error of the mean. Top of bars represent mean.
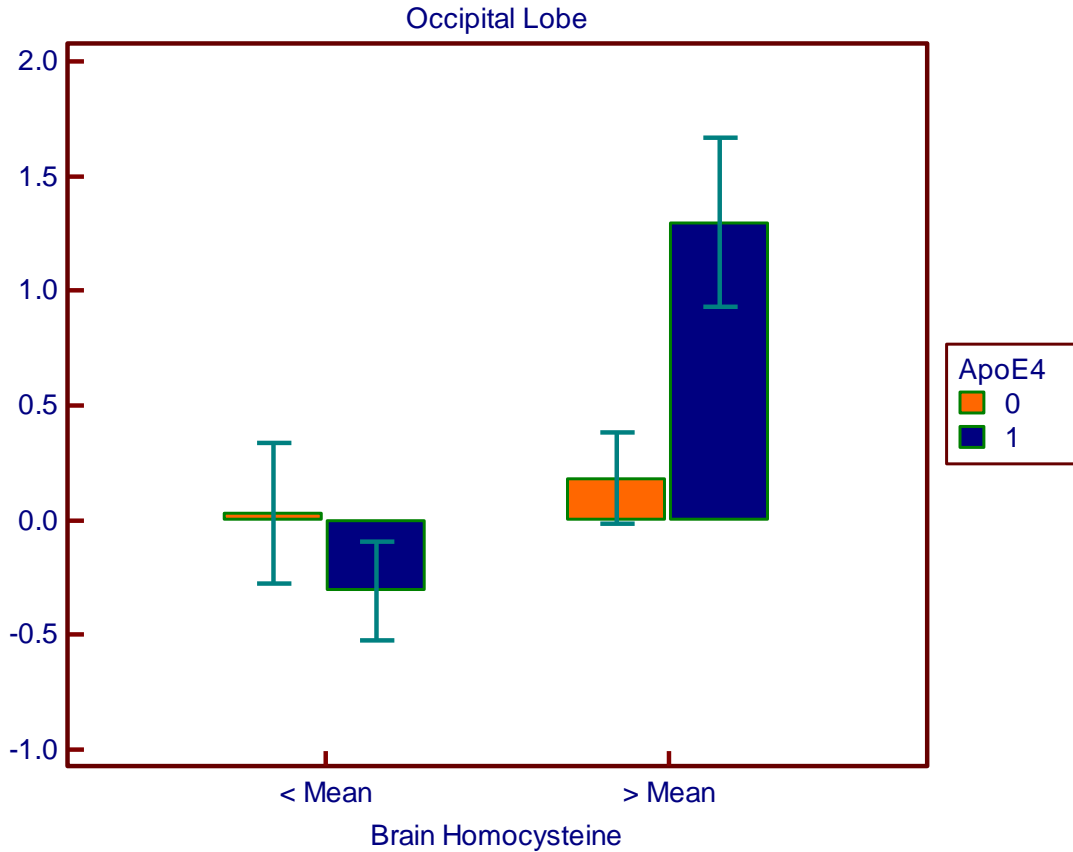
Figure 42

The relationship of brain Hcy, ApoEε4 genotype and p57^{Kip2} expression in the occipital lobe. An ANOVA was conducted using p57 expression as the dependent variable and the brain Hcy levels and the ApoE4 genotype as the independent variables. z-score values for p57^{Kip2} expression in the occipital lobe on y-axis. z-score values for brain Hcy levels (dichotomised to smaller than or greater than the mean of the group) on x-axis. ApoEε4 non-carriers (no ApoEε4 allele = 0) and ApoEε4 carriers (either one or two alleles = 1). (p = 0.019, df = 1). Error bars represent standard error of the mean. Top of bars represent mean.

4.2. IN VITRO STUDY

(HYPOTHESIS 3)

To study the effects of Hcy on neurones and its possible interaction with ApoE we set up *in vitro* experiments using the SH-SY5Y human neuroblastoma cell line. This cell line differentiates into cells with morphological characteristics of neurones such as neurite outgrowth, and expresses neurone-specific markers (e.g. β-tubulin III). Additionally this cell line expresses the AD-related proteins tau and amyloid precursor protein (APP). Using this model we could investigate directly the effect of Hcy and ApoE on cell survival, AD-related pathology and cell cycle kinetics.

The SH-SY5Y human neuroblastoma cultures were pre-differentiated for 5 days with 10μM retinoic acid. This was followed by a 24 hour treatment with D-L homocysteine with and without the human recombinant ApoE isoforms. Cell death was quantified by LDH assay. ACUMEN cytometry was used to analyse the cell cycle kinetics. The LDH assay in combination with ACUMEN cytometry allowed calculation of population doubling times and the length of the individual phases of the cell cycle. AD related expression of phospho-tau (AT8) and beta amyloid were measured in different cell populations using the ACUMEN cytometer.

Note: A separate neuroblastoma culture was set up and treated with L-Cysteine (data not shown). The results of the analysis of the L-Cysteine cultures were different the results of the analysis of the D-L homocysteine treated cultures. This confirms that the results seen in the D-L homocysteine treated cultures were due only to Hcy, and not because Hcy was converted to cysteine via the transsulfuration pathway.

4.2.1. The Effect of Homocysteine and ApoE on Cell Proliferation, Cell Death and Cell Cycle Kinetics.

We have used cell cytometry (following propidium iodide staining) to assess cell numbers, apoptotic cells and cell cycle kinetics. Using the cytometry data, coupled with the LDH assay results (measuring necrotic cell death), our standard mathematical model allowed the calculation of the length of the different phases of the cell cycle and the population doubling times.

After 24 hours of Hcy treatment at doses >5uM, we found a significant increase ($p<0.05$) in the cell numbers, with a slight drop in cell numbers at the highest dose (Figure 43a). Necrotic cell death was reduced at lower doses and then returned to control level at high doses, i.e. above 40µM (see Figure 43a grey). The population doubling times significantly decreased with Hcy treatment (Figure 43b).

Key

Homocysteine *only* - Black

Homocysteine & ApoE2 - Green

Homocysteine & ApoE3 - BLUE

Homocysteine & ApoE4 – Red

(Note - Key for Figure 43 to Figure 54)

A

B
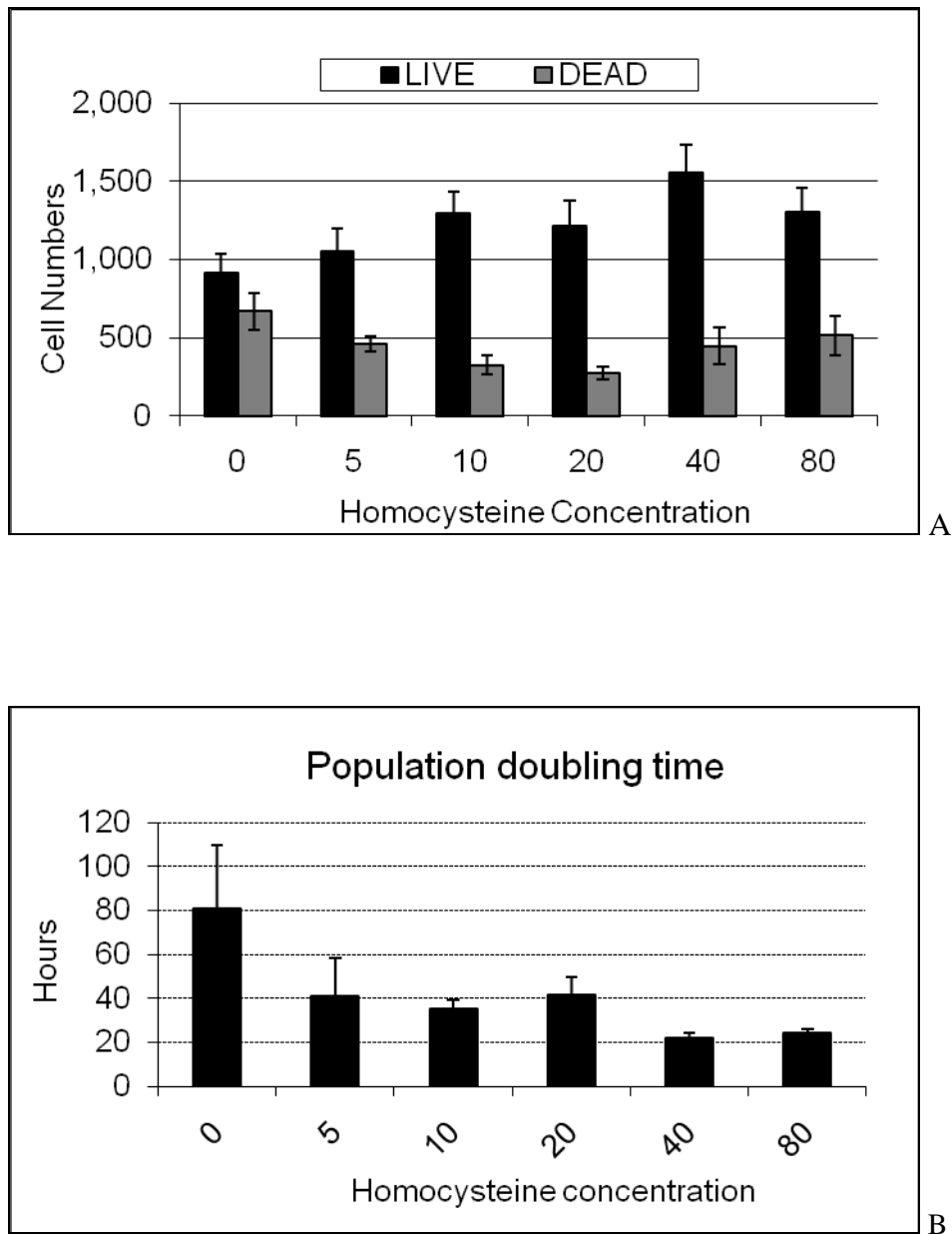
Figure 43

Homocysteine Only. The effect of Hcy (μM) on cell proliferation. A – Live cells (black) and

dead cells (grey). B – Population doubling times (hours).

In the presence of recombinant ApoE2 isoform, the cell numbers significantly decrease with Hcy concentration >20µM, (Figure 44a green). The reduction of live cell numbers is parallel to the increase of dead cell numbers (Figure 44b grey). Significant decrease in the population doubling times is only notable at Hcy concentrations >20µM (Figure 44b).

A

B
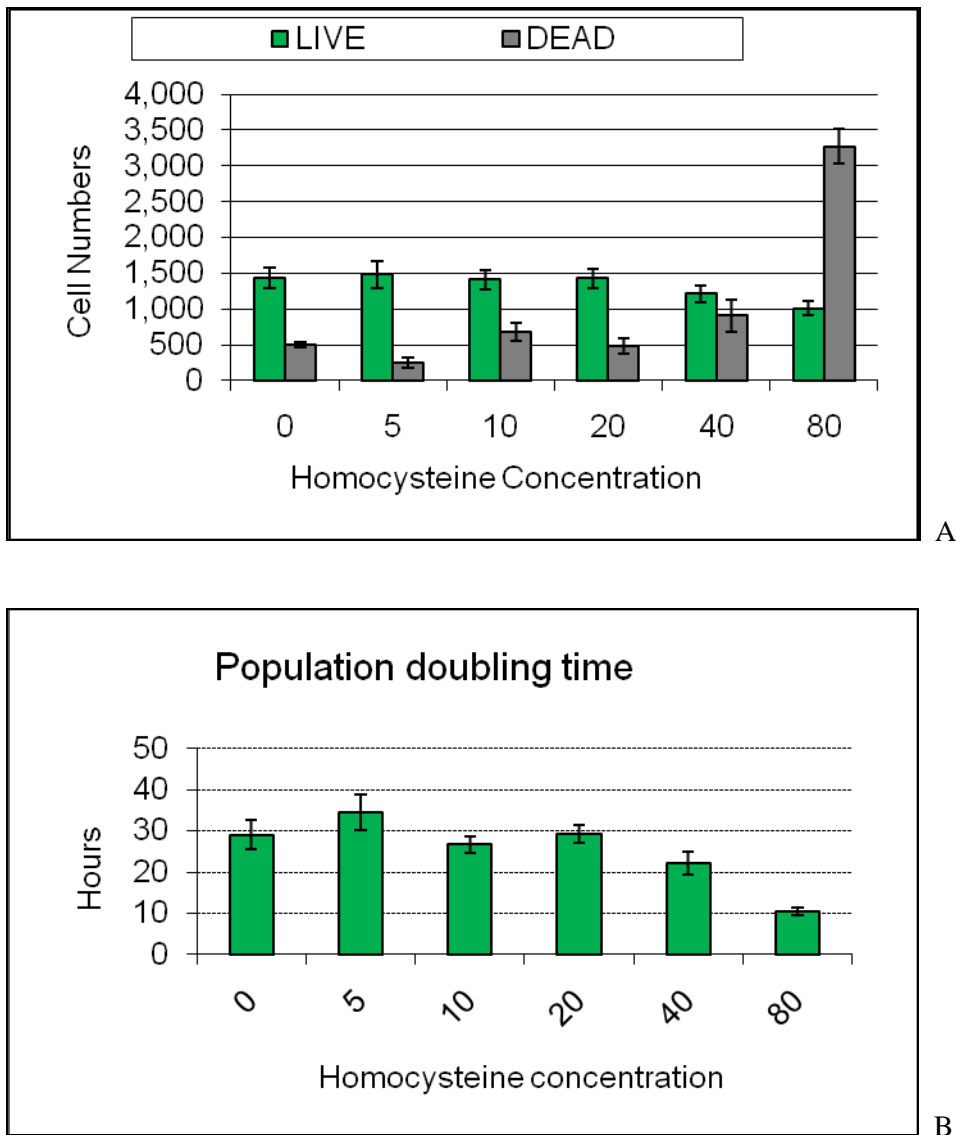
Figure 44

The effect of Hcy (µM) in the presence of ApoE2 on cell proliferation. A – Live cells (green) and dead cells (grey). B – Population doubling times (hours).

With ApoE3 isoform supplementation, there was no significant change in the live cell numbers with Hcy treatment (Figure 45a blue). However dead cell number was found to significantly decrease in Hcy treated cultures (Figure 45a grey). A slight increase in the population doubling times at low doses is associated with a significant reduction in cell death (Figure 45a & b). At high doses, the Hcy-induced inhibition of cell proliferation disappears without a significant increase in cell death.

A

B
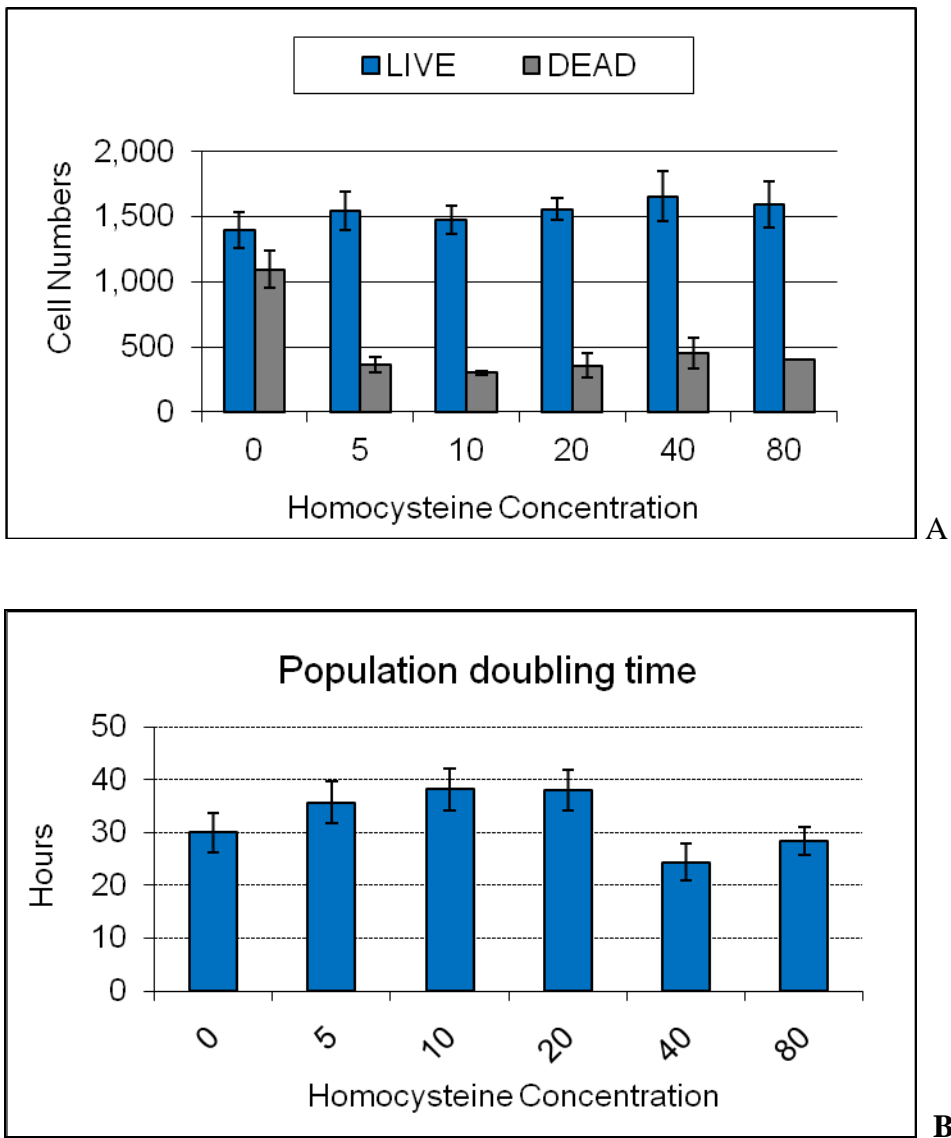
Figure 45

Homocysteine and ApoE3

The effect of Hcy (μM) in the presence of ApoE3 on cell proliferation. A – Live cells (blue) and dead cells (grey). B – Population doubling times (hours).

Finally, in the presence of the ApoE4 isoform, live cell numbers do not change significantly with Hcy treatment in the cultures (Figure 46a red). However, increasing concentrations of Hcy is associated with increasing cell death (Figure 46a grey), leading to a gradually decreasing population doubling time (Figure 46b).

A

B
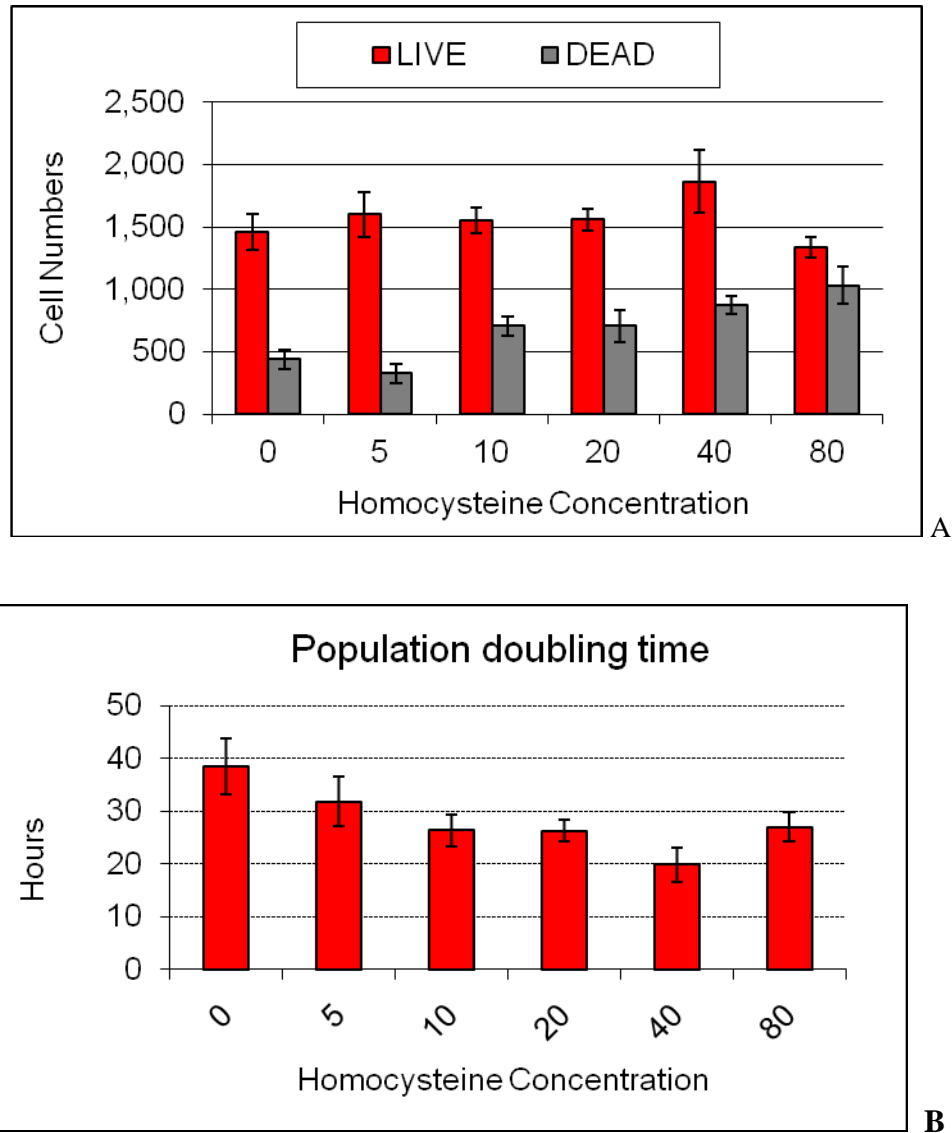
Figure 46

Homocysteine and ApoE4

The effect of Hcy (μM) in the presence of ApoE4 on cell proliferation. A – Live cells (red) and dead cells (grey). B – Population doubling times (hours).

The addition of ApoE to the cultures reduces populations doubling time, significantly reversing some of the differentiating effect of retinoic acid (Figure 47a). The baseline proliferation time in the presence of ApoE is almost identical for the three isoforms.

However, the addition of Hcy to the cultures treated with ApoEelicits a different isoforms dependent effect (Figure 47b). In the presence of ApoE2, Hcy levels up to 20μM have no significant effect on cell proliferation, whereas higher concentrations of Hcy elicit a significant and dose dependent increase in the speed of proliferation (decrease in population doubling times). With ApoE3 treatment, Hcy at low doses (below 20μM) increases baseline population doubling time (slows proliferation). This effect disappears at higher doses. =In ApoE4 treated cultures, Hcy leads to a steady dose dependent decrease in population doubling times that appears to level out with treatment above 40μM (Figure 47b).

A

B
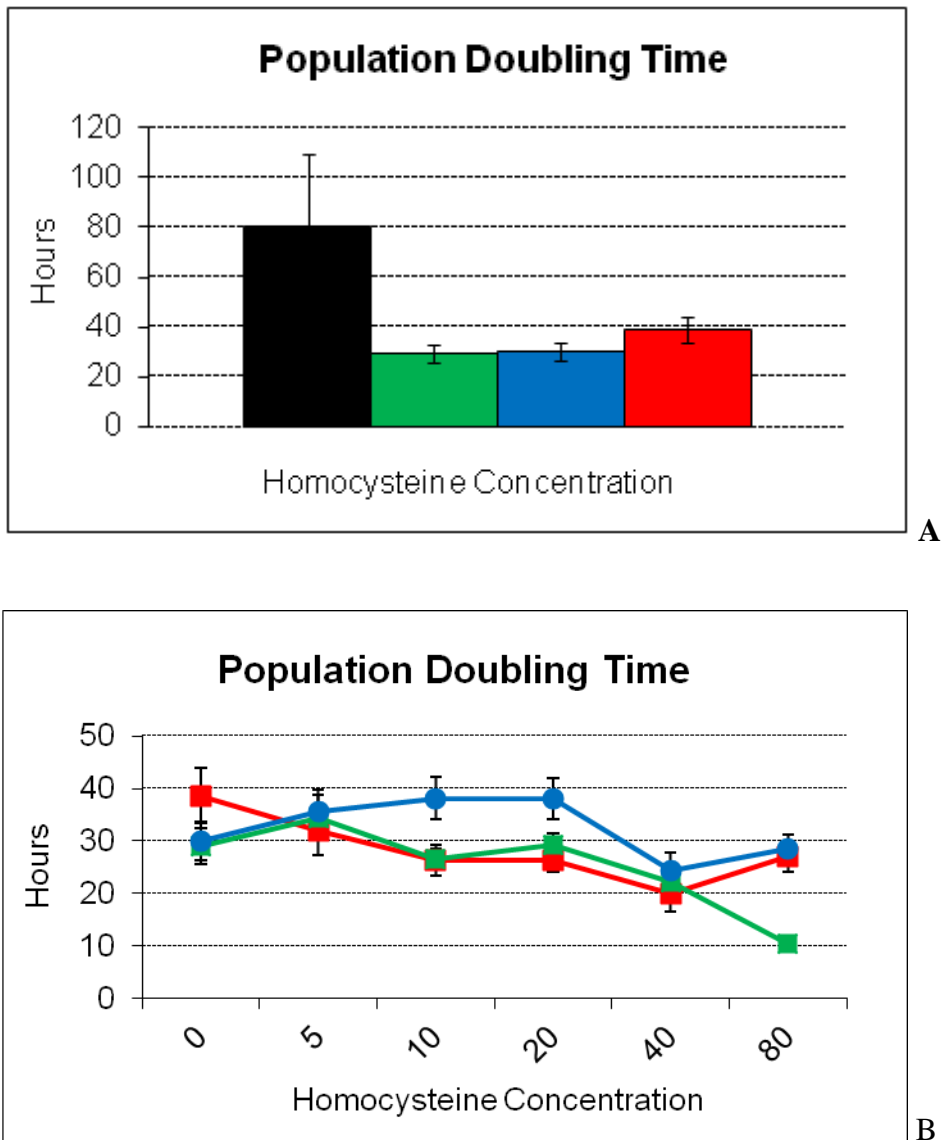
Figure 47

ApoE Isoforms

A - The effect of the ApoE isoforms on cell proliferation. B – The effect of the ApoE isoforms and Hcy (μM) on cell proliferation. ApoE2 (green), ApoE3 (blue), ApoE4 (red).

The changes of the population doubling times in Hcy treated cultures are associated with alterations of the cell cycle kinetics in an isoforms dependent manner.

In the ApoE2 treated cultures, higher doses of Hcy (i.e. above 40µM) leads to an accumulation of cells in the G2 phase of the cell cycle, at the expense of the G1 fraction (Figure 48a). This trend in the ApoE3 cultures is only seen at the highest concentration of Hcy (Figure 48b). While this effect disappears entirely in the presence of ApoE4 (Figure 48c).

A

Figure 48

B

C
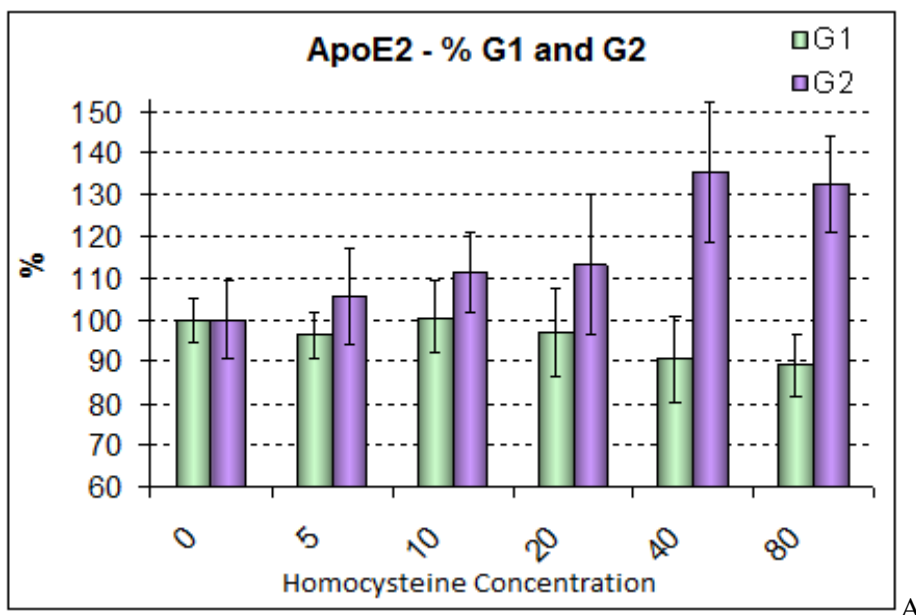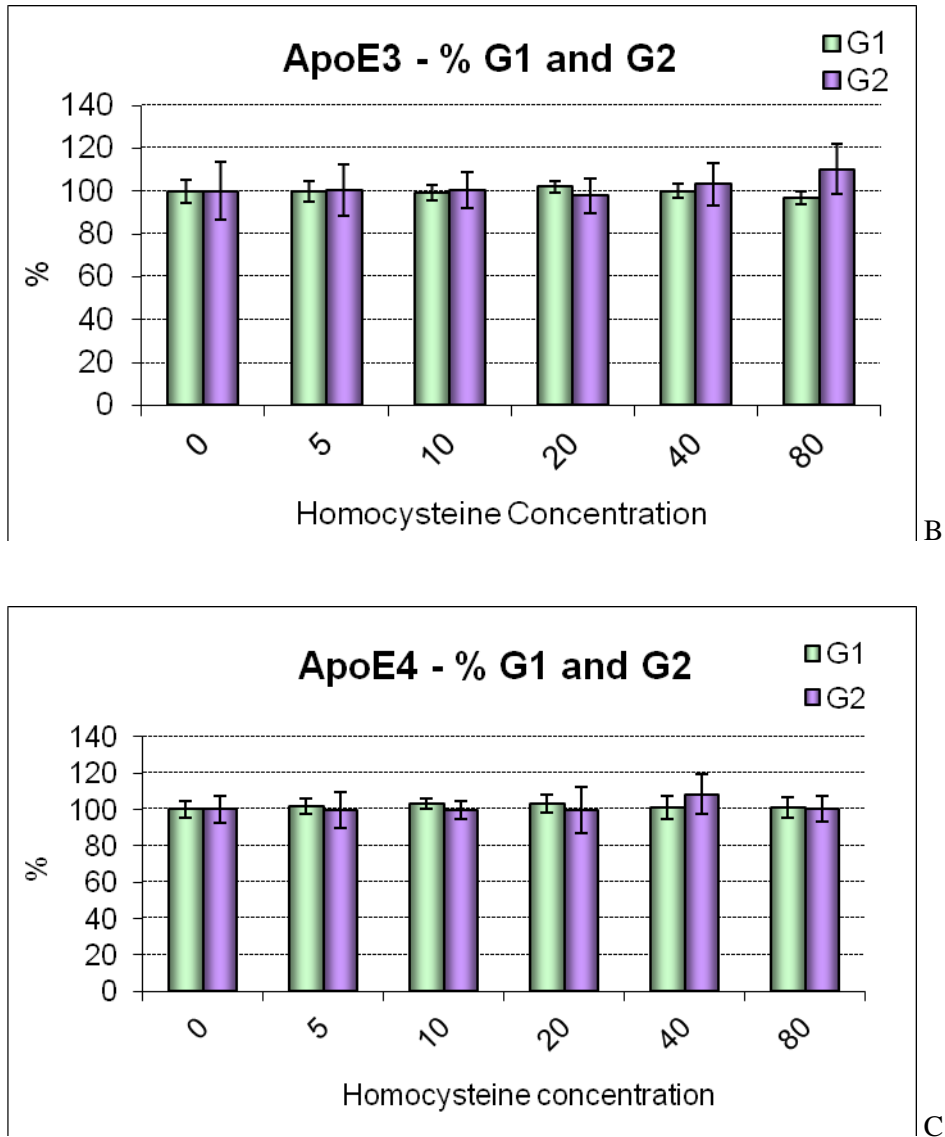
Figure 48

The effect of the ApoE isoforms and Hcy (μM) on the % of G1 and G2 cells. A – ApoE2. B - ApoE3 and C - ApoE4.

4.2.2. The Effect of Homocysteine and ApoE on AD-Related Pathology

4.2.2.1. Phospho-tau production

In the neuroblastoma cell line the baseline p-tau levels (AT8 positive) are significantly higher in G2 phase cells that in G1 cells (Figure 48a). The addition of the fraction of p-tau containing cells is different in the two sub-populations is also significantly different ((Figure 48b).). Baseline levels of p-tau are slightly different in cultures treated with different ApoE isoforms (Figure 48c).

The effects of Hcy are significantly different in cultures treated with the different ApoE isoforms. Hcy alone has very little effect on overall p-tau expression. At very high doses the p-tau content of the G2 cells increases, but there is no alteration in the number of p-tau containing G2 cells (Figure 49). In the presence of ApoE2, high dose Hcy treatment reduces the cellular p-tau expression compared to that of cells treated with no or low dose Hcy (Figure 50a). This reduction in p-tau level is due to a response to high Hcy in both the G1 and G2 cell populations (Figure 50b). In the G1 population, there is a reduction in the number of p-tau positive cells combined with a reduction of p-tau content of the positive cells (Figure 50c and d). While in the G2 population, the reduction in p-tau expression of the whole population is only associated with a reduction in p-tau expression of the positive cells, and not associated with a reduction in the number of cells that express the protein (Figure 50c and d).

A

B

Figure 48

C
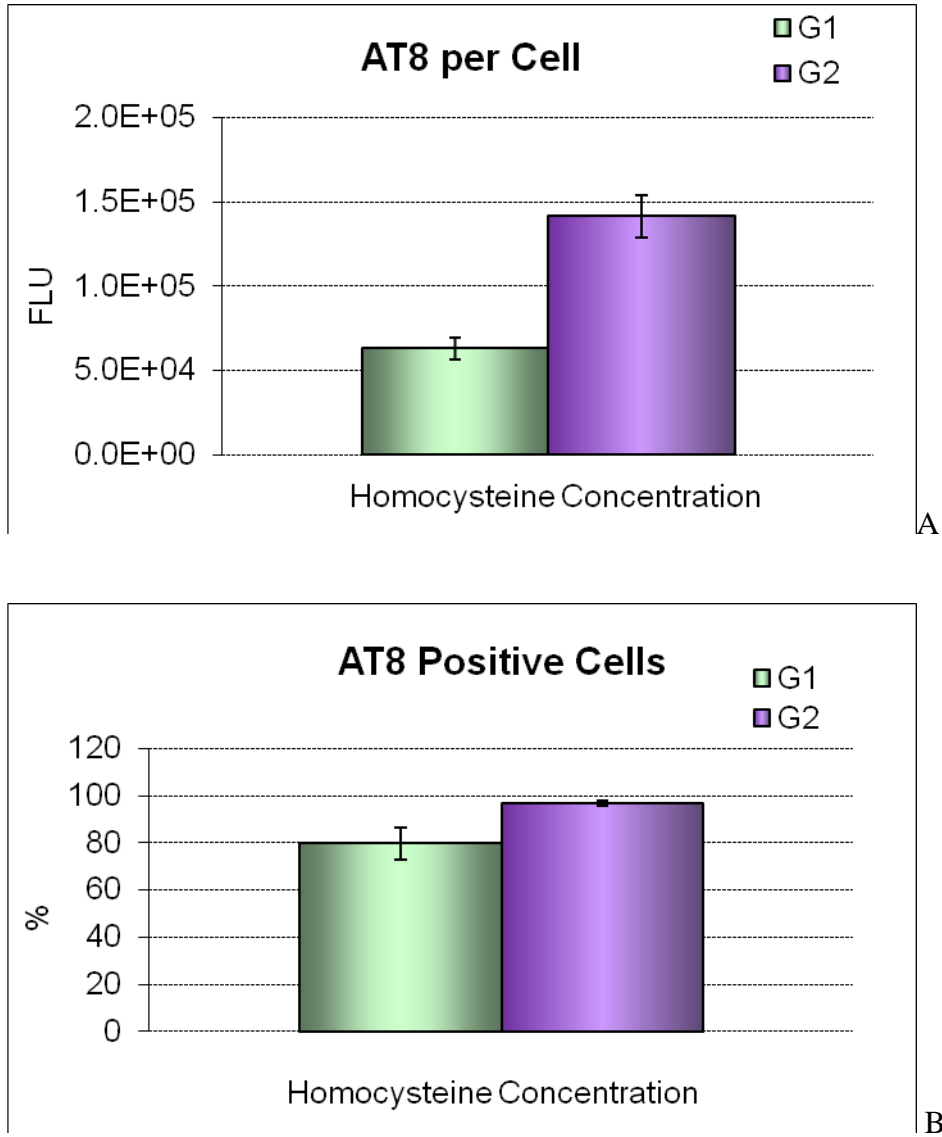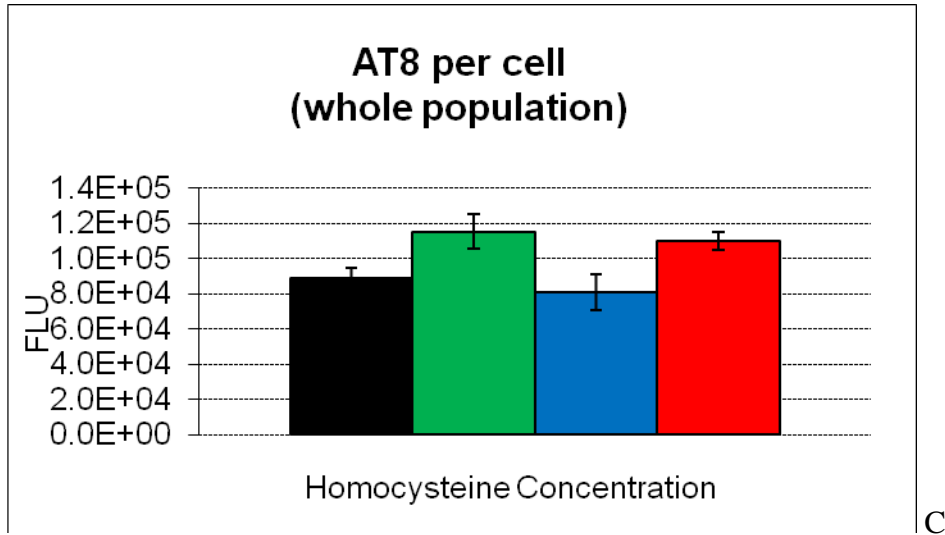
Figure 48

A - The p-tau content in G1 and G2 cells. B - The % of p-tau positive G1 and G2 cells. B - The effect of the ApoE isoforms on p-tau expression. ApoE2 (green), ApoE3 (blue), ApoE4 (red).
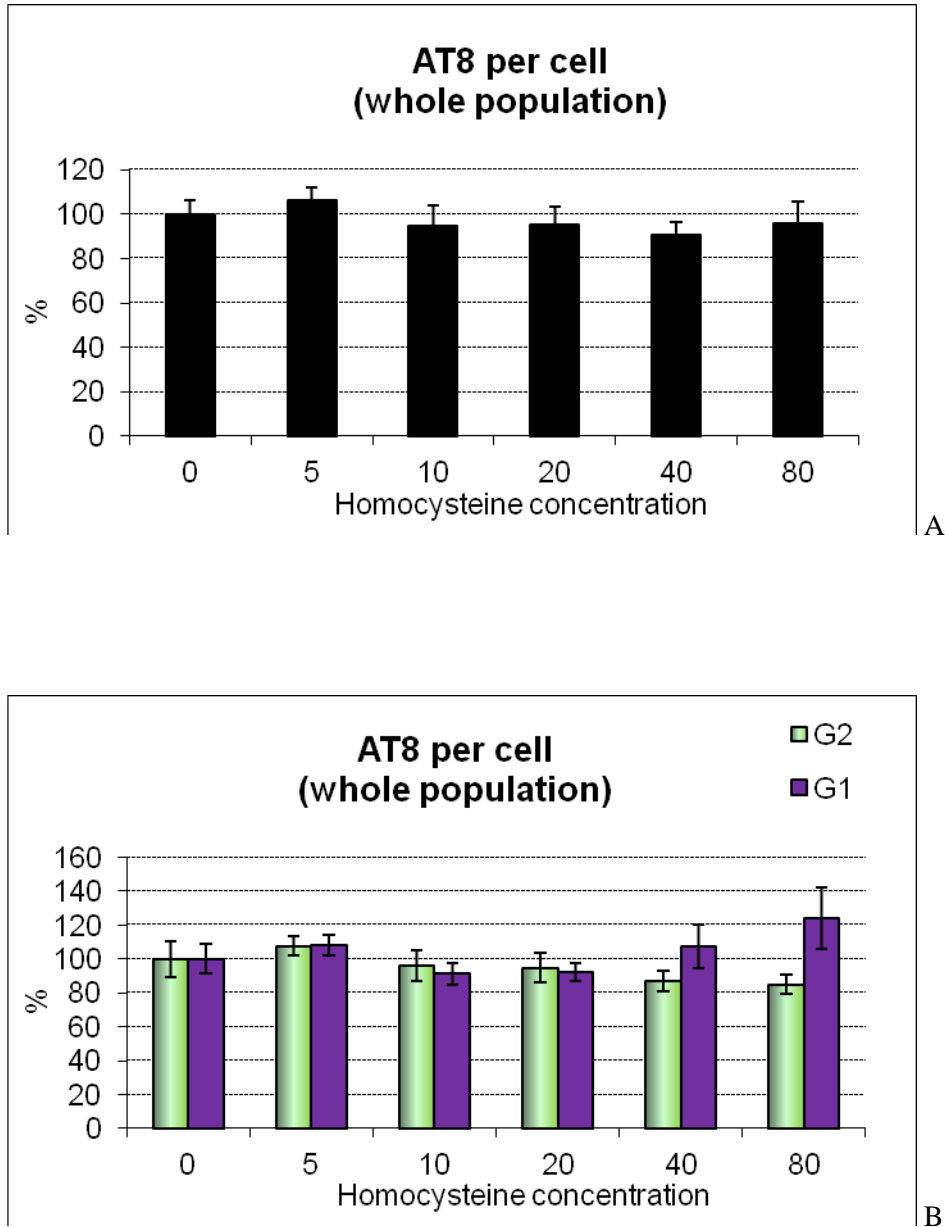
Figure 49

Homocysteine Only - The effect of Hcy (µM) on p-tau accumulation. A – AT8 expression per

cell. B – AT8 expression in G1 and G2 cells. C – Percentage of AT8 positive G1 and G2

cells.

C

Figure 49

Homocysteine Only - The effect of Hcy (µM) on p-tau accumulation. A – AT8 expression per cell. B – AT8 expression in G1 and G2 cells. C – Percentage of AT8 positive G1 and G2 cells.

A

B

Figure 50

C

D
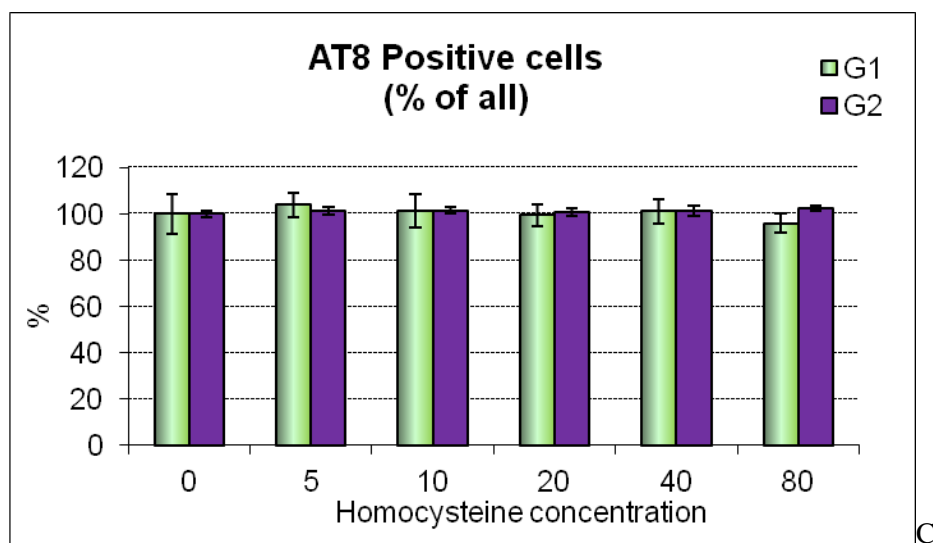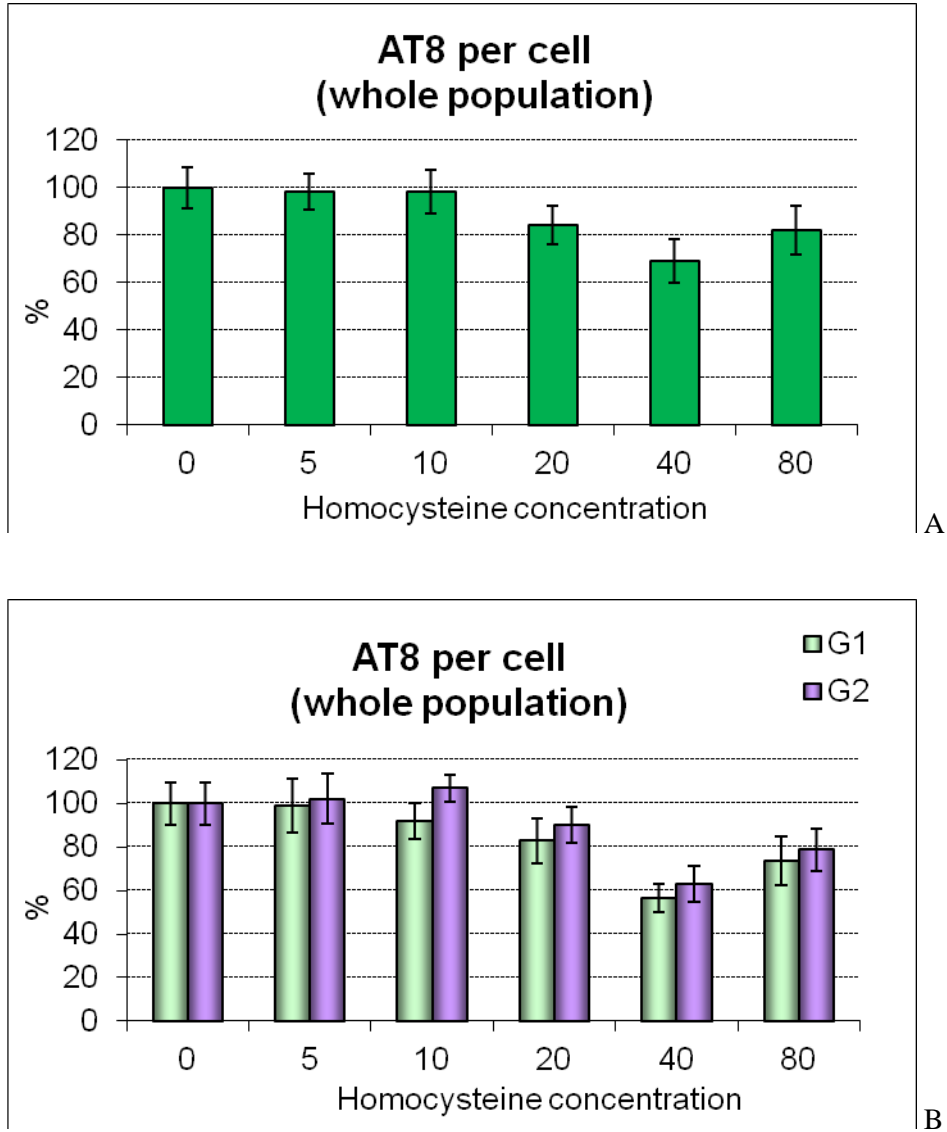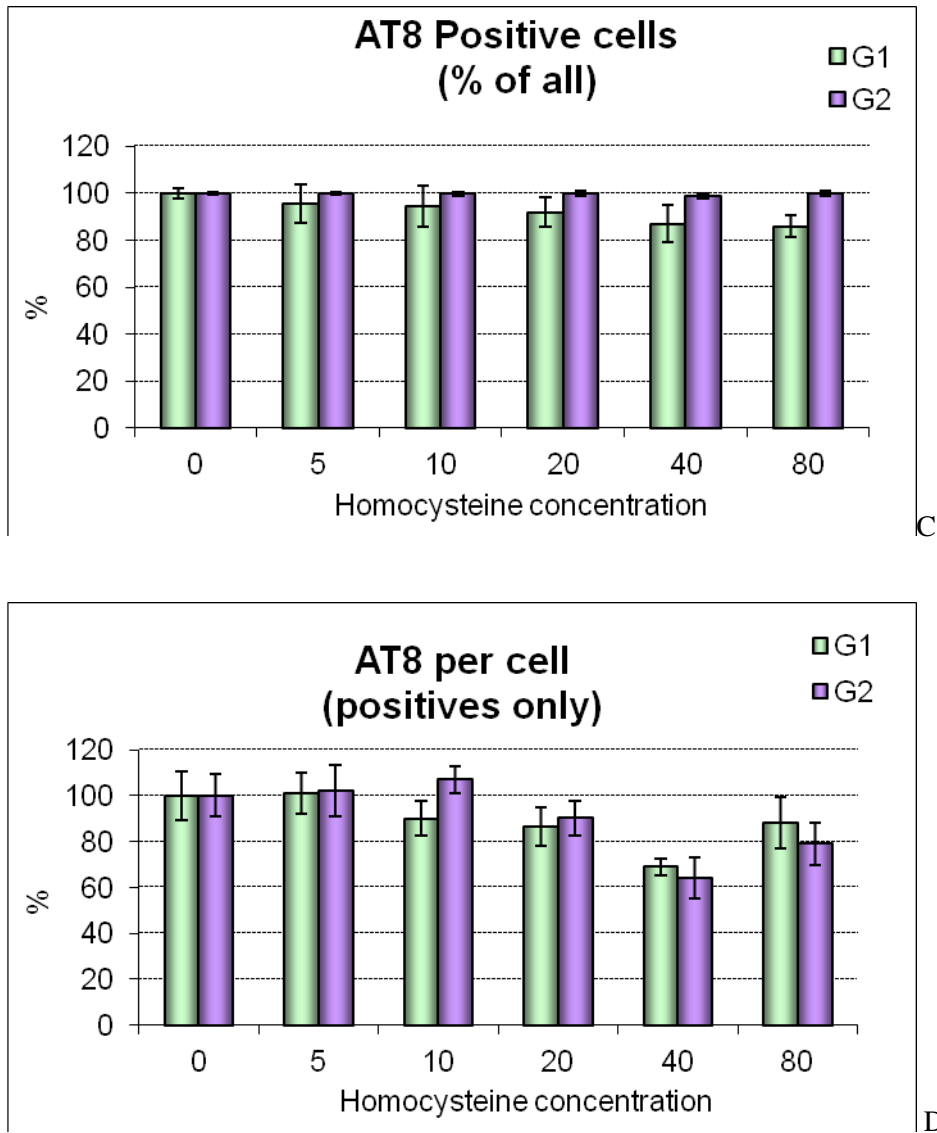
Figure 50

The effect of Hcy (µM) in the presence of ApoE2 on p-tau accumulation. A – AT8 expression

per cell. B – AT8 expression in G1 and G2 cells. C – Percentage of AT8 positive G1 and G2

cells. D - Percentage of AT8 in G1 and G2 positive cells.

In ApoE3 treated cultures, Hcy increases AT8 expression in a dose dependent manner (Figure 51a). This increase is more significant in the G2 cell population with no effect on the G1 population (Figure 51b). The significant change in the G2 population is due entirely to the increase of the p-tau content of these cells as there is no change in the number of positive G2 cells (Figure 51c & d).

ApoE4 with Hcy does not affect p-tau levels significantly in the population as a whole (Figure 52a). The positive cell numbers and p-tau content of both G1 and G2 cell populations seem unaffected by Hcy (Figure 52c-d).

A

B

C

Figure 51

D
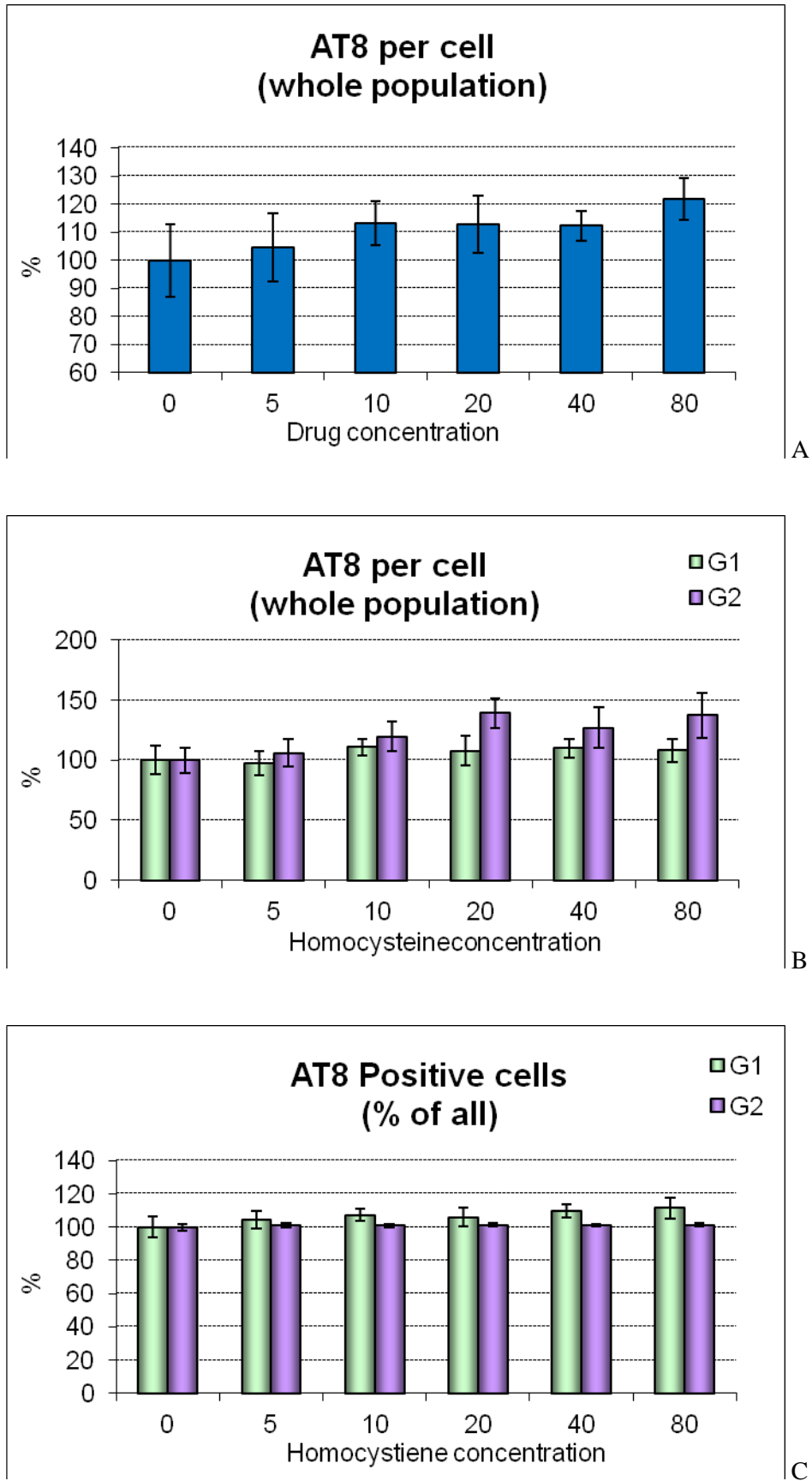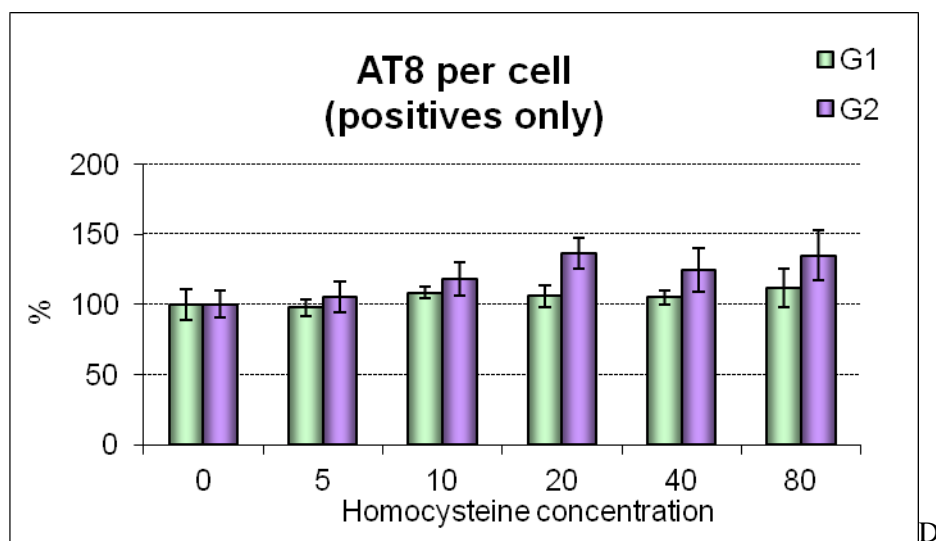
Figure 51

The effect of Hcy (µM) in the presence of ApoE3 on p-tau accumulation. A – AT8 expression

per cell. B – AT8 expression in G1 and G2 cells. C – Percentage of AT8 positive G1 and G2

cells. D - Percentage of AT8 in G1 and G2 positive cells.

AT8 per cell (whole population)

A

AT8 per cell (whole population)

B

AT8 Positive cells (% of all)

C
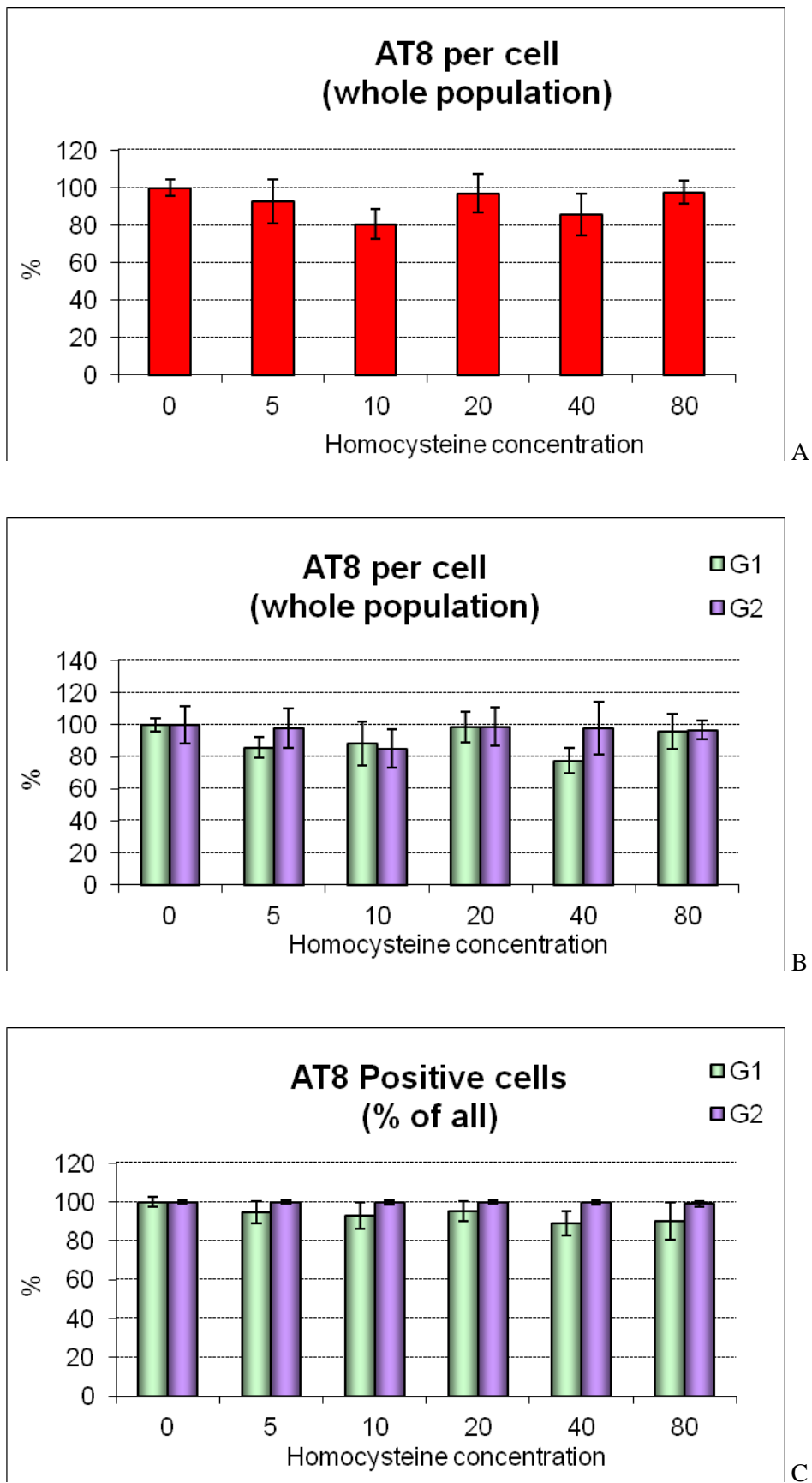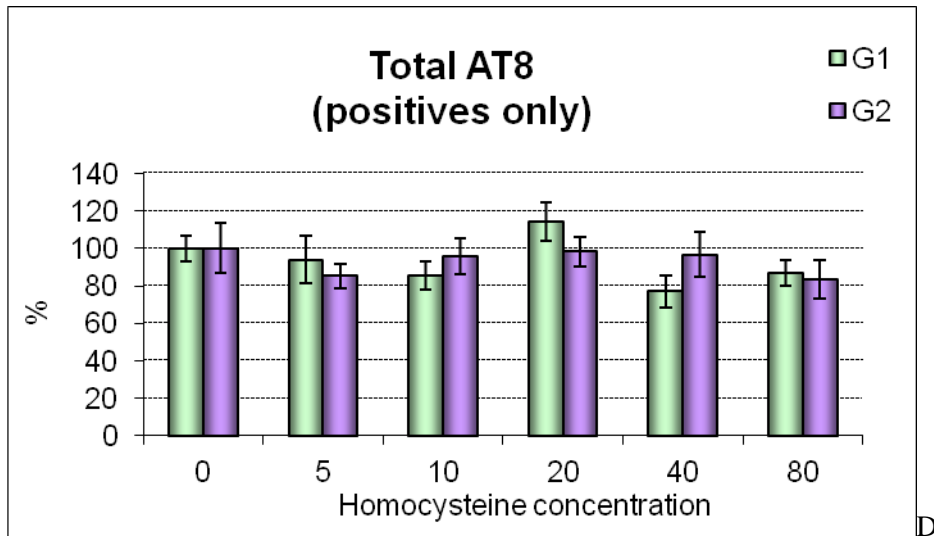
Figure 52

Figure 52

The effect of Hcy (μM) in the presence of ApoE4 on p-tau accumulation. A – AT8 expression

per cell. B – AT8 expression in G1 and G2 cells. C – Percentage of AT8 positive G1 and G2

cells. D - Percentage of AT8 in G1 and G2 positive cells.

When comparing the Hcy induced changes in AT8 expression, in the cultures treated with the different ApoE isoforms, we found that the levels of p-tau increased in the ApoE3 treated cultures. In the presence of ApoE2, there was a decrease from baseline with treatment above 10μM of Hcy. The only change seen in the presence of ApoE4, was at 10μM of Hcy treatment, where there was a decrease from baseline (see Figure 53).
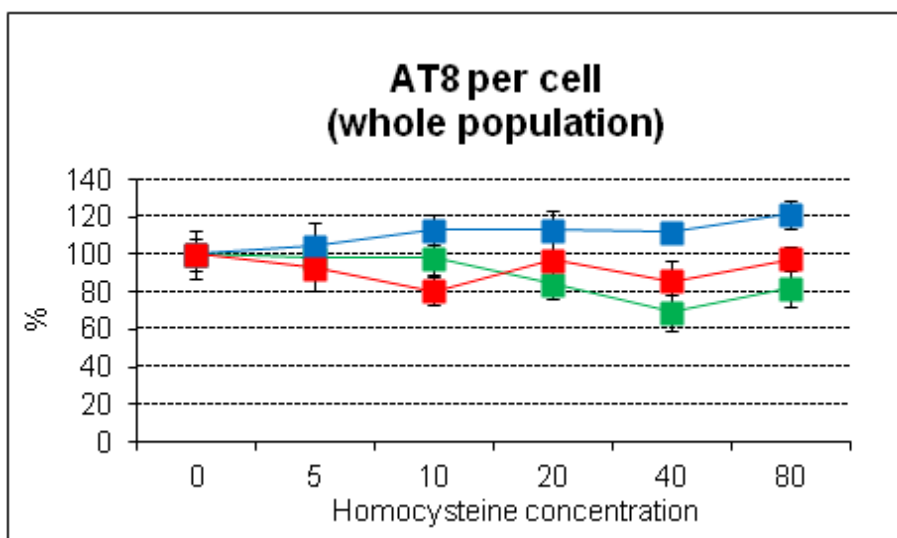
Figure 53

The effect of the ApoE isoforms and Hcy (μM) on AT8 expression. ApoE2 (green), ApoE3 (blue), ApoE4 (red).

4.2.2.2. Beta Amyloid- Positive Cells

Similar to the p-tau cell cytometry results, the beta amyloid content of the G2 cells is always significantly higher than that of G1 cells. Furthermore, a significantly larger fraction of the G2 cell population contains beta amyloid than that of the G1 population (see Figure 54a).

Addition of the ApoE isoforms to the cultures significantly alters the beta amyloid expression per cell compared to that of the control cultures: there is higher beta amyloid expression per cell in the presence of ApoE2 compared to ApoE3 and ApoE4 (Figure 54b).

The beta amyloid levels show minor fluctuations in the cultures treated with the different ApoE isoforms, but there is no obvious dose dependent change induced by Hcy in the different cultures (Figure 54c). However, due to the difference in the baseline beta amyloid level in the three cultures, the absolute levels of beta amyloid are significantly higher in the presence of ApoE2 and ApoE4 compared to ApoE3 (Figure 54d).

Figure 54

Figure title: **Beta Amyloid per cell (whole population)** — D

Figure title: **Beta Amyloid per cell (whole population)** — E
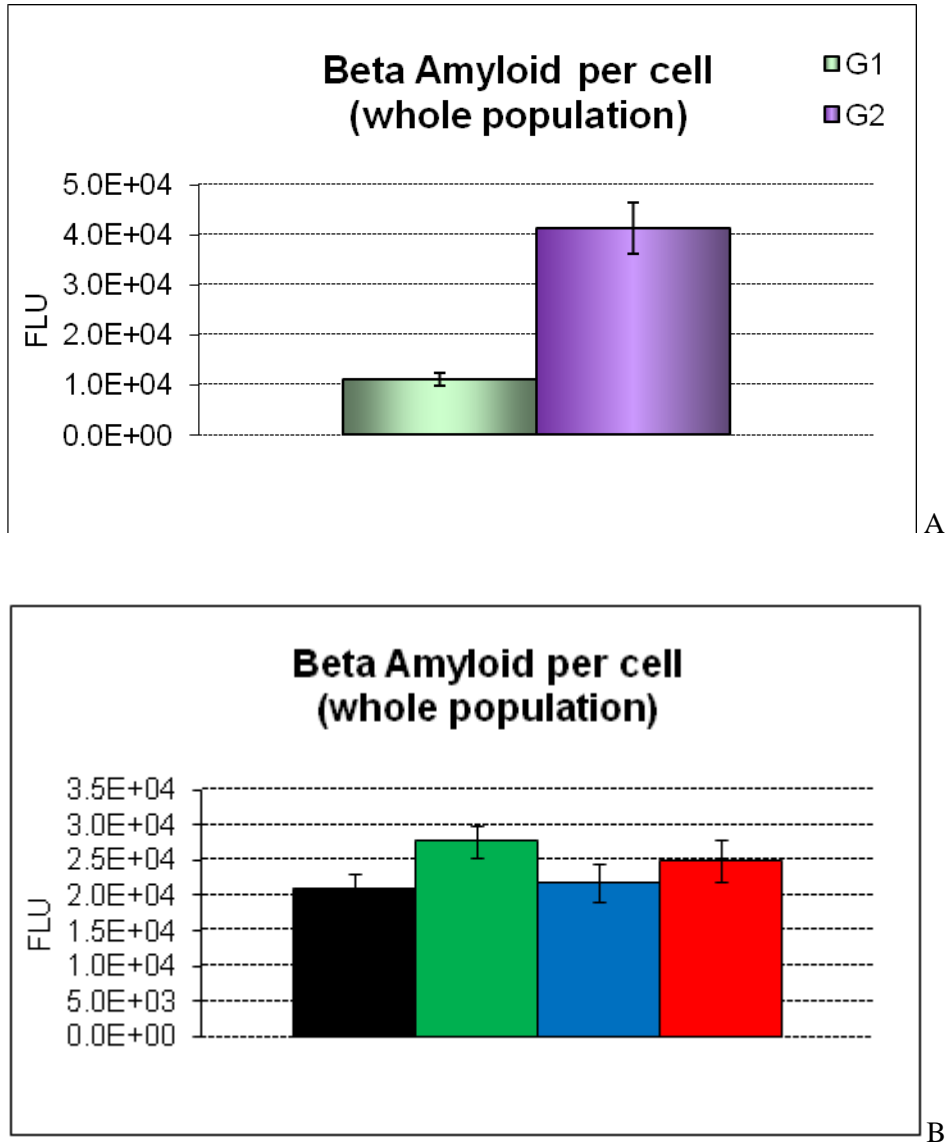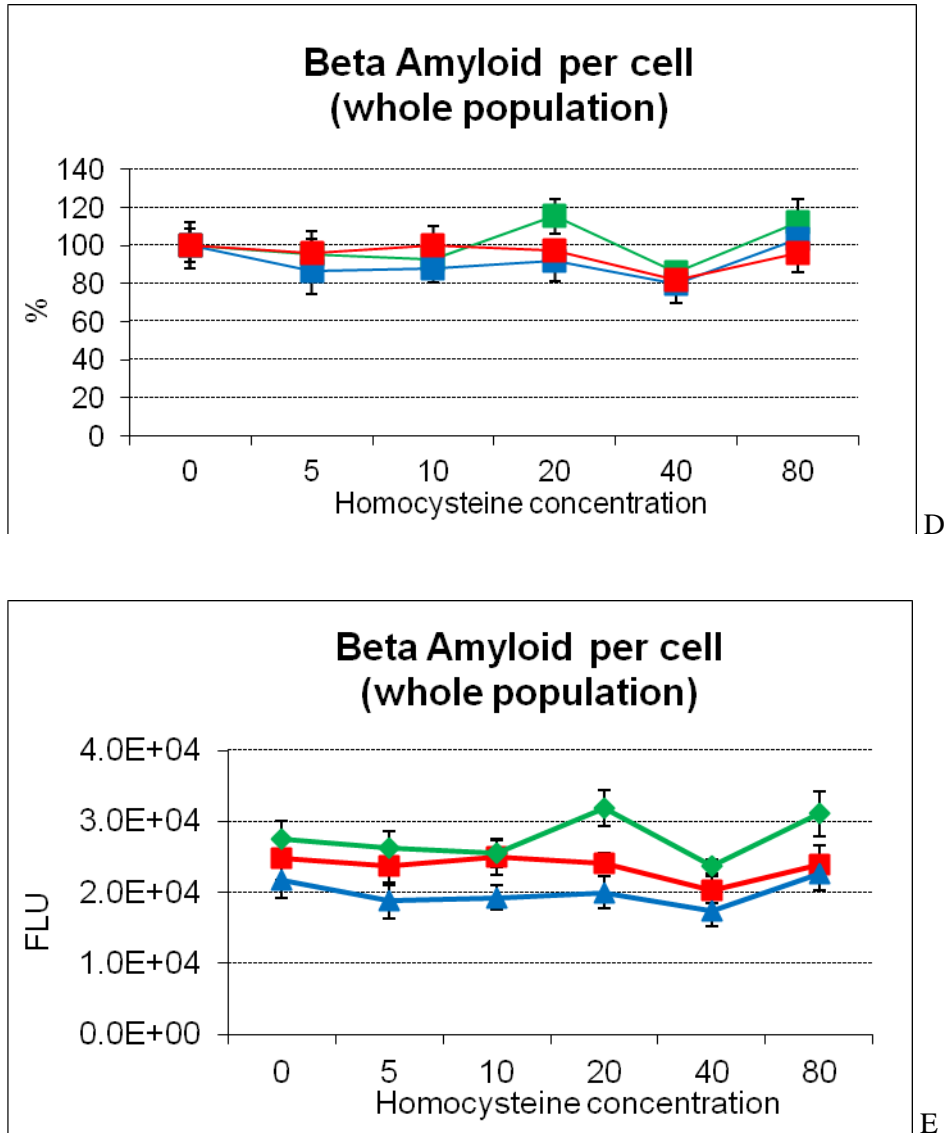
Figure 54

The effect of the ApoE isoforms and Hcy (µM) on beta amyloid expression. A - Beta amyloid content in G1 and G2 cells. B - Beta amyloid expression in the presence of ApoE isoforms. C - Percentage of beta amyloid in the whole population with increase Hcy concentration (µM). D -. Beta amyloid expression (absolute values) in the whole population. ApoE2 (green), ApoE3 (blue), ApoE4 (red).

4.2.3. The Effect of Homocysteine and ApoE on the Methylation of Cell Cycle Regulatory Genes.

Using differentiated SH-SY5Y human neuroblastomas, we could directly investigate the effect Hcy and ApoE isoforms have on the methylation status of CDKI genes.

p16^{INK4a} gene promoter analysis revealed that, in the presence of ApoE3, low doses of Hcy (5 and 20μM) lead to a slight increase in methylation, while the high dose lead to a decrease in methylation of the promoter (see Figure 55a). In the presence of ApoE4, increasing concentrations of Hcy increase the methylation of p16^{INK4a}. In the ApoE4 treated cultures, the methylation status of the promoter is significantly lower at baseline, and significantly higher from 20μM Hcy concentration than in the ApoE3 treated cultures.

p15^{INK4b} promoter methylation status did not change with increasing Hcy concentration in the presence of ApoE3 (see Figure 55b). With ApoE4 supplementation, 80μM of Hcy was found to increase p15^{INK4b} methylation to 0.45%. No significant difference was seen between 5 and 20μM Hcy treatment in the presence of ApoE4 (0.01 & 0.02% respectively).

For p21^{cip1}, p27^{kip1} and p57^{kip2} promoter methylation we calculated an overall average for the methylation status of the three promoter regions. In the presence of ApoE3, we see an interesting bell-shaped dose curve in response to increasing Hcy concentrations. While, in the

presence of ApoE4, the methylation of these genes is upregulated by even the lowest dose of

Hcy concentration, see Figure 56.

A

B
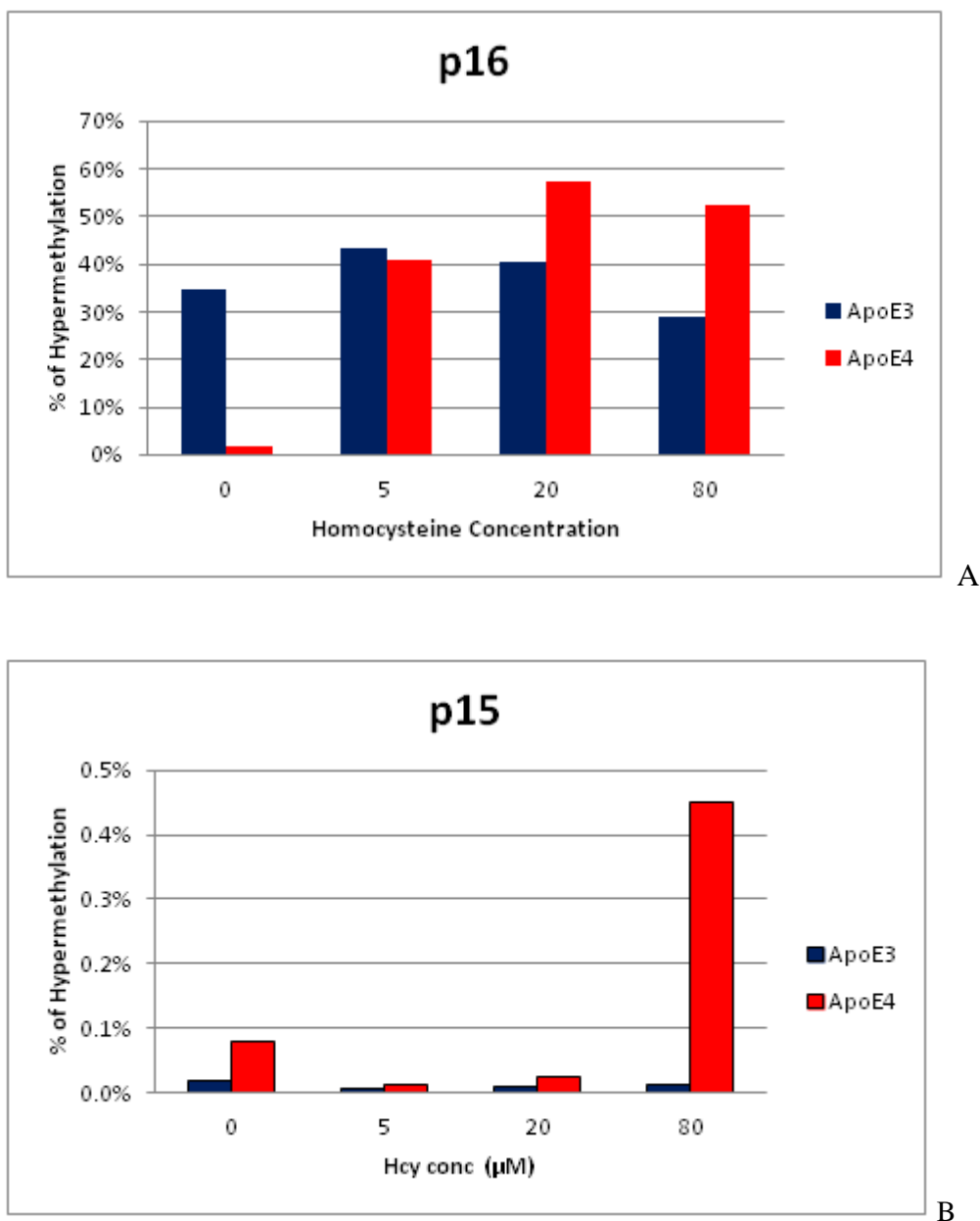
Figure 55

The effect of Hcy (μM) on the methylation status of the INK genes. A. p16^{INK4a} promoter

gene. B. p15^{INK4b} promoter gene.
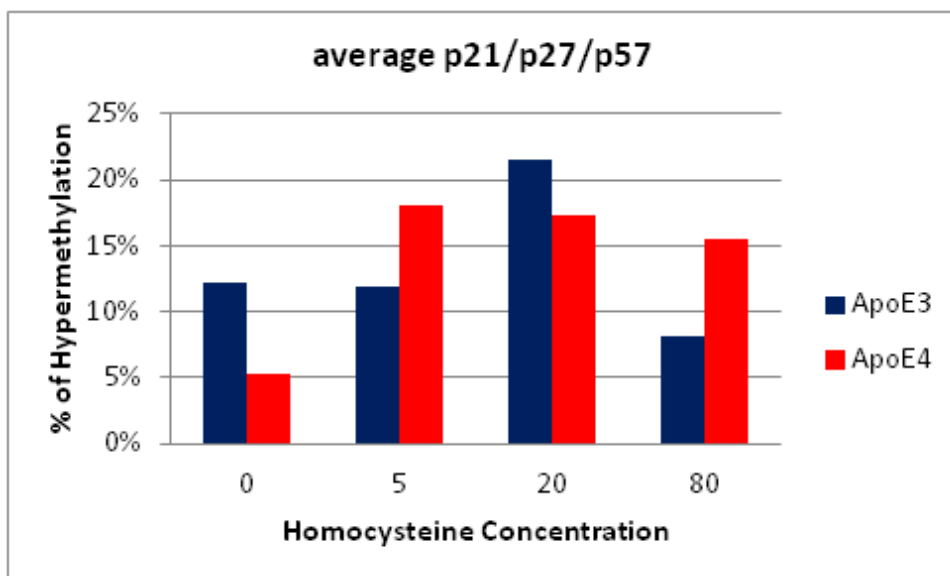
Figure 56

The effect of Hcy (µM) on the methylation status of the cip/kip genes.

5. DISCUSSION

In 1990, Reyland et al were the first to publish findings associating elevated plasma Hcy levels with AD[63]. In 1993, Strittmatter and co-workers found a relationship between late-onset AD and ApoE4 genotype. Elevated plasma Hcy levels and ApoE4 genotype are now considered to be risk factors for both AD and cerebrovascular disease. Since the early 1990s, a number of studies have investigated the possible pathogenic mechanisms by which these factors may influence the development of AD. We hypothesise that there could be a possible interaction between the two risk factors and their pathogenic effect may depend on the two risk factors being present together.

5.1. Frequency of Elevated Homocysteine levels in Alzheimer's Disease

Normal levels of plasma Hcy range from 5 to 15μmol/L. Plasma levels above 15μmol/L are regarded as hyperhomocysteinemia. Hyperhomocysteinemia can vary in severity: levels between 15 and 30μmol/L are regarded as moderate; the range from 30 to 100μmol/L is regarded as intermediate; and levels >100μmol/L is regarded as severe. From our cohort, last plasma Hcy level measurements taken before death were available to study. Plasma Hcy levels were dichotomised to below 15μM and above 15μM; where below 15μM was considered as normal and above 15μM was considered as elevated. There was no difference in the frequency of elevated plasma Hcy in individuals in different stages of AD.

The prevalence of hyperhomocysteinemia in the elderly population is ~40%[64;65]. In a large group of hospitalised elderly patients investigated, 63% of dementia patients were found to

have hyperhomocysteinemia. The lack of difference seen in our cohort is very difficult to interpret due to the low patient numbers compared to other studies.

With regards to the brain Hcy levels, there are very few studies that have examined levels of Hcy in brain tissue. In our cohort, severe AD patients appeared to be more likely to have higher brain Hcy levels; however this was not statistically significant and in light of the small patient numbers is difficult to interpret.

5.2. Plasma Homocysteine and Brain Homocysteine

It has been shown that serum Hcy, stored at -20$^{\text{o}}$C, is stable for 20 years[73].Considering this, we decided to measure Hcy levels in brain tissue that had been stored at -80$^{\text{o}}$C. This would allow us to analyse the direct effect of Hcy on the central nervous system; and gives a measure of Hcy at the time of death.

In a study with cystathionine beta-synthase deficient (CBS$^{-/-}$) mice, that were fed on a methionine rich diet, it was postulated that elevated plasma Hcy levels could disrupt the integrity of the blood brain barrier and expose the brain to toxic levels of Hcy[74]. Furthermore, in a study involving patients with hyperhomocysteinaemia, that were given vitamin B supplements, the supplementation was found to improve blood brain barrier function[75]. It is interesting to note that the ApoE4 genotype has also been linked to compromising the integrity of the blood brain barrier[76].

In the brain, levels of Hcy are found to be 5-30% of that of plasma[32;33]. Active transport via carrier proteins occurs at the blood brain barrier. However, a literature search has shown no specific carrier for Hcy. Furthermore, inducing folate deficiency in the brain via intraventricular administration of methotrexate (anti-folate drug) was found to increase CSF Hcy levels. This may suggest that the Hcy that is found in the brain may originate from the brain itself. Levels of Hcy in the CSF and plasma have been analysed in amyotrophic lateral sclerosis (ALS) patients: this study showed no relationship between CSF Hcy and plasma Hcy[77]. This is further supported by our data where no association was found between plasma Hcy and brain Hcy levels (see Figure 30).

We analysed the relationship between brain Hcy levels and methionine levels and found no association (see Figure 31). However, elevation of brain Hcy is associated with an increase in the Hcy/methionine ratio (see Figure 32), demonstrating that methionine levels remain stable even when Hcy levels are elevated. Studies have shown that folate and vitamin B_{12} deficiencies result in elevated levels of Hcy and low levels of methionine and SAM. The authors suggest that the lack of folate and vitamin B_{12} inhibit conversion of Hcy to methionine[78]. This is not supported by our findings that indicate that brain Hcy and methionine levels change independently of one another.

5.3. The Effect of Homocysteine on the Onset of Disease and disease Duration

Numerous studies have associated increases in plasma Hcy levels with age[4]. However, there are very few studies investigating the influence of plasma Hcy levels on age of onset of AD.

Guidi et al found that patients with late-onset AD (>65 years) had significantly elevated levels of plasma Hcy compared to early-onset patients (<65 years), (20.1 ± 0.9µM versus 14.3 ± 1.2µM respectively)[79]. The lack of association of elevated plasma Hcy with early-onset AD suggest that elevated plasma Hcy may not play a role in this form of the disease. The authors explain that the difference in plasma Hcy levels between early and late-onset age-matched AD patients was a result of vascular disease, which is prevalent in late-onset patients[80]. This is one of the reasons why patients with vascular disease were excluded from our study and only *pure* AD patients were considered.

To ascertain if plasma Hcy is a possible contributor to the pathogenesis of AD, studies have examined levels of Hcy over the duration of the disease. Clarke et al showed that plasma Hcy measurements remained stable over a 3 year disease period[34]. Furthermore, in a 2004 study, it was shown that patients with elevated plasma Hcy levels at initial stages of the disease did not exhibit further increases in plasma Hcy levels several years into the disease period (initial and final plasma Hcy recorded - 13.0 ± 2.8µM and 13.2 ± 2.8µM respectively)[81]. These studies call into question whether elevated plasma Hcy is a consequence of AD. The lack of association of plasma Hcy levels with disease duration in these studies suggest that elevated plasma Hcy levels occurs early on in AD.

In our study we looked at the age of disease onset in relation to plasma Hcy levels. Patients with elevated plasma Hcy levels had a significantly higher age of onset (p=0.015), see Figure 10. On first observation, this could suggest that elevated plasma Hcy levels delay AD onset. On closer analysis, we found that patients with elevated plasma Hcy levels that had a higher age of onset also had a significantly shorter disease duration (p=0.024), see Figure 11. Whilst

their symptoms may have presented at a later age, they had a more rapid decline, causing death in a shorter period of time. Nilsson et al's 2004 study found no relationship between plasma Hcy and disease duration[81]. However, another 2004 study by McCaddon et al[82] showed that patients with a longer disease duration had lower levels of plasma Hcy. This finding is replicated by our results.

A second aim of the study was to see if the effects of Hcy are dependent on the ApoE genotype. We found no indication that the ApoE genotype would have an influence on the effect of Hcy on the age of onset or disease duration. When looking at the effect of the ApoE genotype alone, we found that ApoEε4 carriers had an earlier age of onset with a longer duration of AD (see Figure 14 and Figure 15): an opposite trend to that of patients with elevated plasma Hcy. These findings replicate the results from the Gomez-Isla et al study that demonstrated a younger age of onset of AD in patients that were ApoEε4 carriers. They also showed that ApoEε4 carriers had a longer disease duration. ApoE4 carriers did not have a faster rate of disease progression than non-carriers of ApoE4. As there was no association of ApoEε4 genotype with the rate of progression of the disease, the authors concluded that the longer disease duration in ApoEε4 carriers was due to the earlier age of onset of the disease[83]. From our study, as we do not have a measure of rate of progression, we cannot conclude whether the longer disease duration seen in ApoE ε4 carriers is only due to an earlier age of onset.

To summarise, we found that elevated plasma Hcy levels were associated with a later age of onset of AD and a shorter disease duration. This may suggest that elevated plasma Hcy levels accelerate the rate of progression of the disease. In the literature there are inconsistencies

between studies examining relationships between disease duration and plasma Hcy levels. This can be explained by the difficulty in defining the 'disease duration'. Although onset of disease is defined as the time when the symptoms of AD first present, obtaining an exact measure is complicated. Firstly, symptoms of AD could go unnoticed for a long period of time by both the patient and relatives. Secondly, the amount of pathology associated with the appearance of symptoms may differ significantly between patients.

5.4. The Effect of Homocysteine on Disease Severity

Higher plasma or brain Hcy levels were not associated with more severe AD in our *pure* AD patients. This finding has been previously observed in past studies[84-87]. Nilsson et al looked at the severity of dementia using the Katz ADL-Index and Berger Scale to assess physical and social dependency respectively. They also classified severity of disease as mild, moderate and severe. The study found that plasma Hcy levels positively correlated with the severity of AD type dementia[81]. The majority of studies looking at AD severity and plasma Hcy levels support the notion that elevated plasma Hcy is associated with AD[34;64;85;88-94]. .

We analysed patients with vascular disease in addition to AD, and found that a higher frequency of the patients had elevated plasma Hcy levels in the neocortical (severe) stage of AD compared to earlier stages, although the analysis failed to reach statistical significance (see Figure 9). A similar trend is also seen in other studies[81;95]. This does suggests that plasma Hcy levels may not be related to AD severity but could be a reflection of a relationship between vascular disease and plasma Hcy. Clarke et al found that both patients with histologically confirmed AD with vascular disease, and patients with vascular disease alone, had elevated plasma Hcy levels. But patients with histologically confirmed AD with no evidence of macroscopic vascular disease present also showed elevated levels of plasma Hcy. This suggests that elevated plasma Hcy levels are not a result of concomitant vascular disease in AD patients[34]. This highlights the need for us to exclude patients with vascular disease from our cohort, as a relationship between plasma Hcy and vascular disease could potentially mask the association between Hcy and AD.

The lack of relationship between elevated plasma Hcy and AD that we see in our cohort was also seen by Nilsson and co-workers. They initially did not find a difference in plasma Hcy

levels between control and AD patients without vascular disease. However, when they corrected plasma Hcy levels for plasma creatinine concentration, AD patients without vascular disease had significantly higher levels of plasma Hcy compared to control patients. Elevated Hcy in AD could be a consequence of renal dysfunction or vitamin deficiencies[96;97]. Plasma creatinine concentrations were used to normalise plasma Hcy levels as creatinine concentration is thought to relate to renal function and muscle mass[81]. One limitation of our study is that we do not have plasma creatinine levels. The lack of association between plasma Hcy and AD severity in our cohort could be partly due to the fact that no adjustment were made for levels of plasma creatinine.

5.5. The Effect of Homocysteine on Cognitive Performance

From my review of the literature I have been able to find only nine publications to date that do not show a relationship existing between elevated plasma Hcy levels and cognitive performance[84;85;87;98-102]. A 2000 study published by Ravaglia et al examined 54 healthy elderly subjects and found no association between plasma Hcy levels and cognitive performance[102]. However, 4 years later Ravaglia and co-workers published findings from a larger healthy elderly cohort and found that elevated plasma Hcy was associated with poorer cognitive performance[103]. This suggests that a larger cohort is needed to reveal a relationship between plasma Hcy and cognition.

Contrary to the above, there are a large number of cross-sectional studies that report an association between elevated plasma Hcy and cognitive decline[100;104-107]. It is difficult with these types of studies to ascertain that the elevated plasma Hcy is a cause of poor cognition. Prospective or longitudinal studies allow observation of cognitive performance over time and allow more accurate correlations between plasma Hcy levels and cognition to be made. A

study by Garcia et al, followed a large cohort of subjects (n = 180) with normal cognitive performance at baseline. The study showed that at follow-up subjects with elevated plasma Hcy levels had significantly lower cognitive scores compared to their baseline values. Whilst cognitive scores remained at baseline in subjects with decreased plasma Hcy levels at follow-up [108-110].

Opposite to expectations set by the literature, we found that elevated plasma Hcy levels in life was associated with higher CAMCOG scores (close to significance) just prior to death. The lack of association between plasma Hcy levels and cognitive performance in our cohort could be due to us only using cross-sectional analysis on a relatively small number of patients. Also, using single measurements of plasma Hcy, as we have done in this study, have been shown to underestimate the relationship between Hcy and cognition by 15% [111;112]. Additionally, it important to note that many of our patients had severe dementia (very low cognitive scores) that may have been present for several years and this plateau effect may obscure the relationship between Hcy levels and dementia severity. However, there may be an alternative explanation. As patients with elevated plasma Hcy levels did not show a more rapid cognitive decline but were found to have a shorter disease duration, it is possible to envisage that elevated plasma Hcy levels may be associated with the premature death of the patient independently of their cognitive decline.

There are a number of studies that have looked at the effect of plasma Hcy on cognitive functioning, but very few studies have investigated the combined effect of ApoE genotype and plasma Hcy on cognition. There are inconsistencies in the few studies that have examined the relationship between plasma Hcy, cognitive function and ApoEε4 genotype, Dufouil and co-workers conducted a longitudinal study, where plasma Hcy levels and cognition function were monitored in a healthy elderly cohort over a period of 4 years. Using baseline plasma

Hcy levels, and cognitive decline assessed by loss of MMSE scores, they found a significant association between elevated plasma Hcy levels and cognitive decline. Furthermore, Dufouil et al analysed the possible interaction of plasma Hcy and ApoEε4 genotype. They found that ApoE genotype did not modify the effect that plasma Hcy had on cognition[109]. Two years later, Schafer et al published findings from a study also involving a large group of healthy elderly subjects, and found that elevated plasma Hcy were associated with a worse neurobehavioral test score. Furthermore, contradictory to the 2003 Dufouil study, Schafer and co-workers found that ApoE genotype modified the effect of plasma Hcy levels. Subjects that were homozygous for the ApoEε4 allele (ε4ε4) had a significantly worse neurobehavioral test score compared to ApoEε4 non-carriers[113]. Finally in 2008, Elias et al provided further support to the Schafer et al study. They found that in subjects who were ApoEε4 non-carrier, plasma Hcy did not have an effect on cognitive performance. Whilst subjects carrying either one or two ApoEε4 alleles were able to modify the effect that elevated plasma Hcy had on cognitive function: analysis showed significantly worse cognitive test scores compared to ApoEε4 non-carriers[50]. In our cohort, no relationship between cognitive function and plasma Hcy was seen. This was also true when the ApoE genotype was taken into account. Furthermore, the ApoEε4 genotype alone did not influence cognitive performance, see Figure 17. It is possible that our results just reflect the shortcomings of a cross sectional postmortem study (as discussed above) or it may be that the relationship between cognitive functioning and Hcy levels seen in the healthy population disappear in Alzheimer's disease where cognitive functioning is affected mainly by the presence of pathology.

5.6. The Effect of Homocysteine on Pathology

5.6.1. OPTIMA Cohort

The two pathological hallmarks of AD are neurofibrillary tangles and neutric plaques. The accumulation of pathology varies between different brain regions and is related to the severity of AD[114]. The accumulation of pathology with disease progression in our cohort was consistent with previous studies[62].

The neurofibrillary tangles are composed of hyperphorylated tau. Tau plays an important function in maintaining the stability of microtubules. Therefore, tau has a fundamental role in maintaining neuronal structure and neuronal activity. The function of tau is regulated by the degree of phosphorylation: with hyperphosphorylation inhibiting microtubule binding and microtubule assembly. In AD brains, abnormally hyperphosphorylated tau accumulates to form of pair helical filaments (PHF), the major component of tangles[115-119]. In the current study we used AT8 to label hyperphosphorylated tau (p-tau) in its native state at Ser202 and Thr205. The AT8 antibody recognizes hyperphosphorylated tau prior to tangle formation. We also used another tau antibody (clone DC11), which recognises a tangle specific tau. The accumulating tau pathology relates to disease severity, see Figure 18. Using z-score values we were able to prevent the disease severity from masking the effect of Hcy and ApoE4 genotype on tau pathology.

We found that elevated levels of Hcy (whether in plasma or the brain) were associated with greater accumulation of p-tau and PHF-tau, and this association was independent of AD severity, see Figure 19.

There are a number of studies that report a relationship between tangle pathology and ApoEε4 genotype[19;120-122]. When analysing ApoEε4 genotype and its relationship to tau pathology, we found no relationship, see Figure 20. Contrary to studies that support a link between tau pathology and ApoEε4 genotype, there are a number of studies like ours that fail to find an association between tau pathology and ApoEε4 genotype[70;106;123-126]. There is a lack of studies looking at the combined effect of Hcy and ApoE genotype on tau pathology. We found that the association between elevated Hcy levels and more severe tau pathology in our cohort was mainly true in patients who did not carry the Apoε4 allele. In Apoε4 carriers the Hcy effect on tau pathology disappeared.

Neuritic plaques composed of beta amyloid are another hallmark of AD. Beta amyloid is generated from the cleavage of the amyloid precursor protein (APP). Studies have associated APP gene mutations to early onset AD.

In our cohort we see that with increasing disease severity there is an increase in the accumulation of beta amyloid in the frontal and occipital lobe (see Figure 23), regions of the brain that are affected later in the disease process. We found that patients with elevated Hcy levels (in plasma and the brain) had significantly higher levels of beta amyloid in the lateral temporal lobe, irrespective of disease severity (see Figure 24 and Figure 25). The lateral

temporal lobe was a region of the brain where beta amyloid accumulation might have reached a ceiling and was not associated with the disease severity.

Few studies have examined the relationship between plasma Hcy levels and beta amyloid expression in AD brain tissue. A number of studies have examined levels of plasma beta amyloid in relation to plasma Hcy, and demonstrated a strong correlation between the two variables[127-129]. One study has shown that, although levels of beta amyloid and Hcy in plasma are related, treatments such as vitamin B_{12} supplementation that lower plasma Hcy levels do not have an equivalent effect on beta amyloid levels. This suggests that once the pathological process has started it may be difficult to reverse it, or that the levels of beta amyloid are regulated independently of plasma Hcy[129].

Since both elevated Hcy levels and the ApoE ε4 status has a significant effect on amyloid accumulation, we analysed the combined effect of the two risk factors on this variable (see Figure 27 and Figure 28). We see a trend showing that patients with low Hcy levels and no ApoE ε4 have the lowest beta-amyloid expression in the lateral temporal lobe, whereas ApoE ε4 carriers with elevated Hcy have the highest amyloid load in the brain. Luchsinger et al's study examined the combined effect of ApoE and Hcy on beta amyloid expression. They showed that although plasma Hcy was related strongly to beta amyloid levels in plasma, the association was unaffected by the ApoE genotype[128]. Our study shows a possible interaction between Hcy and ApoE genotype: indicating that elevated Hcy levels affect ApoE ε4 carriers more significantly in terms of beta amyloid accumulation.

5.6.2. *In Vitro* study

To study the interaction between Hcy and ApoE at the cellular level and their effect on AD-related protein expression, *in vitro* experiments were carried out using the SH-SY5Y neuroblastoma cell line. The cells were treated with physiological concentrations of Hcy combined with one of the three ApoE isoforms, and p-tau and beta amyloid expression was investigated.

We chose our experimental range of Hcy concentrations to include normal and the highest plasma Hcy recorded in the OPTIMA cohort (~60µmol/L). The concentration of the human recombinant ApoE used in the cultures was 5µg/ml to match the physiological CSF concentrations of ApoE[130].

Anti-p-tau antibody (clone AT8) was used to detect hyperphosphorylated tau (p-tau) in the cultured neuroblastomas, and p-tau content was measured using ACUMEN cytometry. Several studies have indicated that increased Hcy levels are found to increase tau phosphorylation in SH-SY5Y neuroblastoma cells and other neuronal cells lines[131;132]. In the current study, a clear relationship between Hcy and tau expression is not seen in the Hcy *only* treated cultures. It was only when we analysed the different cell populations separately (defined by the cell cycle phase) that a significant increase in p-tau content was seen. At high Hcy doses, p-tau content per cell significantly increased in the G2 population. As the increase is only seen in the G2 population it could suggest that the intracellular signalling pathways activated by Hcy may cause aberrant upregulation of kinase activity leading to hyperphosphorylation of tau. Studies have shown that Hcy can induce cell proliferation[133], and that entry into the cell cycle has been associated with increased tau phosphorylation[134].

From our results it is evident that Hcy alone contributes to the development of AD not merely by de-regulating the cell cycle, but also increasing the p-tau content of the G2 cells. It is also interesting that the trend in p-tau accumulation in G2 cells is parallel to changes in cell death seen in the cultures, see Figure 43a. Could it be possible that high p-tau content in G2 cells is contributing to cell death? It has been shown in a number of studies that tau hyperphosphorylation and the accumulation of tau pathology correlates to cell death, as high p-tau content in neurones disrupts intracellular trafficking, which is critical for cell functioning[135;136].

When analysing the combined effect of Hcy and ApoE on p-tau expression, we see an isoform dependent effect. The presence of ApoE4 is shown to reverse the p-tau accumulation in G2 cells, which was induced by increasing Hcy concentration (see Figure 52). This is not what we expected as ApoE4 is considered a strong genetic risk factor of AD. In ApoE2 treated cultures, we see a decrease in p-tau expression with high dose Hcy treatment ($>10\mu M$) in both G1 and G2 cells (see Figure 50b). In the presence of ApoE2, increasing Hcy concentrations are also found to reduce the rate of cell proliferation (see Figure 44a and Figure 51a respectively). This suggests that the influence of Hcy treatment alone on cell proliferation and tau phosphorylation is reversed in the presence of ApoE2. In G1 cells, we see that p-tau cell content, and the number of p-tau containing cells, is reduced with increasing Hcy dose (see Figure 51b and c); whilst in G2 cells there is only a reduction in p-tau content with no change in the number of p-tau positive cells. This suggests that the protective effect of ApoE2 occurs earlier on in the cell cycle. The findings from our study are consistent with the results of genetic studies that indicate that the ApoE ε2 allele is protective in AD[137].

Finally, in the presence of ApoE3 increasing Hcy concentration was found to increase the p-tau content in G2 cells (see Figure 53). When analysing the p-tau cell content in relation to the cell death data (see Figure 45a), we can see that there is no significant change in cell death even though p-tau expression has significantly increased. This suggests that, in the presence of ApoE3, the cell death response is prevented even when p-tau is upregulated. Based on previous studies, ApoE3 has been shown to be more protective against apoptosis than ApoE4. In one particular study, ApoE3 was found to protect against apoptosis in retinal ganglion cells deprived of trophic additives, whilst ApoE4 did not protect the cells. ApoE can activate anti-apoptotic signalling pathways via low density lipoprotein receptors. One proposed mechanism is that binding to LRP receptors leads to increased phosphorylation and inactivation of glycogen synthase kinase-3β (a pro-apoptotic kinase). Inactivation of glycogen synthase kinase-3β inhibits apoptosis[138] is associated with decreased tau phosphorylation[139]. The ApoE ε3 allele is considered a neutral genotype in AD when compared to ApoE ε2 and ε4. Based on the p-tau and cell death data from our in vitro study, we can say that ApoE3 may not be able to inhibit the accumulation of tau induced by Hcy treatment, but may protect against apoptosis, allowing cells to survive for longer, despite tau accumulation within the cell.

From our results Hcy does not seem to have a profound effect on the expression of beta amyloid. Based on our cohort analysis we see that elevated Hcy in the brain was associated with beta amyloid accumulation in the lateral temporal lobe, therefore we would have predicted a relationship with dose-dependent increases in beta amyloid content in our cells. One study has shown that Hcy potentiates the neurotoxic effects of beta amyloid when differentiated neuroblastoma cells are co-treated with beta amyloid peptides and high levels of Hcy[140]. The study suggests that the effects of Hcy may come into play once there already is an

accumulation of beta amyloid, and that Hcy is not directly a cause of beta amyloid accumulation.

Cultures treated with ApoE2 and ApoE4 showed higher beta-amyloid expression than the cultures left untreated or treated with ApoE3, see Figure 54b. The lack of effect of Hcy treatment on beta amyloid cell content was not altered by the presence of the ApoE isoforms (data not shown). Finally, G2 cells showed a significantly higher beta amyloid content than G1 cells, see Figure 54a. This suggests that the upregulation of kinase activity in G2 cells could be contributing to aberrant phosphorylation of APP leading to the accumulation of beta amyloid[141]. Hcy may induce a proliferative response that activates mitogenic signalling pathways, but this proliferative response does not induce beta amyloid accumulation.

In a recent study, severe hyperhomocysteinemia was induced through diet in an AD mouse model. After a period of 7 months, no change in the beta amyloid expression was found compared to the control mice[142]. Both this study and our in-vitro study suggest that high levels of Hcy do not induce amyloidogenesis.

5.7. The Effect of Homocysteine on Oxidative Stress in Alzheimer's Disease

Multiple studies suggest that oxidative stress and free-radical damage are involved in the pathogenesis of AD[84;143-145]. Oxidative stress results from an increase in free-radical production or a reduction in antioxidants. The brain is especially vulnerable to oxidative stress because of its high oxygen consumption and high lipid content[146]. The exact cause for the shift in oxidative homeostasis in AD is still unclear. We hypothesized that elevated Hcy levels would induce oxidative stress in the brain.

In the current study, to identify lipid peroxidation and DNA oxidation we used anti-4-hydroxynonenal (4-HN) and anti-8-hydroxyguanosine (8-HG) respectively. We initially investigated the relationship between oxidative stress and disease severity, and compared our results to the results of other studies[140;147]. We found that oxidative stress in the brain did not increase with AD progression. When analysing 4-HN and 8-HG expression in relation to Hcy levels using logistic regression, we found that oxidative stress predicted the levels of Hcy in the brain. This was close to significance in the lateral temporal lobe, and statistically significant in the frontal lobe (a region of the brain that is affected later on in the disease process). Patients that have oxidative stress (increased 4-HN expression) in the frontal lobe tended to be patients who were ApoE ε4 carriers with elevated brain Hcy levels ($p = 0.0057$). No relationship between oxidative stress and plasma Hcy was seen in our cohort, suggesting that only high levels of Hcy in the brain make the neurones susceptible to oxidative stress.

Few studies have examined the combined effect of Hcy and ApoE genotype on oxidative stress. In a 2006 *in-vitro* study, folate deficiency (inducing elevated Hcy) in ApoE-/- mice was found to increase oxidative stress. The effect of folate deficiency on oxidative

homeostasis was potentiated by ApoE deficiency[148]. It is well documented that 30% of Hcy is in its free form, with the vast majority of Hcy protein bound. Of the unbound free Hcy 1-4% is in its reduced form[149]. When levels of Hcy in plasma increase, the protein binding sites for Hcy become saturated, and therefore it can be envisaged that there would be more free circulating reduced forms of Hcy[52]. As Hcy can undergo auto-oxidisation this would lead to the generation of reactive oxygen species, and would explain the relationship between oxidative stress and Hcy. We have found that the effect of brain Hcy on oxidative stress is ApoE dependent. Hcy can form disulfide bonds with cysteine residues on lipoproteins. Structural differences between the ApoE variants would influence Hcy binding. Hcy may have a lower binding capacity for ApoE4 due to the lack of cysteine residues on ApoE4 compared to ApoE2 and ApoE3. Therefore, ApoE ε4 carriers would have higher amounts of free circulating Hcy, thus exposing the brain tissue to harmful levels of Hcy. In theory ApoE2 and E3 carriers would be able to compensate for elevated Hcy levels by having more lipoprotein bound Hcy, thus reducing oxidative stress. We hypothesized that elevated Hcy levels induce oxidative stress, and that this effect is ApoE isoform dependent. Our results support this hypothesis.

5.8. The Effect of Homocysteine on Global DNA in Alzheimer's Disease

DNA methylation plays an important role in gene regulation. Promotor region hypermethylation results in transcriptional silencing of genes, while hypomethylation allows transcription factor binding and gene upregulation. Aging has been associated with the loss of global DNA methylation. Considering that aging is the biggest risk factor for AD, could aberrant changes in DNA methylation play a role in the pathogenesis of AD? Diseases such as

cancer and atherosclerosis have also been associated with global DNA hypomethylation and gene-specific hypermethylation[150-156]. This further supports the need for investigating DNA methylation in AD.

The methyl groups needed for DNA methylation are derived from dietary methyl donors such as methionine. Methionine is converted to s-adenosylmethionine, and then s-adenosylhomocysteine, allowing methyl donations. S-adenosylhomocysteine is then converted to Hcy which is then remethylated to methionine (see Figure 2). Changes to the homeostasis of the folate cycle may alter the supply of methyl groups and therefore impact the biochemical pathways needed for DNA methylation.

Initially we investigated the relationship between disease severity and global DNA methylation in our cohort. We found a trend showing that global DNA methylation decreases with AD progression, see Figure 33. The loss of global DNA methylation would increase genome instability which has been related to the aging process. Furthermore, extensive genomic hypomethylation could account for the upregulation of genes associated with AD pathology, as has been suggested in a number of papers[157-162]. In one paper looking at the methylation status of the APP gene, they found CpG island methylation at the APP promoter region of non- demented subjects, whilst there was a complete absence of DNA methylation in AD subjects. The hypomethylation of the APP gene could be one of the factors contributing to beta amyloid accumulation[162]. Furthermore, the regulation of tau phosphorylation is maintained by the equilibrium of activity of kinases and phosphatases. Abnormal tau hyperphosphorylation is a consequence of an imbalance of the activity of kinases and phosphotates, which may have resulted from aberrant DNA methylation[163;164].

We also found that there was no relationship between global DNA methylation and Hcy levels (whether in the plasma or brain), and this lack of relationship was not altered when we included ApoE status in the analysis. A negative correlation between plasma Hcy levels and DNA methylation has previously been reported in a number of studies[53;165]; however results have not always been replicated[166-168]. Studies have shown that the effect of elevated Hcy levels on global DNA methylation is tissue-specific[108;169-171]. The lack of relationship between Hcy levels and global DNA methylation status was therefore not all together surprising, as other studies have shown very similar findings[168;170]. Heil and co-workers found that patients with cystationine beta-synthase (CBS) deficiency, which can result in a 30-fold increase in plasma Hcy, showed no alteration in global DNA methylation compared to subjects with no deficiency Furthermore, Brombery et al induced a 10-fold increase in plasma Hcy levels in mice and found no significant change in global DNA methylation in the frontal cortex[168;172]. These studies suggest that the lack of association between Hcy levels and global DNA methylation is due to the SAM/SAH ratio remaining constant even when there are considerable changes to the levels of Hcy, which may explain why the global DNA methylation status is preserved in our cohort even when Hcy levels are high.

5.9. Effect of Homocysteine on the Cell Cycle

We have used propidium iodide staining followed by cytometry to assess the cell cycle kinetics and cell numbers in our cultures. The LDH assay quantitatively measures cystosolic lactate dehydrogenase, which is released on cell lysis. This gave us a measure of the proportion of cells that died in our cultures prior to the completion of the experiments. By combining the data from the cytometry and LDH assay, we were able to calculate population doubling times and the length of the individual phases of the cell cycle.

With no ApoE added to the cultures, the cell numbers were found to significantly increase with increasing Hcy concentration, see Figure 43a. This mitogenic effect is consistent with previous studies that have shown that Hcy is able to induce proliferation in different cell types[133;166;173-175]. We found that population doubling times decreased with Hcy treatment (see Figure 43b): with the length of G1 and G2 time also decreasing proportionately. This indicates that Hcy can induce cell cycle entry allowing neuroblastomas to leave their retinoic acid induced differentiated state and begin to replicate their DNA. Cell proliferation and cell death where found to be discrepant at low doses of Hcy and parallel at higher doses, see Figure 43a. Hcy is converted to cysteine through the transsulfuration pathway. Cysteine is an essential amino acid: Hcy treatment at normal physiological doses provides extra nutrition, which may drive cell proliferation. With increasing Hcy concentration cell death begins to increase, suggesting that Hcy becomes toxic at high doses. A number of studies have shown that high Hcy is associated with oxidative stress; this may be the trigger for apoptosis in our cultures [166;176-178].

In the presence of ApoE2, there was a significant decrease in the number of cells with high dose Hcy treatment ($>20\mu M$), see Figure 44a. ApoE2 has a protective effect in differentiated neuroblastomas by inhibiting the proliferative effect of Hcy. The 'protective' influence of ApoE2 is lost at the highest Hcy concentration as the number of dead cells in the culture increased significantly. This indicates that ApoE2 cannot compensate for the effect of high dose Hcy on the cultured neuroblastomas, suggesting that ApoE2 is only protective at normal physiological concentrations of Hcy.

Unlike the ApoE2 isoform effect, in the presence of ApoE3 there was no change in cell numbers with increasing Hcy concentration. Furthermore, the number of dead cells remained stable at all Hcy doses, see Figure 45a. The length of the population doubling time decreased at high doses of Hcy (>20μM), showing that the inhibition of the Hcy-induced proliferative response was lost, see Figure 45b. This suggests that ApoE3 has more of a protective effect in the culture than ApoE2. ApoE3 is able to reduce the proliferative effect of Hcy and inhibit cell death.

Similar to the ApoE3 treated cultures, the presence of ApoE4 inhibits the proliferative effect of Hcy (see Figure 46a). This may suggest that ApoE4 is protective. However, the population doubling time significantly decreased with Hcy treatment of above 5μM concentration, with the number of dead cells increasing significantly in a dose dependent manner (see Figure 46a and b). Even at physiologically normal levels of Hcy (10μM), ApoE4 could not compensate for the proliferative effect of Hcy.

ApoE has been shown to have an anti-proliferative effect on a number of cell types[58;179]. From these studies, ApoE3 was shown to have the greatest anti-proliferative effect, which was also seen in our *in vitro* study. In AD, ApoE2 is considered protective: with the neuroprotective efficiency of ApoE2 greater than that of ApoE3[10;15;28;137]. This is not explained by our *in vitro* results or those of other studies[58;179]. However, it is difficult to compare the human brain to an *in vitro* model. Exogenous recombinant human ApoE may not be able to target all the signalling pathways that are targeted by endogenous ApoE. This would result in an altered neuroprotection efficiency of the ApoE isoforms in cell culture. Physiologically, the levels of ApoE4 in plasma are found to be much lower than the levels of ApoE2 and ApoE3[10] in

plasma; however, in our culture model we used identical concentrations for all ApooE isoforms. Nevertheless, even with the levels of ApoE4 being the same as the other two isoforms, the effect of ApoE4 on protecting the cells against toxic levels of Hcy is still the lowest. This shows us that the influence of ApoE isoforms is not based on the relative amount of protein produced but on the functionality of the isoform.

Adult neurones are considered to be in a quiescent state, in a similar way to the retinonic acid induced differentiated neuroblastomas. Cell cycle inhibitors keep neurones differentiated; however the cells retain their capacity to proliferate. It is only with a mitogenic stimuli and the loss of the cell cycle inhibitor effect that cells are able to re-enter the cell cycle. Aberrant cell cycle re-entry is thought to play a fundamental part in AD pathogenesis. The trigger for the proliferative response in the current *in vitro* study was shown to be high levels of Hcy. Hcy *alone* triggered proliferation in the differentiated neuroblastomas. The addition of any of the three ApoE isoforms to the culture seems to be protective, by reducing the rate of Hcy induced proliferation. The extent of the neuroprotection is ApoE isoform dependent. From our *in vitro* model, the ApoE3 seems to be most neuroprotective, and ApoE4 the least protective (ApoE3>ApoE2>ApoE4). This demonstrates that the Hcy-induced effect is modulated by ApoE in an ApoE isotype dependent manner.

5.10.   The Effect of Homocysteine on CDKI Methylation in Alzheimer's Disease

In the adult brain, neurones are in a differentiated state, but retain synaptic plasticity. In AD, the regions of the brain that are primarily affected by pathology are associated with a high degree of synaptic plasticity and higher cognitive functioning. It is therefore hypothesized that

in AD tightly controlled cell cycle regulation somehow fails during synaptic remodelling, and consequently neurones are allowed to re-enter the cell cycle and unable to revert back to their differentiated state.

As explained in the previous chapter, some studies have shown that some genes are hypermethylated in cancer and that DNA methylation status of gene promoter regions can be altered and respond to changes in physiological conditions. We hypothesised that elevated Hcy levels cause aberrant DNA methylation of cell-cycle related genes, which may contribute to the failure of neuronal cell cycle control leading to the development of AD pathology.

The cell cycle is a tightly controlled process. The progress of the cell through the different cell cycle phases is regulated by the activity of cyclin, cyclin-dependent kinases (CDKs) and cyclin-dependent kinases inhibitors (CDKIs). In the current study, we decided to investigate the DNA methylation status of the CDKI genes using DNA extracted from AD brain samples. We hypothesised that elevated Hcy levels result in hypermethylation of CpG islands on the CDKI gene promoter regions leading to aberrant cell cycle reactivation in neurones.

5.10.1. AD Cohort

We investigated the methylation status of five CDKI genes: $p16^{INK4a}$, $p15^{INK4b}$, $p21^{cip1}$, $p27^{kip1}$ and $p57^{kip2}$ in the lateral temporal lobe. We found that CDKI gene methylation did not relate to disease severity. Multiple regression analysis showed that hypermethylation of the $p16^{INK4a}$ gene was related to brain Hcy levels showing a positive relationship, whereas hypermethylation of the $p16^{INK4a}$ gene related inversely to the brain Hcy/methionine ratio (close to significance, $R^2 = 0.29$, $p = 0.053$). The relationship between brain Hcy and $p16^{INK4a}$ gene methylation was not dependent on the ApoE genotype. The methylation statuses of the

other CDKI genes were found to be independent of the Hcy concentration and the ApoE genotype (i.e. $p15^{INK4b}$, $p21^{cip1}$, $p27^{kip1}$, $p57^{kip2}$).

$p16^{INK4a}$ acts as a potent inhibitor of CDK4. Cyclin D1/CDK4 complex phosphorylates retinoblastoma protein (Rb). Rb is known to regulate the activity of a gene regulatory protein called E2F. Phosphorylation of Rb by cyclin/CDK complexes reduces the binding affinity of Rb to E2F, and E2F is free to activate S-phase related gene expression and further expression of cyclin D1 and CDK4. $p16^{INK4a}$ protein inhibits the formation of Cyclin D1/CDK4 complexes and therefore inhibits cell cycle progression. Mutations in the $p16^{INK4a}$ gene are rare. Studies have shown that downregulation of p16 is due to silencing of the $p16^{INK4a}$ gene by DNA methylation[180-182]. Hypermethylation of the $p16^{INK4a}$ gene promoter would alter p16 protein expression and affect the balance between p16 and CDK4. In the current study we see that in AD brains $p16^{INK4a}$ hypermethylation is associated with elevated brain Hcy levels. The increased amount of Hcy in the brain would indicate an imbalance in the folate cycle and changes in the methylation potential that could potentially lead to altered $p16^{INK4a}$ promoter methylation.

5.10.2. *In Vitro* study

The changes in the population doubling times in the cultures are not associated with alterations of the cell cycle kinetics: all phases of the cell cycle were found to change equally. The changes to cell proliferation induced by Hcy and ApoE affect all phases of the cell cycle equally. Investigating the methylation status of CDKI genes would help us understand a possible mechanism by which Hcy may induce proliferation, and how this effect may be modulated by the different ApoE isoforms. Using our in vitro model we could confirm our

findings of CDKI gene methylation from the OPTIMA cohort. The custom-made SA Bioscience Methyl-Prolifer Arrays were also used for this part of the study, and the same CDKI genes were examined as for the OPTIMA cohort. Three treatments of Hcy were selected (5, 20 and 80μM) in the presence of either human recombinant ApoE3 or ApoE4 isoform.

p16^{INK4a} gene promoter methylation status analysis revealed a differential effect of Hcy in the presence of the different ApoE isoforms. With high dose Hcy treatment, in the presence of ApoE3, we see a decrease in the methylation status of the p16^{INK4a} promoter region, see Figure 55a. This suggests that ApoE3 may suppress the proliferative response triggered by Hcy, via hypomethylation of the p16^{INK4a} promoter, which leads to the upregulation of the p16^{INK4a} gene. When comparing the p16^{INK4a} methylation status to the cell cycle analysis data, we see that at 5 and 20μM of Hcy the population doubling slightly increases (see Figure 45b), suggesting that p16^{INK4a} hypomethylation has influenced cell proliferation and reduced cell death (see Figure 45a). At the highest dose, where p16^{INK4a} is hypomethylated population doubling times remain at baseline. This suggests that ApoE3 can inhibit the Hcy induced proliferation, by allowing p16^{INK4a} gene hypomethylation, which would increase expression of p16 protein to suppress G1 progression.

With ApoE4 supplementation, there is increased p16^{INK4a} promoter hypermethylation with increasing Hcy concentration (see Figure 55a). p16^{INK4a} hypermethylation would lead to gene silencing and decrease in p16 protein expression. This in turn reduces the effect p16 has on inhibiting cell cycle re-entry. It seems that ApoE4 has less of an effect on inhibiting the Hcy induced proliferation, as p16^{INK4a} gene hypomethylation would allow cell cycle re-entry and G1 progression. From the cell numbers in ApoE4 treated cultures we see that the increase

hypermethylation of p16^{INK4a} is not accompanied by changes cell numbers (see Figure 46a). However, the hypermethylation of p16^{INK4a} is parallel to the increase in cell death seen in these cultures (see Figure 46a). This finding has been documented in other studies, including a study by Lau et al, where gene silencing of p16^{INK4a} by small interfering RNA (siRNA) did not alter cell proliferation. However, when the cells were put under UV-stress, increased apoptosis was seen in the siRNA treated cells[183]. This suggests that a relationship exists between elevated Hcy levels, p16^{INK4a} hypermethylation and increase cell death.

In the presence of ApoE3, no change in the p15^{INK4b} methylation status is seen. However, in the presence of ApoE4, the highest Hcy dose was found to significantly increase p15^{INK4b} promoter methylation (from 0.02% to 0.45%), see Figure 55b. This suggests that at this dose the p15^{INK4b} promoter is highly methylated and may result in complete gene silencing. When looking at the cell cycle analysis of the ApoE4 cultures at 80μM of Hcy, we see a slight reduction in live cell numbers and high cell death when compared to the lower Hcy doses (see Figure 46a). This again suggests that hypermethylation, and subsequent gene silencing, of the INK family of CDKI genes is associated with cell death.

Both p16^{INK4a} and p15^{INK4b} are inhibitors of CDK4 and CDK6. These CDKIs inhibit the interaction of CDK4/6 with cyclin D1, thereby preventing G1 progression. Both p16^{INK4a} and p15^{INK4b} show an increase in promoter methylation in the presence of ApoE4. When comparing p16^{INK4a} and p15^{INK4b} methylation in the presence of ApoE3 and ApoE4, we can see that ApoE4 is less effective at inhibiting promoter methylation compared to ApoE3, and that cells are more susceptible to G1 progression caused by Hcy in the presence of ApoE4.

The members of the cip/kip family of genes (i.e. p21^{cip1}, p27^{kip1}, and p57^{kip2}) were grouped together, and the average methylation status of these genes examined (see Figure 56). The members of the cip/kip family of CDKI induce cell cycle arrest at the G1/S and G2/M checkpoints by inhibiting various cyclin/CDK complexes. p21 is up-regulated in response to activation of a tumor suppressor p53 by DNA damage and apoptosis. p21 inactivates CDK2, which forms complexes with cyclin A, cyclin D1 or cyclin E. Therefore p21 can inhibit several phases of the cell cycle and protect against DNA damage induced apoptosis[184]. p27 is highly expressed in quiescent cells: with expression declining once cells begin to proliferate[185]. Finally, p57 is imprinted by DNA methylation, where the paternal allele is transcriptionally repressed and the maternal allele is expressed[186].

We found that in the presence of ApoE3 the changes in cip/kip promoter methylation had a polynomial response to increasing Hcy concentrations. This effect is altered by ApoE4, such that significant alterations in methylation appear at lower Hcy concentrations and do not fall significantly as with the increasing Hcy concentrations. The methylation pattern of the cip/kip CDKI genes is parallel to the population doubling times in the cultures treated with ApoE and Hcy (see Figure 45, Figure 46 and Figure 55).

5.11.   The Effect of Homocysteine on CDKI protein expression

Since CDKI expression is regulated at multiple levels, not just by promoter methylation, we regarded it important to assess the effect of Hcy on CDKI expression at the protein level. There was a trend showing an accumulation of p16 at the later stages of AD. The methylation status of the p16^{INK4a} gene did not relate to p16 protein expression. However, elevated levels

of brain Hcy were related to reduced expression of p16 protein in the occipital lobe (p = 0.042). This relationship was not significantly affected by the ApoE genotype.

Aging has been associated with increasing levels of p16 protein[187]. Low levels of p16 have been found to significantly increase susceptibility to tumours[188]. There are well-documented changes in p16 protein expression in AD. p16 protein expression has been shown to be increased in brains of AD patients compared to aged match controls[108;189;190]. The increased p16 expression in late stages of AD appears contradictory to expectations if we accept the cell cycle hypothesis for the pathogenesis of AD. In theory, for neurones to re-enter the cell cycle and bypass the G1/S phase checkpoint you would expect reduced levels of p16 in the brain. However, the increased p16 immunoreactivity in the brain does not necessarily indicate increased p16 activity. It may only indicate an inappropriate accumulation of p16 where the neurones are attempting to abort the aberrant cell cycle activation.

In the current study we see that elevated brain Hcy levels are associated with reduced p16 immunoreactivity. Looking at the whole cohort we found that p16 protein immunoreactivity does not relate to the p16^{INK4a} methylation status. However, in patients with elevated brain Hcy levels, we found that the p16^{INK4a} promoter is hypermethylated, which in turn inhibits p16 protein production. This demonstrates that Hcy can induce aberrant gene methylation causing changes at the protein levels that would lead to cell cycle re-activation.

Looking at the other CDKIs examined in this study, we found that p21 protein expression was not related to levels of Hcy or to the ApoE genotype. p27 and p57 expression in the occipital lobe were related to elevated levels of brain Hcy, and these relationships were ApoE4

dependent. This increased expression of p27 and p57 could be due to an inappropriate accumulation of these CDKIs as the cell attempts to rescue itself from aberrant cell cycle activation. One further explanation could be that the increased expression of p27 and p57 could potentially be an artifact, as tau is sticky and antibodies tend to bind to it. ApoE4 carriers with elevated brain Hcy levels have shown accumulation of tau in the occipital lobe, the same region of the brain where both p27 and p57 proteins expression is increased. Although this may supports the notion that antibodies could be binding to tau rather than the CDKIs themselves, the use of highly specific antibodies reduces this risk to minimum.

6. CONCLUSION and FUTURE DIRECTIONS

In conclusion, both our cohort analysis and the *in vitro* study demonstrate that Hcy affects the development of Alzheimer's disease at multiple levels, cell cycle regulation, DNA methylation, induction of oxidative stress and direct effect on AD-type protein accumulation. These effects are modulated by the ApoE genotype. Our findings in the human brain are partially confirmed in our *in vitro* model. The discrepancies seen in the neuroblastoma cultures and the human brain are not wholly unexpected, as the findings in the brain reflect the long lasting exposure to elevated levels of Hcy while the cell culture model reflects the acute effects of relatively higher concentrations of Hcy.

Our study provides a good starting point for the elucidation of the mechanistic molecular interactions between ApoE and Hcy in human disease. Further studies in human brains, animal model and cellular models of ageing and Alzheimer's are needed to fully understand the interplay between these two risk factors for Alzheimer's disease.

7. REFERENCES

1. CP Ferri. Global prevalence of dementia: a Delphi consensus study. The Lancet 2006.

2. Nagy Z. The last neuronal division: a unifying hypothesis for the pathogenesis of Alzheimer's disease. Journal of Cellular and Molecular Medicine 2005;9:p 531-541.

3. Arendt et al. Linking cell-cycle dysfunction in Alzheimer's disease to a failure of synaptic plasticity. Biochimica et Biophysica Acta 2007;1772:p 412-421.

4. Brookmeyer R. Forecasting the global burden of Alzheimer's disease. Alzheimers Dementia 2007;3:p 186-191.

5. Shalat et al. Risk factors for Alzheimer's disease. Neurology. Neurology 1987;37:p 1630-1633.

6. Tyas AL et al. Risk factors for Alzheimer's disease a population-based, longitudinal study in Manitoba, Canada. International Journal of Epidemiology 2001;30:p 590-597.

7. Seshadri S. Plasma Homocysteine as a Risk Factor for Dementia and Alzheimer's Disease. The New England Journal of Medicine 2002;346:p 476-483.

8. Breteler M. Vascular risk factors for Alzheimer's disease: An epidemiologic perspective. Neurobiology of Aging 2000;21:p 153-160.

9. Mahley R. Plasma lipoproteins: apolipoprotein structure and function. Review 1984;25:p 1277-1297.

10. Mahley R. Apolipoprotein E: far more than a lipid transport protein. Annual Review of Genomics and Human Genetics 2000;1:p 507-537.

11. Rall SC. Human apolipoprotein E: the complete amino acid sequence. The Journal of Biological Chemistry 1982;257:p 4171-4178.

12. Weisgraber KH. Human E apoprotein heterogeneity:cysteine-arginine interchanges in the amino acid sequence of the apo E isoforms. The Journal of Biological Chemistry 1981;256:p 9077-9083.

13. Weisgraber KH. Abnormal lipoprotein receptor-binding activity of the human E apoprotein due to cysteine-arginine interchange at a single site. The Journal of Biological Chemistry 1982;257:p 2518-2521.

14. Corbo RM SR. Apolipoprotein E (APOE) allele distribution in the world. Is APOE*4 a 'thrifty' allele? Annals of Human Genetics 1999;63:p 301-310.

15. Allen D et al. Apolipoprotein E alleles as risk factors in Alzheimer's disease. 1996. Annual Reviews Medicine 1996;47:p 387-400.

16. Saunders AM. Association of apolipoprotein E allele epsilon 4 with late-onset familial and sporadic Alzheimer's disease. Neurology 1993;43:p 1467-1472.

17. Corder EH. Gene dose of apolipoprotein E type 4 allele and the risk of Alzheimer's disease in late onset families. Science 1993;261:p 921-930.

18. Wilson RS. The apolipoprotein E epsilon 4 allele and decline in different cognitive systems during a 6-year period. Archives of Neurology 2002;59:p 1154-1160.

19. Nagy Z. Influence of the apolipoprotein E genotype on amyloid deposition and neurofibrillary tangle formation in Alzheimer's disease. Neuroscience 1995;69:p 757-761.

20. Tiraboschi P. Impact of APOE genotype on neuropathologic and neurochemical markers of Alzheimer disease. Neurology 2004;62:p 1977-1983.

21. Bradley T.Hyman, E.Tessa Hedley-Whyte, G.William Rebeck, Jean-Paul Vonsattel, Howard L.West, John H.Growdon. Apolipoprotein E epsilon-4/4 in a neuropathologically normal very elderly individual. Archives of Neurology 1996;53:p 215.

22. Growdon JH. Apolipoprotein E genotype does not influence rates of cognitive decline in Alzheimer's disease. Neurology 1996;47:p 444-448.

23. Jungsu Kim. The Role of Apolipoprotein E in Alzheimer's Disease. Neuron 2009;63:p 287-303.

24. Ma J. Amyloid-associated proteins alpha 1-antichymotrypsin and apolipoprotein E promote assembly of Alzheimer beta-protein into filaments. Nature 1994;372:p 92-94.

25. Tokuda T. Lipidation of apolipoprotein E influences its isoform-specific interaction with Alzheimer's amyloid beta peptides. The Biochemical Journal 2000;348:p 359-365.

26. Nagy et al. Influence of the apolipoprotein E genotype on amyloid deposition and neurofibrillary tangle formation in Alzheimer's disease. Neuroscience 1995;69:p 757-761.

27. Martins IJ. Cholesterol metabolism and transport in the pathogenesis of Alzheimer's disease. Journal of Neurochemistry 2009;111:p 1275-1308.

28. Bellosta S. Stable expression and secretion of apolipoproteins E3 and E4 in mouse neuroblastoma cells produces differential effects on neurite outgrowth. The Journal of Biological Chemistry 1995;270:p 27063-27071.

29. S Ramakrishnan, K N Sulochana, S Lakshmi, R Selvi, N Angayarkanni. Biochemistry of homocysteine in health and diseases. Indian Journal of Biochemistry and Biophysics 2006;43:p 275-283.

30. Andersson et al. Plasma homocysteine before and after methionine loading with regard to age, gender, and menopausal status. European Journal of Clinical Investigation 1992;22:p 79-87.

31. welch and Loscalzo. Homocysteine and Atherothromobosis. The New England Journal of Medicine 1998.

32. Hyland K BT. Measurement of total plasma and cerebrospinal fluid homocystine by fluorescence following high-performance liquid chromomatography and precolumn derivatization with o-phthaldialdehyde. Journal of Chromatography A 1992;579:p 55-62.

33. Smith AD. The worldwide chanhhenge of the dementias: A role for vitamins and homocysteine? Food and Nutrition Bulletin 2008;29:p S143-S172.

34. Clarke R. Folate, vitamin B12 and serum total homocysteine levels in confirmed Alzheimer disease. Arch Neurol 1998;55:p 1449-1455.

35. Davies G, McCaddon A. Total serum homocysteine in senile dementia of Alzheimer type. International Journal of Geriatric Psychiatry 1998;13:p 239.

36. Nilsson et al. Plasma homocysteine concentration relates to the severity but not to the duration of Alzheimer's disease. International Journal of Geriatric Psychiatry 2004;19:p 666-672.

37. de Silva HA. Medial temporal lobe atrophy, apolipoprotein genotype, and plasma homocysteine in Sri Lankan patients with Alzheimer's disease. Experimental Aging Research 2005;31:p 345-354.

38. Lehmann M. Identification of cognitive impairment in the elderly: Homocysteine is an early biomarker. Dement Geriatr Cogn Disord 1999;10:12-20. Dementia and Geriatric Cognitive Disorders 1999;10:p 12-20.

39. Teunissen CE. Homocysteine: A marker for cognitive performance? A longitudinal follow-up study. Journal of Nutrition, Health & Aging 2003;7:p 153-159.

40. Teunissen CE. Homocysteine in relation to cognitive performance in pathological and non-pathological conditions. Clinical Chemistry and Laboratory Medicine 2005;43:p 1089-1095.

41. Nilsson K. Plasma homocysteine, apolipoprotein E status and vascular disease in elderly patients with mental illness. Clinical Chemistry and Laboratory Medicine 2010;48:p 129-135.

42. Hasegawa T. Homocysteic acid induces intraneuronal accumulation of neurotoxic Abeta42: implications for the pathogenesis of Alzheimer's disease. Journal of Neuroscience Research 2005;80:p 869-876.

43. Luo Y. Homocysteine induces tau hyperphosphorylation in rats. Neuroreport. 2007 Dec 3;18(18):2005-8. Neuroreport 2007;18:p 2005-2008.

44. Ho PI. Folate deprivation induces neurodegeneration: roles of oxidative stress and increased homocysteine. Neurobiology of Disease 2003;14:p 32-42.

45. Weiss N. Influence of hyperhomocysteinemia on the cellular redox state-impact on homocysteine-induced endothelial dysfunction. Clinical Chemistry and Laboratory Medicine 2003;41:p 1455-1461.

46. Lipton SA. Neurotoxicity associated with dual actions of homocysteine at the N-methyl-D-aspartate receptor. Proc Natl. Acad. Sci. Proceedings of the National Academy of Sciences 1997;94:p 5923-5928.

47. Fuso A. Changes in Presenilin 1 gene methylation pattern in diet-induced B vitamin deficiency. Neurobiology of Aging 2009.

48. Fuso A. S-adeno-sylmethionine/homocysteine cycle alterations modify DNA methylation status with consequent deregulation of PSI and BACE and beta-amyloid production. molecular and cellular neuroscience 2005;28:p 195-204.

49. Jamaluddin MD. Homocysteine inhibits endothelial cell growth via DNA hypomethylation of the cyclin A gene. Blood 2007;110:p 3648-3655.

50. Elias et al. Homocysteine and cognitive performance: Modification by the ApoE genotype. Neuroscience Letters 2008;430:p 64-69.

51. Ventura P. Relevance of different apolipoprotein content in binding of homocysteine to plasma lipoproteins. Nutr Metab Cardiovasc Dis 3 A.D.;13:p 218-226.

52. Togawa T, Senqupta S, Chen H, Robinson K, Nonevski I, Majors AK, Jacobsen DW. Mechansims for the formation of protein-bound homocysteine in human plasma. Biochemical and Biophysical Research Communications 2000;277:p 668-674.

53. Yi et al. Increase in plasma homocysteine associated with parallel increases in plasma S-adenosylhomocysteine and lymphocyte DNA hypomethylation. J Biol Chem 2000;275:p 29318-29323.

54. Zieminska EL. Excitotoxic neuronal injury in chronic homocysteine neurotoxicity studied in vitro: the role of NMDA and group I metabotropic glutamate receptors. Acta Neurobiologiae Experimentalis 2006;66:p 301-309.

55. Kimberly M Korwek. ApoE isoform-dependent changes in hippocampal synaptic function. Molecular Neurodegeneration 2009;4:p 21.

56. Ishigami M. Apolipoprotein E inhibits platelet-derived growth factor-induced vascular smooth muscle cell migration and proliferation by suppressing signal transduction and preventing cell entry to G1 phase. The Journal of Biological Chemistry 1998;273:p 20156-20161.

57. Zeleny M. Distinct apolipoprotein E isoform preference for inhibition of smooth muscle cell migration and proliferation. Biochemistry 2002;41:p 11820-11830.

58. Chan et al. Inhibition of cell proliferation by apolipoprotein E isoform expression. Archives of Biochemistry and Biophysics. Archives of Biochemistry and Biophysics 2011;451:p 97-102.

59. Tsai JC. Induction of cyclin A gene expression by homocysteine in vascular smooth muscle cells. The Journal of Clinical Investigation 1996;97:p 153.

60. Bailey B et al. Direct determination of tissue aminothiol, disulfide and thioether levels using HPLC-ECD with a novel stable boron-doped diamond working electrode. Methods in Molecular Biology 2010;594:p 327-339.

61. Sandhu J et al. Determination of 5-methyl-2'-deoxycytidine in genomic DNA using high performance liquid chromatography-ultraviolet detection. J Chromatogr B Analyt Technol Biomed Life Sci 2009.

62. Braak et al. Staging of Alzheimer's disease-related neurofibrillary changes. Neurobiology of Aging. Neurobiology of Aging 1995;16:p 271-284.

63. Regland B. Vitamin B12 analogues, homocysteine, methylmalonic acid, and transcobalamins in the study of vitamin B12 deficiency in primray degenerative dementia. Dement Geriatr Cogn Disord 1990;1:p 272-277.

64. Joosten et al. Is metabolic evidence for vitamin B-12 and folate deficiency more frequent in elderly patients with Alzheimer's disease? J Gerontol A Bio Sci Med Sci 1997;52:p 79.

65. Joosten et al. Metabolic evidence that deficiencies of vitamin B12 (cobalamin), folate and vitamin B6 occur commonly in the elderly. Am J Clin Nutr 1993;58:p 468-476.

66. Bednarska-Makaruk M et al. Apolipoprotein E genotype, lipid levels and coronary heart disease in a Polish population group. Eur J Epidemiol 2001;17:p 789-792.

67. Corbo et al. Apolipoprotein E polymorphism in Italy investigated in native plasma by a simple polyacrylamide gel isoelectric focusing technique. Comparison with frequency data of other European populations. Ann Hum Genet 1995;59:p 197-209.

68. Lehtimaki et al. Apolipoprotein E phenotypes in Finnish youths: a cross-sectional and 6-year follow-up study. J Lipid Res 1990;31:p 487-495.

69. Schiele F et al. Apolipoprotein E serum concentration and polymorphism in six European countries: the ApoEurope Project. Atherosclerosis 2000;152:p 475-488.

70. Assmann G et al. Apolipoprotein E polymorphism and hyperlipidemia. Clin Chem 1984;30:p 641-643.

71. Crean et al. Apolipoprotein E å4 prevalence in Alzheimer's disease patients varies across global populations: a systematic literature review and meta-analysis. Dement Geriatr Cogn Disord 2011;31:p 20-30.

72. Crean et al. Apolipoprotein E å4 prevalence in Alzheimer's disease patients varies across global populations: a systematic literature review and meta-analysis. Dement Geriatr Cogn Disord 2011;31:p 20-30.

73. Uelan PM. Total homocysteine in plasma or serum: methods and clinical application. Clin Chem 1993;39:p 1764-1779.

74. Atul F et al. Elevated levels of homocysteine compromise blood-brain barrier integrity in mice. 2006. Blood 2006;107:p 591-593.

75. Lehmann M et al. Vitamin B12-B6-folate treatment improves blood-brain barrier function in patients with hyperhomocysteinaemia and mild cognitive impairment. Dement Geriatr Cogn Disord 2003;16:p 145-150.

76. Fullerton SM et al. Impairment of the blood-nerve and blood-brain barriers in apolipoprotein e knockout mice. Exp Neurol 2001;1:p 13-22.

77. Valentino F et al. Elevated cerebrospinal fluid and plasma homocysteine levels in ALS. 2010. European Journal of Neurology 2010;17:p 84-89.

78. Miller et al. Folate-deficiency-induced homocysteinaemia in rats: disruption of S-adenosylmethionine's co-ordinate regulation of homocysteine metabolism. Biochem J 1994;298:p 415-419.

79. Guidi et al. Influence of the Glu298Asp polymorphism of NOS3 on age at onset and homocysteine levels in AD patients. Neurobio Aging 2005;26:p 789-794.

80. Prohovnik et al. Dissociation of neuropathology from severity of dementia in late-onset Alzheimer disease. Neurology 2006;66:p 49-55.

81. Nilsson et al. Plasma homocysteine concentration relates to the severity but not to the duration of Alzheimer's disease. International Journal of Geriatric Psychiatry 2004;19:p 666-672.

82. McCaddon et al. Absence of macrocytic anaemia in Alzheimer's disease. Clin Lab Haem 2004;26:p 256-263.

83. Gomes-Isla et al. Clinical and pathological correlates of apolipoprotein E4 in Alzheimer's disease. Ann Neurol 1996;39:p 62-70.

84. Ariogul et al. Vitamin B12, folate, homocysteine and dementia: are they really related? Arch Gerontol Geriatr 2005;40:p 139-146.

85. Mizrahi et al. Plasma total homocysteine levels, dietary vitamin B6 and folate intake in AD and healthy aging. J Nutr Health Aging 2003;7:p 160-165.

86. Nilsson et al. Relation between plasma homocysteine and Alzheimer's disease. Dement Geriatr Cogn Disord 2002;14:p 7-12.

87. Serot et al. Homocysteine and methylmalonic acid concentrations in cerebrospinal fluid: relation with age and Alzheimer's disease. J Neurol Neurosurg Psychiatry 2005;76:p 1585-1587.

88. Gallucci et al. Homocysteine in Alzheimer disease and vascular dementia. Arch Gerontol Geriatr 2004;Suppl 9:p 195-200.

89. Genedani et al. Studies on homocysteine and dehydroepiandrosterone sulphate plasma levels in Alzheimer's disease patients and in Parkinson's disease patients. Neurotox 2004;6:p 327-332.

90. McCaddon et al. Total serum homocysteine in senile dementia of Alzheimer type. International Journal of Geriatric Psychiatry 1998;3:p 235-239.

91. Nagga et al. Cobalamin, folate, methylmalonic acid, homocysteine, and gastritis markers in dementia. Dement Geriatr Cogn Disord 2003;16:p 269-275.

92. Quadri et al. Homocysteine, folate, and vitamin B-12 in mild cognitive impairment, Alzheimer disease, and vascular dementia. Am J Clin Nutr 2004;80:p 114-122.

93. Selley et al. The effect of increased concentrations of homocysteine on the concentration of (E)-4-hydroxy-2-nonenal in the plasma and cerebrospinal fluid of patients with Alzheimer's disease. Neurobio Aging 2002;23:p 383-388.

94. Selley et al. Increased concentrations of homocysteine and asymmetric dimethylarginine and decreased concentrations of nitric oxide in the plasma of patients with Alzheimer's disease. Neurobio Aging 2003;24:p 903-907.

95. Refsum et al. Homocysteine and cardiovascular disease. Annu Rev Med 1998;49:p 31-62.

96. Nilsson et al. Role of impaired renal function as a cuase of elevated plasma homocysteine concentration in psychogeriatric patients. Scand J Clin Lab Invest 2002;62:p 390.

97. Spindler et al. Nutritional status of patients with Alzheimer's disease. A 1-year study. J Am Diet Assoc 1996;96:p 1013-1018.

98. Aisen et al. High-dose B vitramin supplementation and cognitive decline in Alzheimer's disease: a randomized controlled trial. JAMA 1999;300:p 1774-1783.

99. Kalmijn et al. Total homocysteine and cognitive decline in a community-based sample of elderly subjects. American Journal of Epidemiology 1999;150:p 283-289.

100. Mooijaart et al. Homocysteine, vitamin B12, and folic acid and the risk of cognitive decline in old age: The Leiden 85-Plus study. Am J Clin Nutr 2005;82:p 866-871.

101. Ravaglia et al. Elevated plasma homocysteine levels in centenarians are not associated with cognitive impairment. Mech Aging 2000;121:p 251-261.

102. Ravaglia et al. Blood homocysteine and vitamin B levels are not associated with cognitive skills in healthy normally ageing subjects. J Nutr Health Aging 2000;4:p 218-222.

103. Ravaglia et al. Homocysteine and cognitive performance in healthy elderly subjects. Arch Gerontol Geriatr 2004;9:p 349-357.

104. McCaddon et al. Total serum homocysteine in senile dementia of Alzheimer type. International Journal of Geriatric Psychiatry 1998;3:p 235-239.

105. Budge et al. Plasma total homocysteine and cognitive performance in a volunteer elderly population. Ann NY Acad Sci 2000;903:p 407-410.

106. Adunsky et a. Plasma homocysteine levels and cognitive status in long-term stay geriatric patients: A cross-sectional study. Arch Gerontol Geriatr. Arch Gerontol Geriatr 2005.

107. Robbins et al. Homocysteine, type 2 diabetes mellitus, and cognitive performance: The Maine-Syracuse Study. Clin Chem Lab Med 2005;43:p 1101-1106.

108. Arendt et al. Neuronal expression of cyclin dependent kinase inhibitors of the INK4 family in Alzheimer's disease. J Neural Trans 1998;105:p 949-960.

109. Dufouil et al. Homocysteine, white matter hyperintensities, and cognition in healthy elderly people. Ann Neurol 2003;53:p 214-221.

110. Garcia et al. Increases in homocysteine are related to worsening of Stroop scores in healthy elderly persons: A prospective follow-up study. J Gerontol A Bio Sci Med Sci 2004;59:p 1323-1327.

111. Clarke et al. Variability and determinants of total homocysteine concentrations in plasma in an elderly population. Clin Chem 1998;44:p 102-107.

112. Refsum et al. Facts and recommendations about total homocysteine determinations: An expert opinions. Clin Chem 2004;50:p 3-32.

113. Schafer et al. Homocysteine and cognitive function in a population-based study of older adults. American Geriatrics Society 2005;53:p 381-388.

114. Perl DP. Neuropathology of Alzheimer's disease. Mt Sinai J Med 2010;77:p 32-42.

115. Grundke-Iqbal et al. Microtubule-associated protein tau: a component of Alzheimer paired helical filaments. J Bio Chem 1986;261:p 6084-6089.

116. Grundke-Iqbal et al. Abnormal phosphorylation of the microtubuleassociated protein (tau) in Alzheimer cytoskeletal pathology. Proc Nat Acad Sci 1986;93:p 4913-4917.

117. Iqbal et al. Defective brain microtubule assembly in Alzheimer's disease. Lancet 1986;2:p 421-426.

118. Iqbal et al. Identification and localization of a tau peptide to paired helical filaments of Alzheimer disease. Proc Nat Acad Sci 1989;86:p 5646-5650.

119. Lee et al. A68: a major subunit of paired helical filaments and derivatized forms of normal tau. Science 1991;251:p 675-678.

120. Ghebremedhin et al. High frequency of apolipoprotein E epsilon4 allele in young individuals with very mild Alzheimer's disease-related neurofibrillary changes. Exp Neurol 1998;153:p 152-155.

121. Ohm et al. Apolipoprotein E polymorphism influences not only cerebral senile plaque load but also Alzheimer-type neurofibrillary tangle formation. Neuroscience 1995;66:p 583-587.

122. Polvikoski et al. Apolipoprotein E, dementia, and cortical deposition of beta-amyloid protein. N Engl J Med 1995;333:p 1242-1247.

123. Landen et al. The apolipoprotein E allele epsilon 4 does not correlate with the number of senile plaques or neurofibrillary tangles in patients with Alzheimer's disease. J Neurol Neurosurg Psychiatry 1996;61:p 352-356.

124. Morris et al. Effect of apolipoprotein E genotype on Alzheimer's disease neuropathology in a cohort of elderly Norwegians. Neuroscience Letters 1995;201:p 45-47.

125. Olichney et al. The apolipoprotein E epsilon 4 allele is associated with increased neuritic plaques and cerebral amyloid angiopathy in Alzheimer's disease and Lewy body variant. Neurology 1996;47:p 190-196.

126. Oyama et al. Apolipoprotein E genotype, Alzheimer's pathologies and related gene expression in the aged population. Brain Res Mol 1995;29:p 92-98.

127. Irizarry et al. Association of homocysteine with plasma amyloid beta protein in aging and neurodegenerative disease. Neurology 2005;65:p 1402-1408.

128. Luchsinger et al. Relation of plasma homocysteine to plasma amyloid beta levels. Neurochem Res 2007;32:p 775-81.

129. Viswanathan et al. Plasma Abeta, homocysteine, and cognition: the Vitamin Intervention for Stroke Prevention (VISP) trial. Neurology 2009;72:p 268-272.

130. Carlsson J. Clinical relevance of the quantification of apolipoprotein E in cerebrospinal fluid. Clinica Chimica Acta 1991;1196:p 167-176.

131. Chan A.Y. Folate deprivation increases tau phosphorylation by homocysteine-induced calcium influx and by inhibition of phosphatise activity: alleviation by S-adenosyl methionine. Brain Research 2008;1199:p 133-137.

132. Ho.P.I et al. Multiple aspects of homocysteine neurotoxicity: glutamate excitotoxicity, kinase hyperactivation and DNA damage. J Neurosci Res 2002;70:p 694-702.

133. Zou CG. Homocysteine promotes proliferation and activation of microglia. Neurobiol Aging.2010. (12):2069-79]. Neurobio Aging 2010;12:p 2069-2079.

134. McShea et al. Neuronal cell cycle re-entry mediates Alzheimer disease-type changes. Biochim Biophys Acta 2007;1772:p 467-472.

135. Iqbal et al. Mechanism of neurofibrillary degeneration in Alzheimer's disease. Mol Neurobiol 1994;9:p 119-123.

136. Trojanowski et al. PHFt(A68): from pathological marker to potential mediator of neuronal dysfunction and neuronal degeneration in Alheimer's disease. *Clin Neurosci.* 1993; 1: 184-91][Lee VMet al. The disordered neuronal cytoskeleton in Alzheimer's disease. Curr Opin Neurobiol 1992;2:p 653-656.

137. Corder et al. Protective effect of apolipoprotein E type 2 allele for late onset Alzheimer disease. Nat Genet 1994;7:p 180-184.

138. Hayashi et al. Protection of nerons from apoptosis by apolipoprotein E containing lipoproteins does not require lipoprotein uptake and involves activation of phospholipase Cã1 and inhibition of calcineurin. J Bio Chem 2009;284:p 29605-28613.

139. Noble et al. Inhibition of glycogen synthase kinase-3 by lithium correlates with reduced tauopathy and degeneration in vivo. Proc Natl Acad Sci 2005;102:p 6990-6995.

140. Ho P.I.et al. Homocysteine potentiates beta-amyloid neurotoxicity: role of oxidative stress. Journal of Neurochemistry 2001;78:p 249-253.

141. Suzuki et al. Cell cycle-dependent regulation of the phosphorylation and metabolism of the Alzheimer amyloid precursor protein. EMBO J 1994;13:p 1114-1122.

142. Zhuo J.M.et al. Severe In vivo hyper-homocysteinemia is not associated with elevation of amyloid-beta peptides in the Tg2576 mice. Journal of Alzheimer's Disease 2010;21:p 133-140.

143. Gabbita et al. Increased nuclear DNA oxidation in the brain in Alzheimer's disease. J Neurochem 1998;71:p 2034-2040.

144. Mark RJ et al. A role for 4-hydroxynonenal, an aldehydic product of lipid peroxidation, in disruption of ion homeostasis and neuronal death induced by amyloid -peptide. J Neurochem 1997;68:p 255-264.

145. Smith MA et al. Morphological aspects of oxidative damage in Alzheimer's disease. Mitochondria and Free Radicals in Neurodegenerative Diseases 1997;p 335-342.

146. Coyle et al. Oxidative stress, glutamate and neurodegenerative disorders. Science 1993;262:p 689-695.

147. Shea TB et al. Homocysteine, folate deprivation and Alzheimer's disease. J Alzheimer's Disease 2002;4:p 261-267.

148. Tchantchou et al. Expression and activity of methionine cycle genes are altered following folate and vitamin E deficiency under oxidative challenge: Modulation by apolipoprotein E-deficiency. Nutritional Neuroscience 2006;9:p 17-24.

149. Ueland PM et al. Reduced, oxidized and protein-bound forms of homocysteine and other aminothiols in plasma comprise the redox thiol status - A possible element of the extracellular antioxidant defense system. J Nutr 1996;126:p 1281-1284.

150. Bandyopadhyay et al. The emerging role of epigenetics in cellular and organismal aging. Exp Gerontol 2003;38:p 1299-1307.

151. Hiltunen et al. DNA methylation, smooth muscle cells, and atherogenesis. Arterioscler Thromb Vasc Biol 2003;23:p 1750-1753.

152. Issa et al. Aging, DNA methylation and cancer. Curr Rev Oncol Hematol 1999;32:p 31-43.

153. Liu L et al. Aging, cancer and nutrition: the DNA methylation connection. Mech Ageing Dev 2003;124:p 989-998.

154. Richardson B et al. Impact of aging on DNA methylation. Aging Res Rev 2003;2:p 245-261.

155. Singh et al. Involvement of gene-diet/drug interaction in DNA methylation and its contribution tocomplex diseases: from cancer to schizophrenia. Clin Genet 2003;64:p 451-460.

156. Toyota M et al. CpG island methylator phenotypes in aging and cancer. Cancer Biol 1999;9:p 349-357.

157. Fuso et al. Changes in Presenilin 1 gene methylation pattern in diet-induced B vitamin deficiency. Neurobiology of Aging 2011;32:p 187-199.

158. Fuso et al. The effect of S-adenosylmethionine on CNS gene expression studied by cDNA microarray analysis. J Alzheimer's Disease 2006;4:p 415-419.

159. Fuso et al. S-adenosylmethionine/homocysteine cycle alterations modify DNA methylation status with consequent deregulation of PS1 and BACE and beta-amyloid production. Molecular and Cellular Neurosciences 2005;28:p 195-204.

160. Lin et al. S-Adenosylhomocysteine increases beta-amyloid formation in BV-2 microglial cells by increased expressions of beta-amyloid precursor protein and presenilin 1 and by hypomethylation of these gene promoters. Neurotoxicology 2009;30:p 622-627.

161. Mastroeni et al. Epigenetic changes in Alzheimer's disease: Decrements in DNA methylation. Neurobiology of Aging 2000;31:p 2025-2037.

162. West et al. Hypomethylation of the amyloid precursor protein gene in the brain of an alzheimer's disease patient. J Mol Neuro 1995;6:p 141-146.

163. Brzezianska et al. A minireview: the role of MAPK/ERK and PI3K/Akt pathways in thyroid follicular cell-derived neoplasm. Front Biosci 2011;16:p 422-439.

164. Wang et al. Kinases and phosphatases and tau sites involved in Alzheimer neurofibrillary degeneration. Eur J Neurosci 2007;25:p 59-68.

165. Castro R et al. Increased homocysteine and S-adenosylhomocysteine concentrations and DNA hypomethylation in vascular disease. Clin Chem 2003;49:p 1292-1296.

166. Alam M.M. Homocysteine reduces endothelial progenitor cells in stroke patients through apoptosis. J Cereb Blood Flow Metab 2009;29:p 157-165.

167. Bonsch et al. Homocysteine associated genomic DNA hypermethylation in patients with chronic alcoholism. J Neural Transm 2004;111:p 1611-1616.

168. Bromberg et al. Hyperhomocysteinemia does not affect global DNA methylation and nicotinamide N-methyltransferase expression in mice. J Psychopharmacol 2011;25:p 976-981.

169. Devlin AM et al. Tissue specific changes in H19 methylation and expression in mice with hyperhomocysteinemia. J Biol Chem 2005;280:p 25506-25511.

170. Heil et al. DNA methylation status is not impaired in treated cystathionine beta-synthase (CBS) deficient patients. Mol Genet Metab 2007;91:p 55-60.

171. Lenz et al. Homocysteine regulates expression of Herp by DNA methylation involving the AARE and CREB binding sites. Exp Cell Res 2006;312:p 4055.

172. Ingrosso D et al. Epigenetics in hyperhomocysteinemic states. A special focus on uremia. Biochem Biophys Acta 2009;1790:p 892-899.

173. Zhang Q. Effects of homocysteine on murine splenic B lymphocyte proliferation and its signal transduction mechanism. Cardiovasc Res 2001;52:p 328-336.

174. Zou CG. Homocysteine enhances cell proliferation in hepatic myofibroblastic stellate cells. J Mol Med 2009;87:p 75-84.

175. Zou T. Homocysteine enhances cell proliferation in vascular smooth muscle cells: role of p38 MAPK and p47phox. Acta Biochim Biophys Sin 2010;42:p 908-915.

176. Olas B. Homocysteine and its thiolactone may promote apoptotic events in blood platelets in vitro. Platelets 2010;21:p 533-540.

177. Hirashima Y. Homocysteine and copper induce cellular apoptosis viia caspase activation and nuclear translocation of apoptosis-inducing factor in neuronal cell line SH-SY5Y. Neuroscience Research 2010;67:p 300-306.

178. Ye et al. S phase entry causes homocysteine-induced death while ataxia telangiectasia and Rad3 related protein functions anti-apoptotically to protect neurons. Brains 2010;133:p 2295-2312.

179. M.Zeleny. Distinct apolipoprotein E isoform preference for inhibition of smooth muscle cell migration and proliferation. Biochemistry. Biochemistry 2002;41:p 11820-11823.

180. Little M et al. Methylation and p16: suppressing the suppressor. Nature Med 1995;1:p 633-634.

181. Merlo et al. 5-prime CpG island methylation is associated with transcriptional silencing of the tumour suppressor p16/CDKN2/MTS1 in human cancers. Nature Med 1995;1:p 686-692.

182. Silva et al. Aberrant DNA methylation of the p16^{INK4a} gene in plasma DNA of breast cancer patients. Br J Cancer 1999;80:p 1262-1264.

183. Lau et al. p16INK4a-silencing augments DNA damage-induced apoptosis in cervical cancer cells. Oncogene 2007 26:6050-6060] 2007;26:p 6050-6060.

184. Harper et al. The p21 Cdk-interacting protein Cip1 is a potent inhibitor of G1 cyclin-dependent kinases. Cell 1993;75:p 805-816.

185. Braun-Dullaeus et al. A novel role for the cyclin-dependent kinase inhibitor p27(Kip1) in angiotensin II-stimulated vascular smooth muscle cell hypertrophy. J Clin Invest 1999;104:p 823.

186. Matsuoka et al. Matsuoka, S., Thompson, J. S., Edwards, M. C., Barletta, J. M., Grundy, P., Kalikin, L. M., Harper, J. W., Elledge, S. J., Feinberg, A. P.Imprinting of the gene encoding a human cyclin-dependent kinase inhibitor, p57(KIP2), on chromosome 11p15. Proc Nat Acad Sci 1996;93:p 3026-3030.

187. Janzen et al. Stem-cell ageing modified by the cyclin-dependent kinase inhibitor p16(INK4a). Nature 2006;443:p 421-426.

188. Serrano et al. Role of the INK4a locus in tumor suppression and cell mortality. Cell 1996;85:p 27-37.

189. McShea et al. Abnormal expression of the cell cycle regulators P16 and CDK4 in Alzheimer's disease. Am J Pathol 1996;150:p 1933-139.

190. Rodel et al. Expression of the cyclin-dependent kinase inhibitor p16 in Alzheimer's disease. Neuroreport 1996;7:p 2829-3105.

191. Jellinger et al. Neuropathological evaluation of mixed dementia. Journal of Neurological Sciences. 2007. 257 (1-2):80-7

192. Esiri et al. Neuropathological assessment of the lesions of significance in vascular dementia. 1997. J Neurol Neurosurg Psychiatry. 63 (6): 749-53.

193. Malouf et al. Folic acid with or without vitamin B12 for the prevention and treatment of healthy elderly and demented people. Cochrane Database Systemic Reviews. 2008. 8 (4):CD004514

194. Mark Tranmer and mark Elliot. Binary Logistic Regression. Teaching Paper: Binary Logistic Regression - CCSR

195. The neuropathology of dementia. Margaret M. Esiri, Virginia M.-Y. Lee, John Q. Trojanowski. 2004.

196. Ubbink JB. Assay methods for the measurement of total homocyst(e)ine in plasma. Semin Thromb Hemost. 2000. 26(3); 233-41.